PUBLISHED VERSION

Peter R. Johnson, Galen P. Halverson, Timothy M. Kusky, Robert J. Stern, and Victoria Pease
Volcanosedimentary basins in the Arabian-Nubian Shield: markers of repeated exhumation and denudation in a Neoproterozoic accretionary orogen
Geosciences, 2013; 3(3):389-445

©2013 by the authors; licensee MDPI, Basel, Switzerland. This is an open access article distributed under the Creative Commons Attribution License which permits unrestricted use, distribution, and reproduction in any medium, provided the original work is properly cited.

Originally published at:
http://doi.org/10.3390/geosciences3030389

PERMISSIONS

http://creativecommons.org/licenses/by/3.0/

creative commons

Attribution 3.0 Unported (CC BY 3.0)

This is a human-readable summary of (and not a substitute for) the license.

Disclaimer

APPROVED FOR Free Cultural Works

You are free to:

Share — copy and redistribute the material in any medium or format

Adapt — remix, transform, and build upon the material

for any purpose, even commercially.

The licensor cannot revoke these freedoms as long as you follow the license terms.

Under the following terms:

Attribution — You must give **appropriate credit**, provide a link to the license, and **indicate if changes were made**. You may do so in any reasonable manner, but not in any way that suggests the licensor endorses you or your use.

No additional restrictions — You may not apply legal terms or **technological measures** that legally restrict others from doing anything the license permits.

http://hdl.handle.net/2440/92123

Geosciences **2013**, *3*, 389-445; doi:10.3390/geosciences3030389

OPEN ACCESS

geosciences

ISSN 2076-3263

www.mdpi.com/journal/geosciences

Review

Volcanosedimentary Basins in the Arabian-Nubian Shield: Markers of Repeated Exhumation and Denudation in a Neoproterozoic Accretionary Orogen

Peter R. Johnson [1,*], Galen P. Halverson [2], Timothy M. Kusky [3], Robert J. Stern [4] and Victoria Pease [5]

[1] 6016 SW Haines Street, Portland, OR 97219, USA

[2] Department of Earth and Planetary Sciences/Geotop, McGill University, Montreal, QC H3A 2A7, Canada; E-Mail: galen.halverson@mcgill.ca

[3] Three Gorges Research Center for Geohazards, State Key Laboratory of Geological Processes and Mineral Resources, China University of Geosciences, Wuhan 430074, China; E-Mail: tkusky@gmail.com

[4] Geosciences Department, University of Texas at Dallas, Richardson, TX 75080, USA; E-Mail: rjstern@utdallas.edu

[5] Department of Geological Sciences, PetroTectonics Facility, Stockholm University, Stockholm SE-106 91, Sweden; E-Mail: vicky.pease@geo.su.se

* Author to whom correspondence should be addressed; E-Mail: petergeo@earthlink.net; Tel.: +1-503-293-1776.

Received: 7 May 2013; in revised form: 17 June 2013 / Accepted: 19 June 2013 / Published: 9 July 2013

Abstract: The Arabian-Nubian Shield (ANS) includes Middle Cryogenian-Ediacaran (790–560 Ma) sedimentary and volcanic terrestrial and shallow-marine successions unconformable on juvenile Cryogenian crust. The oldest were deposited after 780–760 Ma shearing and suturing in the central ANS. Middle Cryogenian basins are associated with ~700 Ma suturing in the northern ANS. Late Cryogenian basins overlapped with and followed 680–640 Ma Nabitah orogenesis in the eastern ANS. Ediacaran successions are found in pull-apart and other types of basins formed in a transpressive setting associated with E-W shortening, NW-trending shearing, and northerly extension during final amalgamation of the ANS. Erosion surfaces truncating metamorphosed arc rocks at the base of these successions are evidence of periodic exhumation and erosion of the evolving ANS crust. The basins are evidence of subsequent subsidence to the base level of alluvial systems or below sea level. Mountains were dissected by valley systems, yet relief was

locally low enough to allow for seaways connected to the surrounding Mozambique Ocean. The volcanosedimentary basins of the ANS are excellently exposed and preserved, and form a world-class natural laboratory for testing concepts about crustal growth during the Neoproterozoic and for the acquisition of data to calibrate chemical and isotopic changes, at a time in geologic history that included some of the most important, rapid, and enigmatic changes to Earth's environment and biota.

Keywords: Arabian-Nubian Shield; marine sediments; terrestrial sediments; post-amalgamation basins; transpressional basins; exhumation; erosion; subsidence; Cryogenian; Ediacaran

1. Introduction

The Arabian-Nubian Shield (ANS) is in the northern part (present-day coordinates) of the East African Orogen (EAO) [1], an accretionary orogen that extends from Arabia to East Africa and into Antarctica. The orogen resulted from multiphase convergence and amalgamation of crustal blocks during the late Neoproterozoic-early Cambrian. It was the product of a supercontinental cycle, initiated at the end of Grenvillian orogenesis (~950 Ma) by the break-up of Rodinia and ended by Ediacaran Brasiliano-Pan-African orogenesis during final assembly of eastern and western Gondwana [2]. Whereas orogenesis continued until about 530 Ma in the southern EAO, it was complete in the ANS by about 550 Ma.

The bulk of the ANS consists of Tonian to Ediacaran arcs that originated in the Mozambique Ocean, the ocean basin that opened during the middle Neoproterozoic break-up of Rodinia. The arc assemblages comprise juvenile suites of tholeiitic and calc-alkaline volcanic rocks, large amounts of volcaniclastic sedimentary rocks, and voluminous epizonal TTG-type intrusions. The arcs were active about 870 to 600 Ma [3]; they have Nd model ages close to their crystallization ages, positive εNd(t) values, and are typical juvenile crust [4]. In the eastern and southern ANS, arc assemblages are structurally intercalated with or overlie gneiss that has model ages as old as 3.0 Ga, moderately to strongly negative εNd values, and crystallization ages as old as 1.8 Ga [5,6]. These old units possibly represent fragments of Rodinia that were preserved as microplates in the Mozambique Ocean and were subsequently incorporated in the otherwise juvenile Neoproterozoic rocks of the shield. Assembly of the ANS entailed the amalgamation of the arc systems to form tectonostratigraphic terranes, suturing of the terranes, and the emplacement of a vast array of syntectonic to posttectonic granitoids. Cryogenian-Ediacaran sedimentary and volcanic strata were variously deposited unconformably atop actively deforming or newly amalgamated arcs and sutured terranes. Arc amalgamation began about 780–760 Ma and continued periodically to about 620 Ma [7]. Overall, shield assembly terminated at about 560 Ma, by which time the ANS had been accreted to the Saharan Metacraton [8] and had evolved as part of the southern margin of Paleotethys.

The many sedimentary and volcanic successions unconformable on arc sequences in the ANS are an under-reported aspect of ANS geology. They occupy basins developed on crust being created or newly created by the amalgamation and suturing of the arcs. They were contemporary with or followed episodes of metamorphism, deformation, and syntectonic intrusion. Exhumation and uplift of basement

rocks led to the development of unconformities of local to regional extent, on top of which the sedimentary and volcanic assemblages were deposited (Figure 1). At least one volcanosedimentary sequence overlies a forearc accretional prism; others overlie plutonic rocks from deep in the magmatic core of the arc systems; and some overlap suture zones between amalgamated terranes. Comprehensive detailed information about the tectonic settings of many of the ANS basins is lacking and not all can yet be described in terms of standard basin types. Several basins in the ANS are informally referred to as "post-amalgamation basins" [9] where it can be demonstrated that they overlie newly amalgamated components of composite terranes (Table 1). Basins suspected of being located on the upper overriding plate during terrane collision and suturing are referred to as retroforeland basins [10]. Other basins developed during transtensional extension at releasing bends or transpressional extension at constraining bends in strike-slip fault systems, or during normal faulting associated with orogen-parallel extension and gneiss doming.

Figure 1. Volcanosedimentary basins in the Arabian-Nubian Shield unconformable on basement composed of older arc rocks and amalgamated terranes (terrane names in red italics). (After [11]).

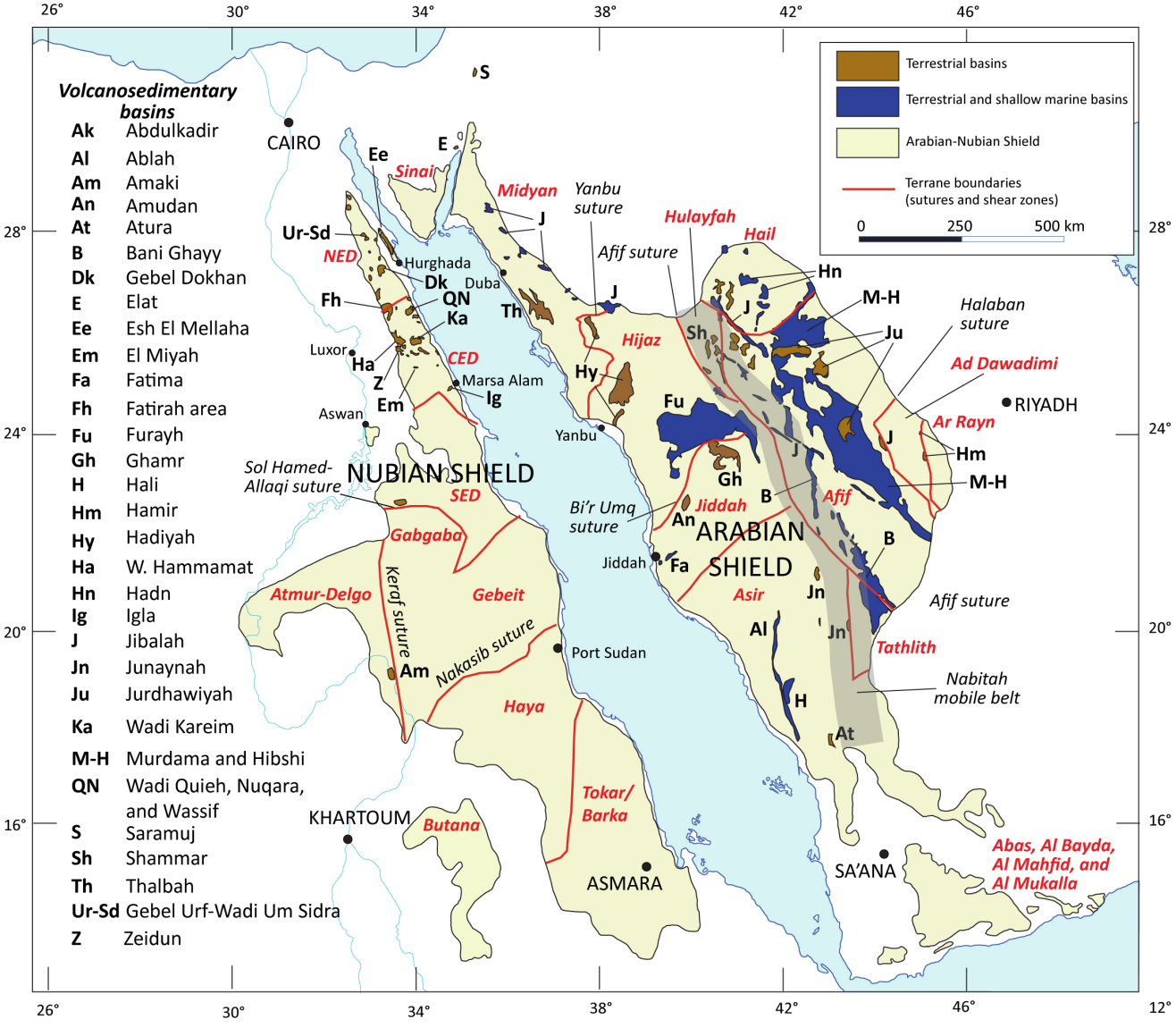

Table 1. Volcanosedimentary successions unconformable on older arc terranes in the Arabian-Nubian Shield (ANS).

Basin	Age, age range (Ma)	Lithology	Thickness	Metamorphism	Tectonic setting/basin type
Hali	795–780	Quartz-biotite schist, actinolite-biotite schist, quartzofeldspathic granofels, amphibolite, minor marble. Protoliths: quartz-rich to arkosic sandstone, mafic volcanic rocks, minor polymict conglomerate, minor limestone	Unknown	Amphibolite facies	Close to convergent margin; unconformable on exhumed core of Shwas volcanic arc; retroforeland basin?
Ghamr	~745	Felsic tuff, pebbly sandstone, rhyodacitic ash-flow tuff, polymict conglomerate, matrix-supported pebble conglomerate, sandstone, siltstone, subordinate limestone	~6000 m	Greenschist facies	Close to convergent margin; suspected location on upper plate; retroforeland basin?
Amudan	755–745	Basaltic andesite to rhyolite flows and tuffs, polymict conglomerate, tuffaceous siltstone or chert, sandstone and siltstone	~8000 m	Greenschist facies	Close to convergent margin; suspected location on upper plate; retroforeland basin?
Hadiyah	~695	Pillow basaltic-andesite flows, basaltic-andesite breccia, rhyolitic ash-flow tuffs, sandstone, polymict pebble to cobble conglomerate, matrix-supported pebble to boulder conglomerate, red and green siltstone and mudstone, limestone	~7000 m	Low greenschist facies	Close to convergent margin; suspected location on upper plate; retroforeland basin?
Furayh	~660–630	Pillow basalt, basalt and andesite flows and breccia, rhyolite, rhyodacite, and dacite flows and tuffs, polymict conglomerate, sandstone, arkose, siltstone, green and purple shale and siltstone, mudstone, carbonate (limestone, dolomitic marble, magnesite), locally stromatolitic.	~6000 m	Low greenschist facies	Close to triple junction between Bi'r Umq and Afif suture zones; basin type uncertain; possibly flexural basin reflecting tectonic loading by the Afif terrane.
Murdama	650–625	Bimodal rhyolite, dacite, andesite, and basalt flows and breccia; polymict conglomerate, sandstone (wacke), carbonate (dolomitic marble), locally stromatolitic, subordinate siltstone.	8000 m or more	Greenschist facies	Type "post-amalgamation basin" overlying newly amalgamated Afif composite terrane; possibly caused by flexure due to tectonic loading of the Halaban ophiolite.

Table 1. *Cont.*

Basin	Age, age range (Ma)	Lithology	Thickness	Metamorphism	Tectonic setting/basin type
Dokhan, Hammamat, Thalbah	630–585	Dokhan—dacitic and rhyolitic welded and non-welded ignimbrite. Hammamat and Thalbah—Cobble and boulder polymict conglomerate, pebbly sandstone, purple sandstone (litharenite), siltstone, and mudstone	~4000 m	Low greenschist facies; locally, in shear zone, mylonite	Close to shear zones and gneiss complexes and belts; variously associated with active margins, transpression, and extension. Variously termed intramontane basin, foreland basin, extensional pull-apart basin, rift, graben, piggy back basin, flexural basin.
Jibalah	600–650	Polymict conglomerate, sandstone, siltstone, carbonate (limestone and dolomite) locally stromatolitic, bimodal basalt, andesite, rhyodacite	As much as 3000 m	Very low-grade metamorphism to none	Close to shear zones; original basin form debated; one or more large basins now preserved in fault basins or many separate pull-apart/extensional basins.

Volcanosedimentary basins have been studied in the ANS for more than 30 years [12]. Recent U-Pb ion-probe zircon dating constrains depositional ages for some basins more precisely than heretofore. A growing body of geologic mapping better constrains the structural settings of several basins, and a small number of $^{40}Ar/^{39}Ar$ cooling ages provide constraints on the timing of late Cryogenian and Ediacaran exhumation. Our improved understanding of the time-space distribution, lithologic character, and depositional environments, structural controls, and shallow marine to terrestrial settings of the ANS basins provides new insights about where and when exhumation and erosion occurred during ANS orogeny. These insights inform our understanding of the complexity of Neoproterozoic orogeny at the northern end of the EAO and allow for the development of an orogenic model that takes into account periodic crustal subsidence as well as mountain building. The objective of this review is to make information about these basins more widely known, and we present data compiled from standard international geologic journals as well as from maps and reports in the archives of national geological surveys and universities less readily available to an international audience. The basins of the ANS are important geologic phenomena; they record important stages in evolution of what is one of the largest expanses of juvenile crust worldwide; they have a tremendous potential to refine aspects of EAO tectonic development; and, more globally, they help elucidate problems in Neoproterozoic Earth history, including calibration of the Ediacaran time scale and timing of final Gondwana assembly.

For the purposes of this paper, selected basins are discussed, chosen because they provide information about some of the main orogenic events in the ANS, because they illustrate a variety of structural controls on basin development and exhumation and erosional features of basin margins, and because they contain a variety of basin fill reflecting varied depositional environments. The locations of basins discussed in this contribution are indicated in Figure 2; they are listed in Table 1.

Figure 2. Index of regions discussed in the text.

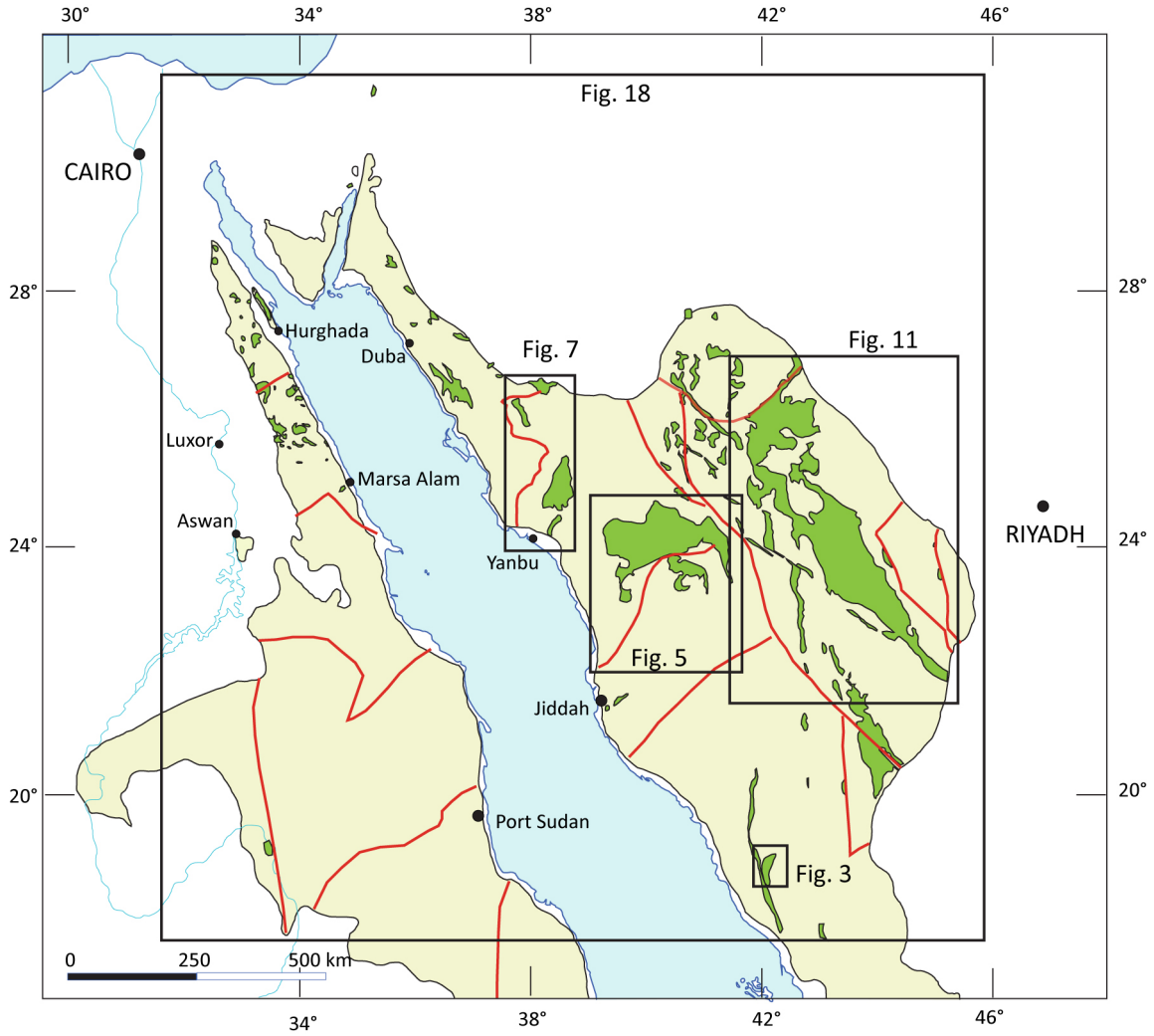

2. Geologic Character

Volcanosedimentary basins are widespread in the ANS (Figure 1). They occur throughout the Arabian Shield and in the northern Nubian Shield, but are absent from the southern Nubian Shield apart from one relatively small location in Sudan. It is not known whether this distribution was an original distribution, results from differential erosion during Cretaceous tectonics (e.g., Sudan and Yemen basins), or reflects Neogene uplift related to the Afar hotspot and separation of the African and Arabian plates. The defining feature of the basins is that they have basal unconformities—that is, they are *in situ*–in depositional contact with basement composed of amalgamated arc systems and terranes. A variety of other Tonian to Ediacaran sedimentary and volcanosedimentary assemblages are also known in the ANS but differ from the basins considered here in that they lack any observable base. These assemblages are intercalated with the volcanic strata as part of the supracrustal rocks that make up the juvenile arcs of the shield and are not a focus of this paper.

The arc rocks beneath the basins are mostly metamorphosed to greenschist facies. The relatively low metamorphic grade and presence of layered and plutonic rocks representing both the supracrust and epizonal magmatic core of the arcs are evidence of only moderate exhumation and erosion of the sutured arcs in most parts of the ANS prior to basin development. In some locations, however, the

basement beneath the basins is almost entirely plutonic or contains high-grade metamorphic rocks, indicating virtual complete removal of the volcanic supracrustal rocks and implying significant amounts of exhumation and erosion prior to basin formation.

All of the volcanosedimentary basin deposits are deformed to some extent. Their strata are gently to vertically dipping in open-to-tight folds, and commonly show pervasive cleavage and lineations. Brittle faults internally disrupt the basins and commonly bound the basins; in places, shear zones transform basin fill into mylonite. Metamorphism is mostly weak to moderate, but in ductile shear zones may reach amphibolite grade and on the flanks of granitoid intrusions basin rocks may be hornfelsed.

The basin assemblages are Cryogenian to Ediacaran, ranging from about 785 Ma (Hali group) to about 560 Ma (Jibalah and Saramuj groups). They vary in size from aggregates of basins extending over as much as 72,000 km^2 to small isolated basins of 200 km^2 and make up about 18 percent of the shield in terms of surface area [3]. The largest basin is in the northeastern Arabian Shield, filled by the Murdama group and Afif and Hibshi formations. Smaller basins are filled by the Atura formation in the far southern Arabian Shield, the Amaki formation in the south-central Nubian Shield [13], and the Hammamat Group, Dokhan Volcanics, and Jibalah group in the northern ANS. Depositional units within the basins may be entirely or largely volcanic or volcaniclastic in origin and contain basalt, andesite, or rhyolite flows, agglomerates, ignimbrites, and tuffs. Other basins are filled dominantly or entirely by sedimentary rocks such as sandstone, siltstone, and limestone. Some post-amalgamation basins are terrestrial whereas others are terrestrial to shallow marine. It should be noted that in this paper we use "Group" and "Formation" if the stratigraphic units are formally defined, that is if measured type sections of the units are well known or have been described in the international literature. Otherwise we use "group" and "formation". In practice, most units in the Nubian Shield are referred to as Groups or Formations; most units in the Arabian Shield are treated as informal. Exceptions in the Arabian Shield are the Shammar Group and formations in the group [14,15].

3. Hali Group Basin

The Hali group, the oldest succession considered in this report, crops out in the west-central part of the Asir composite terrane in the southern Arabian Shield (Figures 1 and 3). It rests unconformably on a deeply eroded diorite-tonalite batholith that originated in the arc rocks of the Shwas-Tayyah structural belt. Its basal contact is one of the oldest unconformities in the ANS. The name of the group was introduced by the US Geological Survey during 1:100,000-scale geologic mapping in the southern shield [16] for a sequence of high-grade quartz-biotite-garnet schist interlayered with amphibolite and subordinate layers of marble, pebble-conglomerate schist, and rhyolitic schist. In later map compilations, the rocks were incorrectly reassigned to the Ablah group [17], which is considerably younger and of lower metamorphic grade. In its type area the Ablah group comprises relatively unmetamorphosed polymict conglomerate, sandstone, siltstone, limestone and rhyolite dated between 640 and 613 Ma [18,19]. The Hali group, in contrast, is metamorphosed to amphibolite facies, and is early Cryogenian.

The Hali group is situated in a key part of the Asir composite terrane, adjacent to the boundary between arc rocks of the Al Lith-Bidah structural belt (L-B) in the west and the Shwas-Tayyah belt

(S-T) in the east (Figure 3 inset). It is underlain by the An Nimas batholith (816–797 Ma) [20], the largest arc-related plutonic complex in the southern Arabian Shield and is intruded by syntectonic tonalite and granodiorite of the Baqarah complex (780–760 Ma) [20] (Figure 3). The Al Lith-Bidah belt contains early Cryogenian arc rocks (~855–815 Ma); the Shwas-Tayyah belt is older than >795 Ma, but possibly younger than the Al Lith-Bidah belt [3]. The join between the two belts is a long-lived zone of structural weakness in the southern Arabian Shield that probably originated by convergence of the two structural belts during 780 and 765 Ma shearing [21] within and on the margin of the An Nimas batholith, emplacement of syntectonic tonalite gneiss in the Baqarah complex (780–765 Ma) (Figure 3) [20], and metamorphism. The dextral Tarj shear zone on the margin of the An Nimas batholith, which partly defines the zone of weakness, is a north-trending shear zone more than 400 km long (Figure 3). The zone of structural weakness was reactivated some 120 million years later as a control on development of the north-south narrow basin of the Ediacaran Ablah group, at which time it became the site of transpressive thrusting and shearing associated with east-west shortening in the southern ANS [3,22,23]. The Hali group itself is not dated, but is constrained between about 795 and 780 Ma by the ages of the An Nimas batholith and the Baqarah complex.

The Hali group is well-bedded (Figure 4A,B) quartz-biotite schist, actinolite-biotite schist, actinolite-biotite-quartz-feldspar schist, quartzofeldspathic granofels, amphibolite, hornblende schist, and white, gray, and brown marble. Its outcrop defines a broad northeast-plunging antiform around the Baqarah complex (Figure 3). The antiform rotates the basal unconformity, with the result that the contact between the Hali group and the stratigraphically underlying An Nimas batholith is overturned and dips northwest (Figure 4A,B), placing the Hali group structurally beneath the batholith. The group has pervasive cleavage and schistosity, tight folding of the foliation, and locally developed intrafolial folds and shear fabric (Figure 4C). Flecks of malachite are present in the quartzofeldspathic rocks and kyanite is present on the flanks of and in roof pendants in the Baqarah complex as kyanite-quartz-muscovite and kyanite-quartz-biotite schists. The Hali group is locally migmatized close to contacts with the Baqarah complex, and in places it is difficult to distinguish from gneissose plutonic rock. Overall, the Hali group protoliths are inferred to be quartz-rich to arkosic sandstone, mafic volcanic rocks, and limestone.

The Hali group basal unconformity is not everywhere apparent because of overprinting by high-grade metamorphism and recrystallization that altered quartzofeldspathic clastic rocks at the base of the Hali to resemble plutonic rocks in the An Nimas batholith. Nevertheless, the unconformity is locally well exposed (for example, at lat 18°58.73' N, long 42°03.16' E) and is evident as a change from massive leucocratic biotite-hornblende tonalite of the batholith to layered granofels of the Hali group. The granofels is composed of quartz, feldspar, biotite, and hornblende and contains rounded tonalite clasts. The unconformity itself is evidence of significant exhumation, uplift, and erosion of the An Nimas batholith and the arc of which the batholith is part. The depth of crystallization of the batholith is not known, but it appears to be a typical mid-level intrusion and exhumation was therefore probably on the order of 10 or more km. The cause of exhumation has not been established but may be related to orogenic uplift resulting from accretion between the Al Lith-Bidah and Shwas-Tayyah belts.

Figure 3. Geologic setting of the Hali group, unconformable on the exhumed and eroded An Nimas batholith (~815–795 Ma) and intruded by ~775–765 Ma syntectonic Baqarah complex tonalite and granodiorite (after [17]). Inset shows the location of the Hali group and younger Ediacaran Ablah group close to and at the junction between the Al Lith-Bidah (L-B) and Shwas-Tayyah structural belts (S-T) in the Asir composite terrane. The Khadra structural belt (K) is a separate belt in the eastern part of the Asir terrane. The Tathlith, Jiddah, and Afif are other terranes east and north of the Asir terrane.

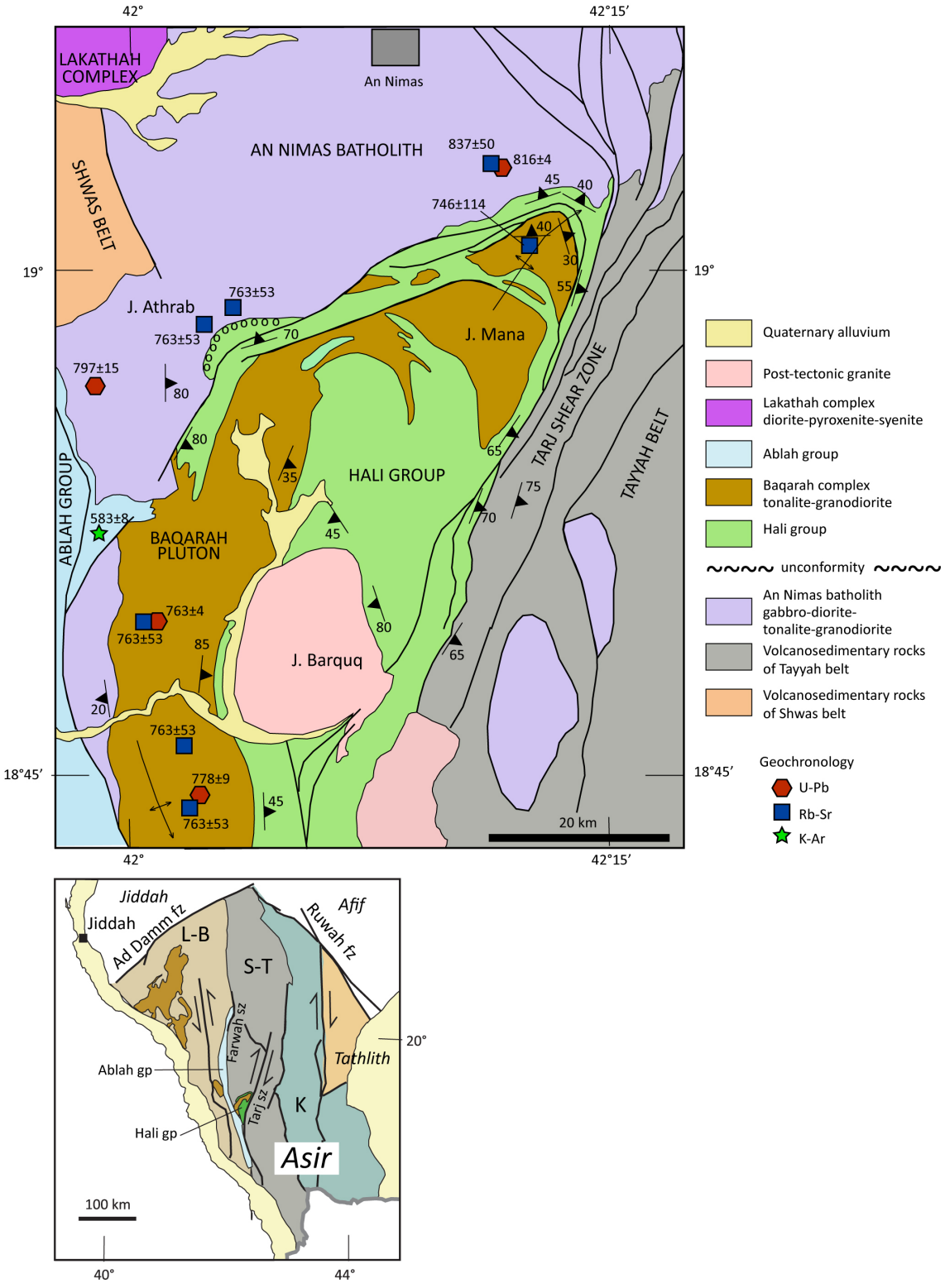

Figure 4. Lithologic and structural features of the Hali group. (**A**) View, looking west, of a narrow zone of well-bedded Hali group rocks in contact with the An Nimas batholith to the north (slopes on the right hand side of the photo) and the Baqarah pluton to the south (on the left). The Hali group unconformably overlies the An Nimas batholith but, as seen in this view, the group dips steeply north beneath the batholith and the unconformity is overturned; (**B**) Another view of overturned, north-dipping Hali group rocks, showing the flaggy character of psammitic schist; (**C**) Close up of psammitic rocks in the Hali group showing their strongly deformed character with transposed, discontinuous layering, sheared-out intrafolial folds, and stretched epidote-rich lenses.

(**A**)

(**B**)

(**C**)

The association of arc convergence, metamorphism, folding, shearing, and syntectonic intrusion in the vicinity of the Hali group is evidence for the oldest recognized Cryogenian orogenic event in the Asir terrane. Exhumation, uplift, and erosion of the underlying 816–797 Ma An Nimas tonalite and diorite was followed by subsidence and the deposition of epiclastic, volcanic, and carbonate rocks of the Hali group. The structural control and depositional environment of the Hali group basin has not been studied and it is not known whether carbonate in the group represents a lacustrine or shallow marine environment. Soon after its deposition, the Hali group was caught up in a major orogenic event that inverted the basin and overturned the unconformity; the rocks were folded and metamorphosed, and intruded by a syntectonic pluton. As a consequence, the Hali basin was relatively short lived, but its strata reveal that stages in early Cryogenian orogeny associated with arc amalgamation in the Asir composite terrane included not only deformation but also exhumation, uplift, erosion, and subsidence.

The basin clearly developed close to an active convergent margin (the join between the Al Lith-Bidah and Shwas-Tayyah structural belts) and may be a type of retroforeland basin.

4. Ghamr and Amudan Basins

These basins, named after the Ghamr group [24] and Amudan formation [25] (Figure 5), contain coeval middle Cryogenian volcanosedimentary assemblages as much as 4000–6000 m thick. The basins unconformably overlie early Cryogenian arc sequences and are discontinuously exposed over an area of about 200 km × 120 km, adjacent to and south of the Bi'r Umq suture zone in the west-central Arabian Shield. The suture joins the Jiddah and Hijaz terranes and resulted from possible ~780–750 Ma southeast-directed convergence between the terranes and amalgamation [26], placing the Ghamr and Amudan rocks on the overriding plate. The suture zone continues southwest into the Nubian Shield as the Nakasib suture between the Haya and Gebeit terranes. The combined suture is nearly 600 km long, extending from the core of the Arabian Shield, at its eastern end, almost to the contact between the Nubian Shield and Saharan Metacraton along the Keraf suture in the west (Figure 1). Deposition of the Ghamr group and Amudan formation overlapped with and immediately followed suturing. The Jiddah terrane is a composite structure comprising a Tonian arc in the south (870–850 Ma), represented by deeply eroded plutonic rocks of the Makkah batholith and flanking amphibolite-grade volcanic strata, and early to middle Cryogenian arc rocks in the north, represented by the Arj, Mahd, and Samran groups and intrusive TTG suites (825–745 Ma) [27]. These rocks are shown in Figure 5 as "Arc rocks of the Jiddah terrane".

The Ghamr group rests on a basement composed of the Dhukhr complex, Arj group, and Mahd group (all shown in Figure 5 as "Arc rocks of the Jiddah terrane") and crops out in three areas separated by intervening basement rocks or Cenozoic alluvium. It is not known whether this distribution represents three original basins or is the effect of post-Ghamr structural and erosional segmentation of a single basin. The Ghamr group is moderately folded with dips varying between 20° and 80° and is metamorphosed in the greenschist facies. The Amudan formation crops out to the southwest. It overlies the Shayban formation (part of an arc assemblage assigned to the Samran group) and is more strongly deformed than the Ghamr group, with moderate to tight folding and extensive shearing, although only metamorphosed in the greenschist facies [25]. The formation is extensively intruded by younger plutonic rocks and only retains its depositional contact with older arc rocks along its northwestern margin, so that its original basin geometry is unknown.

Subvolcanic rhyolite from the Ghamr group yields a Rb-Sr whole-rock isochron age of 748 ± 22 Ma (n = 5; MSWD = 0.98) [28]. Dacite lava and two samples of andesite lava from the Amudan formation yield U-Pb zircon ion-probe concordia ages of 753 ± 6 Ma (MSWD = 0.95), 752 ± 4 Ma (MSWD = 0.016), and 746 ± 6 Ma (MSWD = 0.105), respectively [27]. The arc rocks of the Jiddah terrane that underlie the Ghamr group and Amudan formation are dated between 816 and 775 Ma [27,28]. The contact between the Ghamr group and basement is an angular unconformity, where it rests on eroded volcanic rocks, and nonconformity where it rests on plutonic rocks. The contact between the Amudan formation and underlying arc rocks is structurally conformable and in previous mapping [25] the Amudan was incorporated within the Samran group. However, radiometric dating indicates that the two are separated by a hiatus of about 15 million years [27].

Figure 5. Geologic map of the Ghamr group and Amudan formation and Furayh group (after [24,25]) showing their locations in basins unconformable on arc rocks of the Jiddah and Hijaz terranes, south and north of the Bi'r Umq suture, respectively. Inset schematically shows the tectonic settings of the basins in relationship to the Bi'r Umq and Afif suture zones. Arrows suggest sites of influx of coarse conglomeratic material.

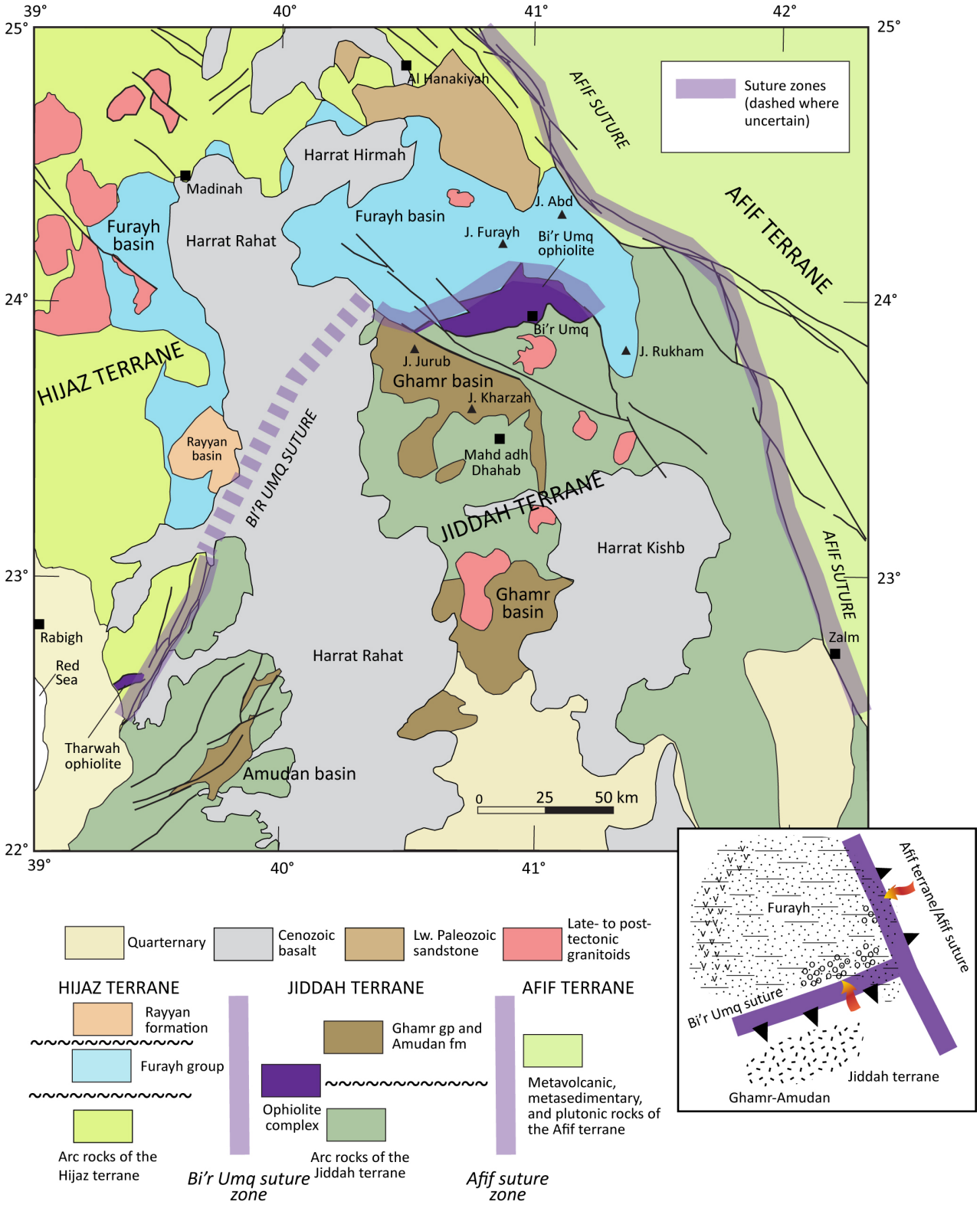

The Ghamr group has a pervasive reddish color and its stratigraphic units abruptly thicken, thin, and change facies along strike. These changes are interpreted as reflecting deposition on a paleosurface of high relief in a fault-controlled basin. The environment is believed to have been subaerial to near-shore marine [24]. The basin was unstable and the group contains internal unconformities so that its upper part oversteps the lower part and rests directly on the Mahd group. In its northern part, the Ghamr group is divided into two formations: the lower Kharzah (800–4000 m thick) and upper Gharmati (as much as 2000 m thick). The Kharzah formation (Figure 6) comprises reddish-gray felsic tuff coarsening upward to pebbly sandstone, and mauve-gray, rhyodacite ash-flow tuff over a thickness of about 300 m. This is followed, in varying amounts in different parts of the Ghamr basin, by polymict conglomerate containing clasts derived from the underlying volcanic and plutonic basement, matrix-supported pebble conglomerate and pebbly sandstone, epiclastic volcanic breccia, and a sequence of reddish-gray sandstone, overlain by siltstone and several tens of meters of basalt flows. Bedding is commonly poorly defined and sedimentary structures sparse, but cross lamination, mud cracks, ripple marks, and mud pebble conglomerates are locally observed indicating shallow water to subaerial conditions. Beds of gray to white limestone are locally present. The Gharmati formation (Figure 6) has a lower member composed of tuffaceous red to gray sandstone, siltstone, and mudstones overlain by an upper sandstone member with intervals of boulder conglomerate containing rhyolitic, basaltic, and plutonic clasts. Laminated calcareous sandstone and limestone crop out at the transition between the lower and upper members. The limestone is dark gray, fetid, and microbially laminated. In its southern areas, the Ghamr group contains a larger proportion of felsic volcanic rocks and is as much as 6000 m thick. Sedimentary rocks in the south include yellow and purple flaggy, laminated siltstone, wacke, and conglomerate containing boulders of sedimentary rocks, diorite, and granite. A rare carbonate is exposed in the south in one small lens of recrystallized calcarenite 30 m thick [29]. The Ghamr group was deposited during the Kaigas glacial event (~755 Ma) but whether the group contains reliable evidence of glaciation, such as diamictic glaciogenic conglomerate, has not been determined.

The Amudan formation (Figure 6) is estimated to be as much as 8000 m thick [25]. It contains a greater proportion of volcanic rocks than the Ghamr group. It is largely basaltic andesite to rhyolite flows and tuffs, interbedded at the base and in its upper part with polymict cobble-boulder conglomerate and breccia and well-bedded tuffaceous siltstone or chert, normally graded pebble conglomerate, laminated sandstone and siltstone. Conglomerate clasts are typically rounded and consist of granite, diorite, rhyolite, laminated ash tuff or siltstone and crystal tuff [27]. Welding and flow-banding are well preserved in the volcanic rocks and grading is present in the epiclastic rocks. The formation is interpreted to represent alluvial fans deposited on the flanks of an emergent volcanic edifice in a maturing arc or rift [27].

The Dhukhr plutonic complex in the basement beneath the Ghamr group is also nonconformably overlain by the Mahd group. The complex was therefore possibly exhumed and eroded at least twice in its history. The first time occurred between about 810 and 775 Ma, resulting in an erosion surface overlain by the Mahd group that in part may reflect erosion by local continental ~780 Ma glaciation [30,31], perhaps as an early part of the Kaigas event. The second episode of exhumation, which caused erosion of the Mahd group and further erosion of the Dhukhr complex, predated the Ghamr group. The depth of crystallization of the Dhukhr complex is not known, but it appears to be a typical mid-level intrusion, and exhumation was therefore probably on the order of 10 or more km. The

angular unconformity between the Ghamr and Mahd groups betokens deformation between ~775 Ma and 750 Ma followed by exhumation and erosion of the Mahd group. The occurrence of basement clasts in the Amudan conglomerate indicate a partial change in depositional environment from submarine to largely subaerial during the 15 million-year hiatus between the underlying Shayban formation and Amudan formation.

Figure 6. Representative stratigraphic columns for the Ghamr group and Amudan formation. Ghamr column after [24]; Amudan column after [25,27]. The thickness of neither column has been accurately measured. Arrows indicate the results of age dating although the exact stratigraphic positions of the dated samples are unknown; they are arbitrarily plotted here for descriptive purposes only.

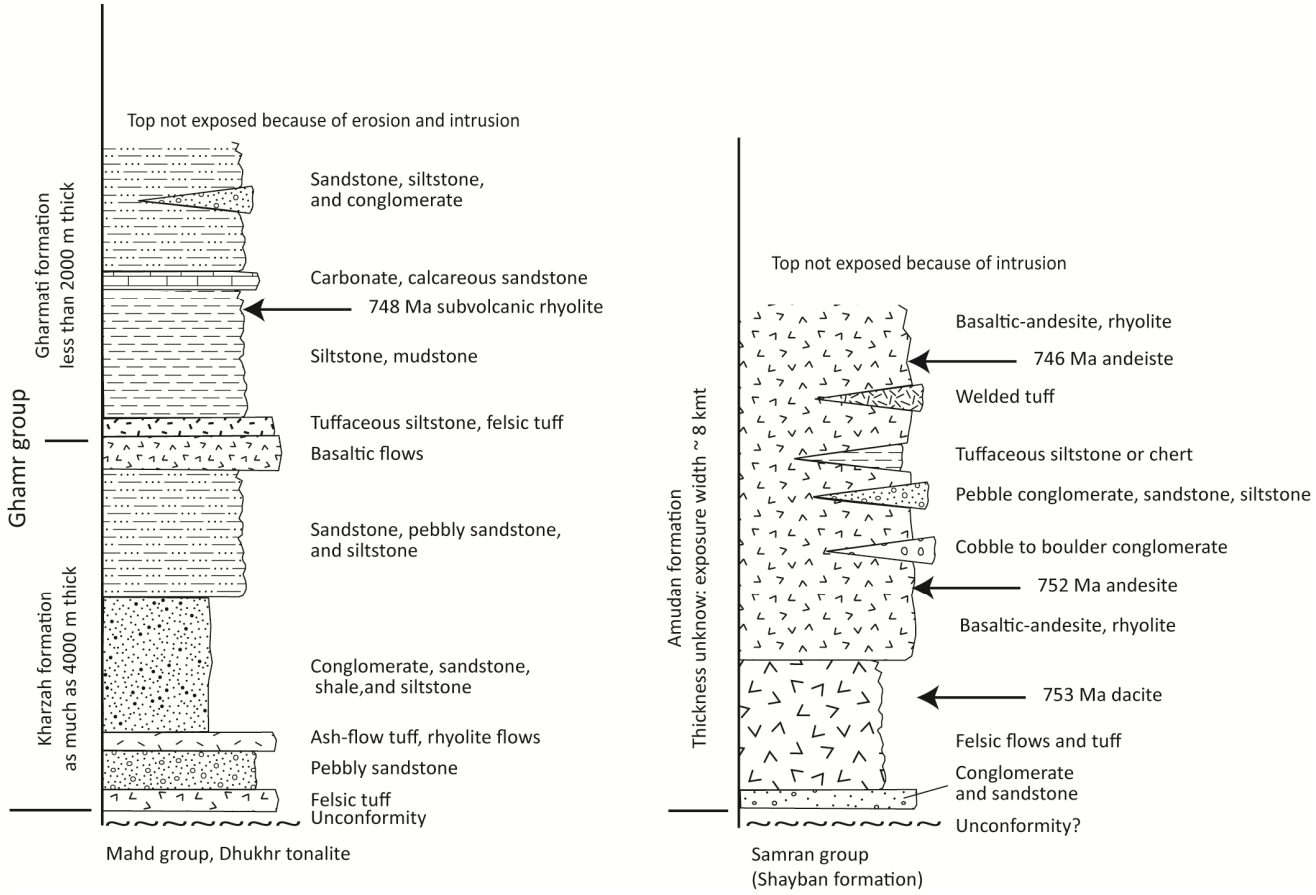

This pre-Ghamr/Amudan period of exhumation, uplift, and erosion overlapped deformation, metamorphism, and two periods of syntectonic intrusive activity along the Bi'r Umq suture. The syntectonic intrusions consist of tonalitic orthogneiss emplaced about 782 ± 7 Ma and 751 ± 5 Ma (U-Pb ion-probe dating) [27]. The gneisses intrude the Samran group with sharp to lit-par-lit transitional contacts. The syntectonic character of tonalite emplacement is evidenced by an increase in metamorphic grade to amphibolite facies in the Samran group toward the gneisses, the development of mylonite, and the presence of syntectonic hornblende aggregates, kinematic markers including sigmoidal tails on felsic porphyroclasts and S-C fabrics, and parallelism of foliation in gneiss and Samran group rocks.

The gneiss is regarded as the most reliable indication of the timing of deformation and amphibolite metamorphism along the Bi'r Umq suture, and by implication of the timing of suturing between the Jiddah and Hijaz terranes sometime between 780 and 750 Ma [27]. The syntectonic intrusions were emplaced during active dextral shear on the suture zone and were deformed while at or very close to solidus temperature in a zone affected by high heat flux [27]. The Bi'r Umq ophiolite at the northeastern end of the Bi'r Umq suture was probably emplaced during the early part of this suturing episode. The ophiolite has a crystallization age of ~838 Ma, but plagiogranite intrusions in peridotite yield single-point zircon U-Pb ages between 782 and 764 Ma [32]. Because the plagiogranite intruded already serpentinized and carbonated peridotite, it is believed to post date ophiolite obduction [32], suggesting that the ophiolite was in place by 780 Ma.

The placement of the Ghamr-Amudan basins close to and inboard into the Jiddah terrane from the Bi'r Umq suture (Figure 5) on what may have been the upper overriding plate of a convergent margin, suggests that they are a type of retroforeland basin. We envisage that suturing resulted in exhumation and uplift of rocks in the Jiddah terrane in the hanging wall of the suture zone, followed by development of a regional erosion surface. Alluvial channels or fault-scarp fronts shed supracrustal and plutonic clasts into fault-controlled basins and the concomitant growth of volcanic edifices gave rise to lava flows, pyroclastic deposits, and volcaniclastic sediments. Local intra-Ghamr unconformities demonstrate basin instability and Ghamr group limestone implies local lacustrine environments or ephemeral marine connections.

5. Hadiyah Group Basins

The Hadiyah group basins (Figure 7), named after the Hadiyah group [33,34], overlie arc rocks assigned to the Al Ays group (735–705 Ma) on the northwestern flank of the Hijaz terrane. The basins parallel the ophiolite-decorated Yanbu suture at the northwestern margin of the terrane, some 25–50 km inboard of the suture. Convergence and suturing along the Yanbu suture, which joins the Hijaz and Midyan terranes and continues into the Nubian Shield as the Sol Hamid-Allaqi suture (Figure 1), was completed by about 700 Ma. Ophiolites along the suture, originating about 780 Ma [32], were in place by about 705 Ma, a time constrained by a U-Pb conventional zircon age of 706 ± 11 Ma obtained from trondhjemite that intrudes already serpentinized and sheared gabbro. The suture is cut by ~695 Ma trondhjemite and tonalite of the Jar-Salajah batholith [32]. The Al Ays group is an assemblage of volcanic and sedimentary rocks forming a middle Cryogenian arc that extends as much as 250 km across strike, east of the Yanbu suture and well east of the area shown in Figure 7. Volcanic rocks representing the magmatic axis of the arc are concentrated more than 100 km east of the suture. The Hadiyah group basins overlie mostly Al Ays group sedimentary rocks located in part of the arc between the arc trench, represented by the suture zone, and the magmatic axis. The sedimentary rocks possibly represent a fore-arc accretionary prism.

Figure 7. Geologic setting of the Hadiyah group showing its location in three basins unconformable on arc rocks of the Hijaz terrane and 25–50 km inboard into the Hijaz terrane from the Yanbu suture (after [33,34]). Inset schematically shows the inferred tectonic setting of the basin.

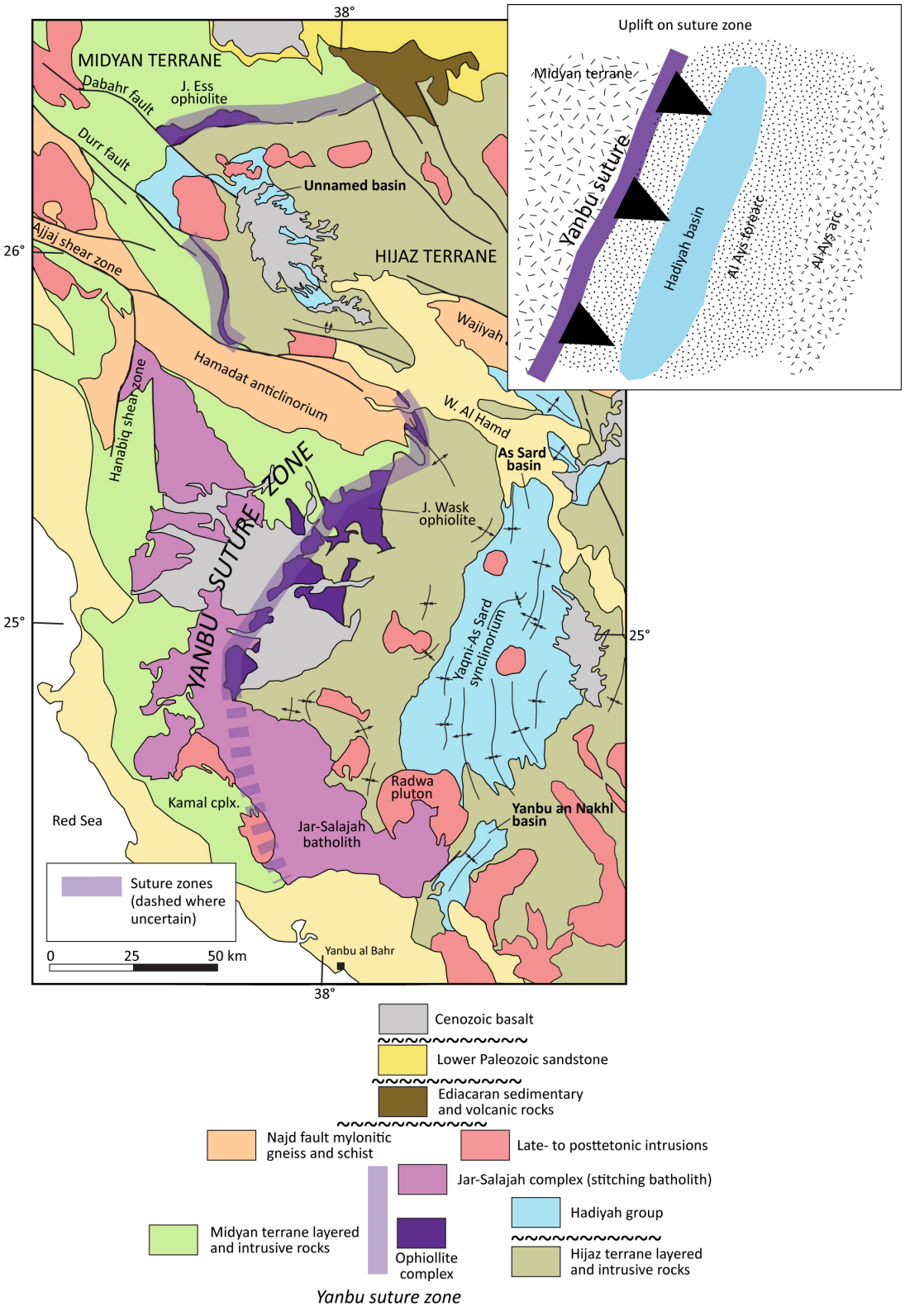

The Hadiyah group basins are three elongate structures exposed over a strike distance of about 300 km (Figure 7). They are individually about 30 to 125 km long and as much as 50 km wide. The largest As

Sard basin is extensively folded as the Yaqni-As Sard synclinorium. The Yanbu an Nakhl basin is a small basin to the south. An unnamed basin to the northwest is largely covered by Cenozoic basalt. It is reasonable to consider that the basins were originally continuous, forming a relatively narrow depositional trough on the northwestern flank of the Hijaz terrane, parallel to the Yanbu suture. Northwest-trending sinistral strike-slip Najd faults associated with en-echelon belts of orthogneiss and paragneiss are part of a shear system extending across the entire Arabian Shield and into the Nubian shield belonging to the largest pre-Mesozoic shear zone on Earth [35]. They deform the Al Ays and Hadiyah groups, and offset the Yanbu suture. Folds in the As Sard and Yanbu an Nakhl basins trend north-south to northeast-southwest. Farther north, the folds veer to the northwest, a result of rotation by sinistral shear along the Najd faults. Folds are mostly upright and open, with wavelengths of several kilometers, subhorizontal plunges and moderately to steeply dipping limbs (Figure 8A,C). Axial-planar cleavage is well developed and, on steep limbs, is parallel to bedding (Figure 8B). Despite deformation however, the Hadiyah group is only slightly metamorphosed and the rocks have assemblages of prehnite, chlorite, clinozoisite and epidote [34]. Folds in the Hadiyah group extend into the Al Ays group (Figure 7) suggesting that the two groups were folded by the same deformation event. Because folds in the Al Ays group are cut by the 695 Ma stitching batholith of the Jar-Salajah complex, it is inferred that the Hadiyah group was also deformed prior to 695 Ma.

Rhyolite from the Siqam formation in the lower part of the Hadiyah group yields an ion-probe U-Pb zircon crystallization age of 697 ± 5 Ma [36]. Zircon grains of 872 ± 23 Ma, 1051 ± 17 Ma, 1089 ± 17 Ma, and 1845 ± 29 Ma indicate inheritance in the rhyolite of material from early Cryogenian, Mesoproterozoic, and Paleoproterozoic sources. The underlying Al Ays group has U-Pb ion-probe ages of 708 ± 4 Ma, 711 ± 10 Ma, and 736 ± 5 Ma [36,37]. The contact between the Hadiyah and Al Ays groups is conventionally described as an unconformity [34] but the nature of the unconformity is debated [38]. In any given exposure, the Hadiyah group appears to be structurally conformable with the Al Ays group and in places the Hadiyah group also appears to be interlayered with the Al Ays group [39]. Nevertheless, some workers argued that the Hadiyah rests on an erosional surface that in places truncates as much as 4000 m of Al Ays group rocks [34]. Undoubtedly, the contact between the Hadiyah and Al Ays groups represents a significant change in depositional environment; we note that the basal contact of the Hadiyah is locally marked by regolith formed by weathering of Al Ays group rocks, hence indicating a period of uplift and erosion between depositions of the two groups. Overall, the geochronology suggests that the Hadiyah group was deposited contemporaneously with or immediately after suturing on the Yanbu suture, and together with the Al Ays group, was folded at about 695 Ma. It was evidently deposited close to an active margin during convergence between the Hijaz and Midyan terranes and was affected by ongoing deformation and intrusion. Similar to the Ghamr group and Amudan formation in the Jiddah terrane, the Hadiyah group was likely located on an overriding plate and is probably a type of retroforeland basin.

The Hadiyah group, divided into three formations, is as much as 7000 m thick (Figure 9). The Siqam formation (~2000 m thick), at the base of the group, is mostly volcanic; the upper formations are entirely sedimentary. The Siqam formation comprises a bimodal assemblage of locally pillowed basaltic to andesitic lava, basaltic and andesitic breccia, and rhyolitic ash-flow tuff. The Tura'ah formation (~3400 m thick) comprises two members differentiated by a lithologic and color change at ~1800 m. The lower Jammazin member mostly contains thin-bedded light green to dark green

sandstone or wacke, interbedded with cross-bedded sandstone and diamictite comprising matrix-supported pebble to boulder sized quartz keratophyre clasts. Limestone occurs at or near the base in several localities and includes several meters of microbial laminite. The upper Qaraqah member is a conspicuous red-bed facies composed of thin-bedded, medium-grained sandstone to mudstone. Abundant ripple marks, cross bedding, current scours, and mud cracks indicate a shallow-water environment. Polymict conglomerate and conglomeratic sandstone with small, well-rounded pebbles are present at the base of the member and as interbeds in the sandstone, siltstone, and mudstone higher in the member.

Figure 8. Features of the Hadiyah group, As Sard basin. (**A**) General view of steeply dipping well-bedded Tura'ah formation sandstone and siltstone; (**B**) Close up of fine-grained sandstone (to left) and siltstone (to right) showing prominent bedding-parallel cleavage in the siltstone; (**C**) Well-bedded sandstone and siltstone in the Qaraqah member of the Tura'ah formation, showing its characteristic purple-red color; (**D**) Aghrad formation clast-supported polymict pebble-cobble conglomerate with well-rounded clasts, which in this exposure include abundant granite and lesser amounts of feldspar porphyry, purple chert, siltstone, and dark green rhyolite.

A

B

C

D

Figure 9. Stratigraphic column of the Hadiyah group. Siqam formation thickness estimated; Tura'ah and Aghrad formations measured. Simplified after [34]. Arrow shows approximate stratigraphic position of dated sample.

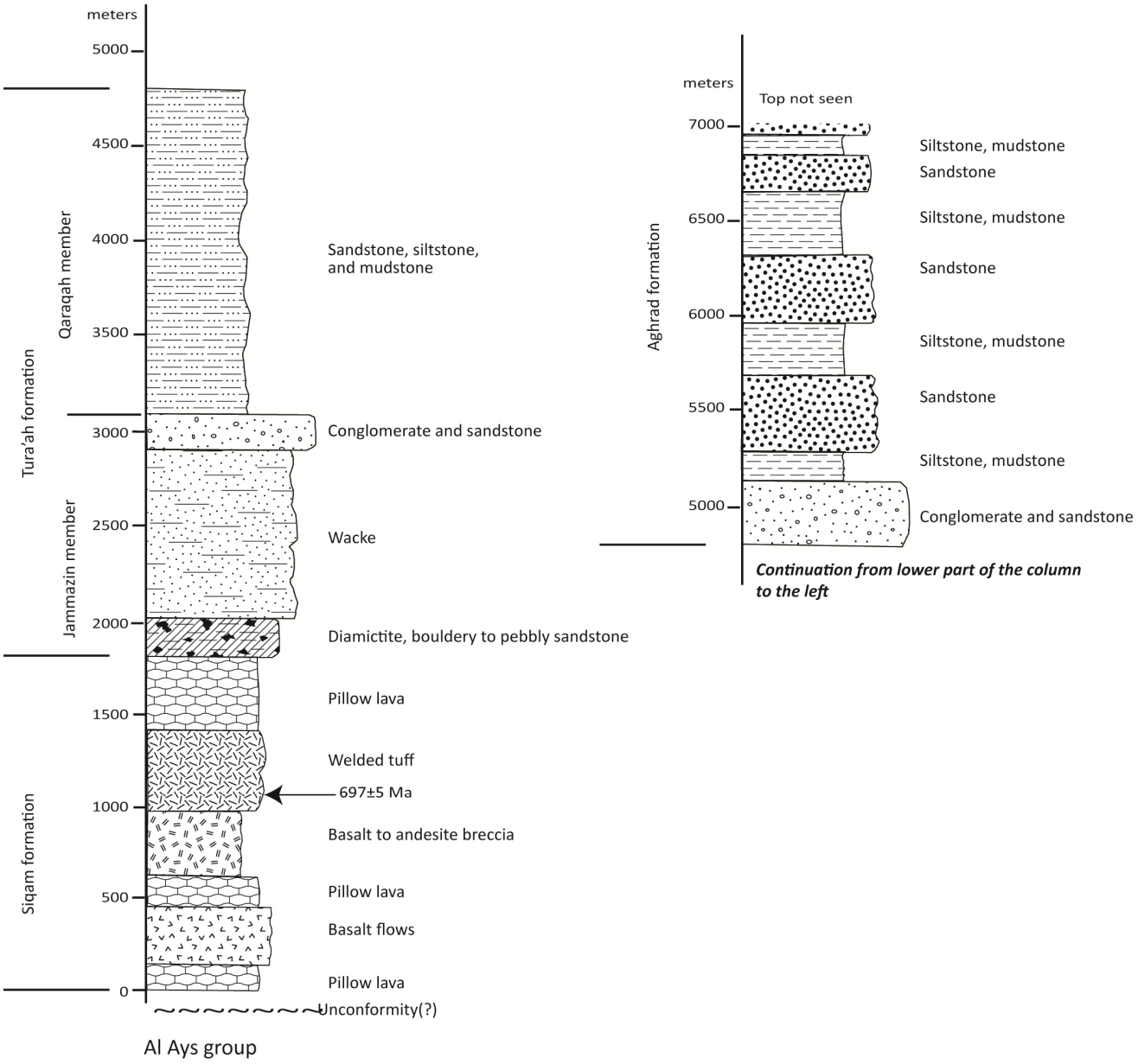

The upper Aghrad formation, estimated at 1000–2000 m thick, begins with 100–150 m of pebble to cobble conglomerate with clasts up to 20 cm in diameter. The clasts are well rounded and include felsic and basalt to andesite volcanic rocks, granite, feldspar porphyry, chert, and siltstone (Figure 8D). Above are 450 m of broadly upward-thinning and fining, red-gray to red shallow-water siliciclastics grading from thick beds of sandstone to thin-bedded siltstone and mudstone. The upper part of the formation comprises gray to red-gray, poorly bedded, planar cross-bedded sandstone with a few thin pebbly to conglomeratic beds and rare carbonate beds. Mineralogically, the Tura'ah and Aghrad formation sandstones are similar. They tend to be immature and contain abundant volcanic (rhyolitic, granophyric, and lesser basaltic) rock fragments, quartz, feldspar, chlorite, epidote and abundant

opaque minerals. The Aghrad formation rocks probably represent an upward continuation of the shallow-water environment of the upper part of the Tura'ah formation.

The Hadiyah group was earlier identified as molasse, peripheral to uprising gneiss domes along the Najd faults [40]. However, because Najd faulting in the Arabian-Nubian Shield is <~630 Ma, such a genetic relationship is unlikely. Alternatively, the elongate geometry of the Hadiyah basins, their parallelism to the Yanbu suture, and their putative retroforeland setting suggest that the Hadiyah group was deposited in response to ongoing deformation and uplift along the Yanbu suture. The character of volcanic clasts in sandstone and conglomerate and rare granitoid clasts is consistent with sources from the underlying Al Ays group and arc-associated intrusions. The putative 4-km depth of erosion into the Al Ays group implies considerable exhumation, uplift, and erosion prior to Hadiyah group deposition, although this is controversial as noted above. Pillow basalt in the Siqam formation and turbidites in the lower member of the Tura'ah formation indicate submerged conditions in the Hadiyah basins during its early history, and the bimodality of volcanic rocks in the Siqam formation is consistent with an episode of extension inboard of the Yanbu suture. The abrupt change to red-bed facies with mud cracks and current scours in the Qaraqah member suggests a rapid shallowing of the basin as deposition continued. The thick conglomerate at the base of the Aghrad formation is evidence of an abrupt influx of coarse detritus into the basin and may reflect a particular episode of uplift and erosion of the basin margins. Carbonate is nowhere significant in the Hadiyah group, and the thin unit of microbial carbonate at the base of the Tura'ah formation could be a lake deposit. We note that the Hadiyah group was deposited during the Sturtian glacial event (~717–680 Ma) [41,42]. Glaciation could have served both as a source of clasts in matrix-supported conglomeratic beds and as a mechanism to enhance deep incision into the Al Ays group, although such a scenario is currently speculative.

6. Furayh Group Basin

The Furayh basin, named after the Furayh group [43], crops out in the west-central part of the Arabian Shield where it unconformably overlies the southern Hijaz terrane and oversteps parts of the Bi'r Umq and Afif sutures (Figure 5). The basin is mostly north of the Bi'r Umq suture and west of the Afif suture, and evidently developed following suturing between the Hijaz and Jiddah terranes and the beginning of the docking between the Afif terrane and the Jiddah and Hijaz terranes. A depositional contact is reported [43] between the Furayh group and mafic-ultramafic rocks in the Bi'r Umq ophiolite along the suture zone, although mylonite at the contact suggests local faulting [44] with thrusting of the ophiolite over the Furayh. In the southeast, the Furayh group transgresses the suture zone, and rests unconformably on arc rocks in the Jiddah terrane over a short distance south of the suture. Along its northeastern margin, the basin oversteps the Afif suture and is in depositional contact with the rocks in the Afif terrane. Along its northern and western margins, the basin appears to have an unconformable contact with the underlying arc rocks of the Hijaz terrane. However, this contact is not well exposed and, east of Al Madinah, the Furayh group appears to be structurally conformable, and lithologically gradational, with the underlying Al Ays group [44]. The basin is partly concealed by Cenozoic basalt of Harrat Rahat, but assuming continuity of the Furayh group beneath the harrats, has an overall size of about 200 km east-west and 150 km north-south. Rhyodacitic tuffs and flows yield

Rb-Sr whole-rock isochrons of 633 ± 15 Ma and 663 ± 44 Ma, respectively [45]. These results are imprecise but indicate an approximate late Cryogenian age, consistent with the wider geologic relationships of the Furayh basin.

The Furayh group comprises mafic to felsic flows and tuffs, sandstone, siltstone, conglomerate, and subordinate carbonate. The rocks are deformed into broadly north-trending folds, displaced by northwest-trending faults of the Najd fault system, and metamorphosed to greenschist facies. Volcanic rocks dominate west of Harrat Rahat; sedimentary rocks are more abundant in the east. Lithologic units thicken and thin across the basin. The stratigraphic columns shown in Figure 10 are generalizations based on published descriptions of the group. East of Harrat Rahat, the group is divided into three formations. These comprise the mainly sedimentary Naslah and Shaqran formations at the base and top, respectively, and the intermediate volcanic Ghuwayt formation. West of Harrat Rahat the Naslah and Shaqran formations are absent, and the group is represented by a thick sequence of volcanic and subordinate sedimentary rocks of the Ghuwayt formation.

The Ghuwayt formation west of Harrat Rahat overlies arc rocks of the Birak and Al Ays groups, and arc-associated plutonic rocks. The immediate contact is marked by a unit of volcanic-rich conglomerate, sandstone, and tuff up to 400 m thick (Figure 10). This is followed by a low-K calc-alkaline assemblage of basalt and andesite several thousand meters thick [46]. Amygdaloidal, locally pillowed, lavas are prominent and intercalated with lesser amounts of andesitic and basaltic volcanic breccia, basaltic lapilli and water-lain tuffs. Rhyolite and rhyodacite flows and tuffs and dacitic lapilli tuff dominate the upper part of the formation. Sedimentary units intercalated with volcanic rocks west of Harrat Rahat include polymict boulder conglomerate, coarse-grained sandstone, arkose, wacke, siltstone, and mudstone. Conglomerate clasts are sub-rounded and poorly sorted. They are commonly volcanic, possibly derived in part from volcanic units in the Furayh group itself as well as the underlying arc rocks; diorite clasts were sourced most likely from plutonic rocks in the basement. Sandstone is green or purple, well bedded, and medium grained with ripple marks and well-developed graded bedding.

East of Harrat Rahat, the Naslah formation contains abundant polymict conglomerate, dark-green sandstone and wacke, massive to poorly bedded green and purple shale and siltstone, and minor carbonate. Conglomerate is prominent immediately north of the Bi'r Umq suture where the formation is about 2000 m thick (Figure 10) and west of the Afif terrane. Conglomerate has cobbles and boulders of rhyolite, marble, red jasper, amygdaloidal andesite-basalt, pink granophyre, and rare magnesite. Along the northeastern margin of the Furayh basin, in the vicinity of Jabal Abd (Figure 5), the Naslah formation oversteps the Afif suture and unconformably overlies volcanic and intrusive arc-related rocks of the Afif terrane, along with ultramafic rocks entrained along the Afif suture. Here the basal conglomerate contains cobbles and boulders as much as 80 cm in size of greenstone, talc-chlorite-actinolite rocks, red rhyolite, ignimbrite, fine- to coarse-grained granite with biotite and(or) amphibole, diabase, siltstone, meta (biotite-bearing) rhyolite, and white quartz. Carbonate units in the Naslah formation crop out over a strike distance of 7 km. They comprise beds of gray to light pink dolomitic marble with lenses of white magnesite and beds of carbonate conglomerate composed of angular to rounded cobbles of gray and red marble and magnesite. Similar rocks crop out at Jabal Rukham (Figure 5) in the tongue of Furayh group in the southeastern part of the Furayh basin, where the Furayh group oversteps the Bi'r Umq suture and rests on Mahd group arc rocks of the Jiddah

terrane. The Ghuwayt formation east of Harrat Rahat is 2000 m thick, thinner than west of the harrat, but as in the west, it contains locally pillowed basaltic and andesitic flows, tuffs, and breccia, interbedded with subordinate green to purple shale, siltstone, and sandstone. The upper Shaqran formation contains green to purple ripple-marked lithic sandstone and wacke, polymict conglomerate, shale, siltstone, carbonate, and rhyolite. The Shaqran formation carbonate consists of gray calcdolomitic marble with domal and tabular stromatolite bioherms in beds 10–20 m thick. Conglomerate has cobbles and pebbles of purple porphyry, pink granophyre, green siltstone, red, beige, and black chert, porphyritic andesite, rhyolite, and white quartz.

The Furayh basin west of Harrat Rahat is interpreted as a high-energy, shallow-water to subaerial environment characterized by rapid emergence and erosion of an active volcanic domain resulting in deposition of poorly sorted, immature material in proximal basins [45]. Ripple marks, microslumping, and cross-bedding are evidence of shallow-water deposition. Mud-cracks, mud-chip intraformational conglomerate, and local unconformities indicate periodic emergence. Color variations from green to purple are consistent with alternating submerged and emerged conditions.

East of Harrat Rahat, the abundance and thickness of conglomerate along the southern and northeastern margins of the basin adjacent to the Bi'r Umq and Afif suture zones suggests proximity to elevated source regions. Depositional contacts between the Furayh group and Bi'r Umq ophiolite and Mahd group bear witness to exhumation and erosion of the arc rocks of the Jiddah terrane and the Bi'r Umq suture between the Jiddah and Hijaz terranes prior to and during Furayh deposition. Depositional contacts between the Furayh group and arc and ultramafic rocks in the Afif terrane and the increase in conglomerate toward the Afif suture suggest that the Hijaz terrane was in place adjacent to the Afif terrane at the time of Furayh deposition and that the Afif terrane had undergone exhumation, uplift, and erosion. The Jiddah and Hijaz terranes were in contact by 750 Ma; the Afif terrane amalgamated with the Jiddah and Hijaz terranes during the Nabitah orogeny or mobile belt (680–640 Ma) [47], an episode of deformation and syntectonic intrusion widely recognized in a north–south zone the central Arabian Shield (Figure 1). As described above, the early Cryogenian Ghamr and Amudan basins reflect volcanism and sedimentation coincident with development of the Bi'r Umq suture zone; the Furayh group reflects volcanism and sedimentation some 100 million years later in an actively evolving depocenter at the triple junction between the Jiddah, Hijaz, and Afif terranes. The type of basin represented by the Furayh group is uncertain. Perhaps it reflects tectonic loading at the Jiddah-Hijaz-Afif triple junction associated with some extension in the west accounting for the bimodal character of the volcanic Ghuwayt formation.

Figure 10. Representative stratigraphic columns for the Furayh group in the Furayh basin. Column west of Harrat Rahat after [45]; column east of Harrat Rahat after [43]. Arrows show approximate stratigraphic positions of dated samples.

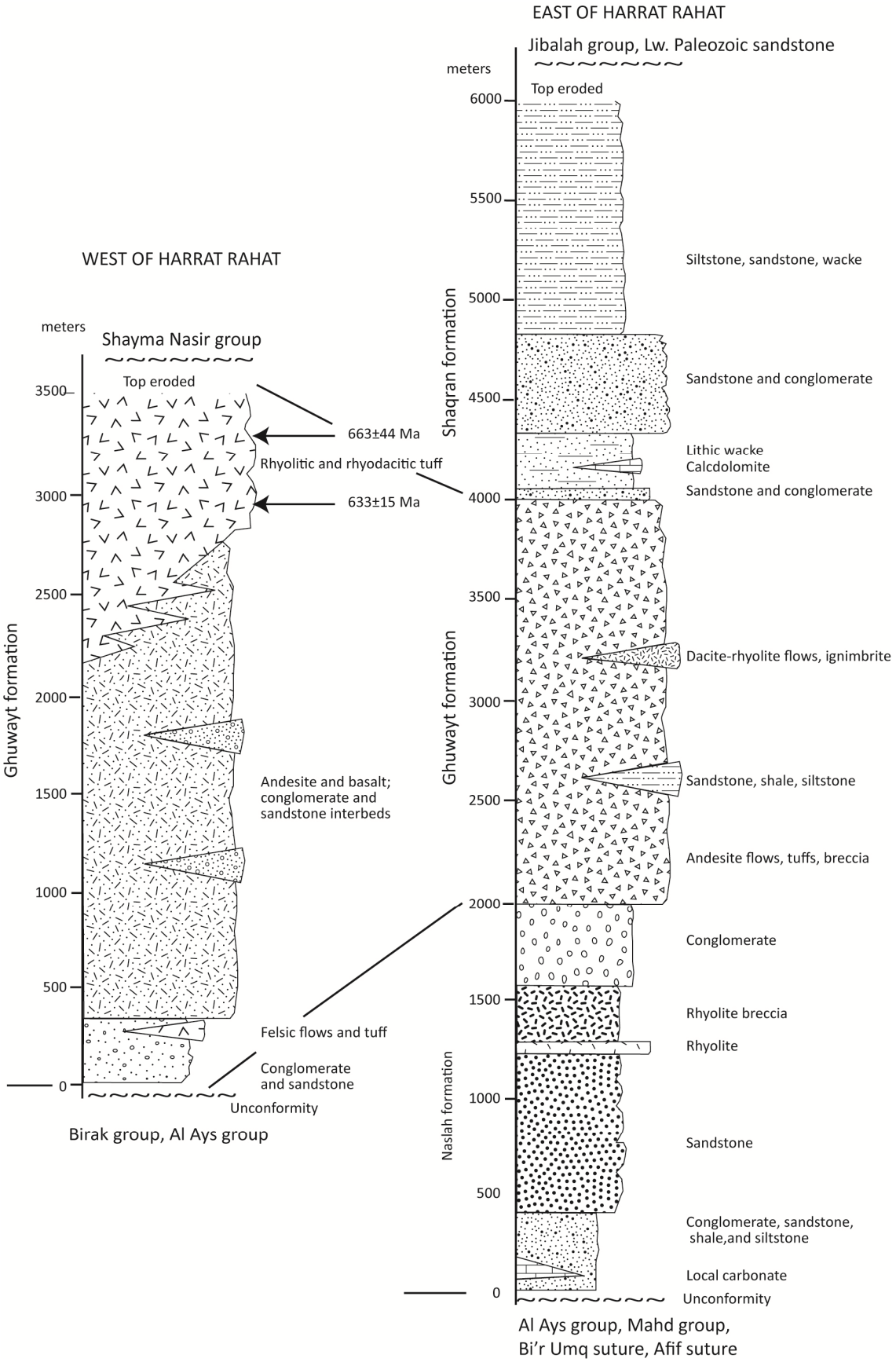

7. Murdama Basin

The Murdama basin, the largest volcanosedimentary basin in the ANS, is filled by a thick succession of late Cryogenian–early Ediacaran sedimentary and volcanic rocks deposited unconformably on middle Cryogenian arc rocks of the Afif composite terrane (Figure 11). It is exposed over an area about 570 km NW-SE and 120 km wide SW-NE and is shown by aeromagnetic data to extend a further 200 km southeast beneath Phanerozoic sediments beyond the edge of the exposed Arabian Shield [48]. The Afif terrane is a collage of pre-Murdama Cryogenian arcs and a fragment of Paleoproterozoic crust (the Khida terrane) that was assembled by or soon after 685 Ma. The basin overlies the inferred joins within the terrane between rocks of the Nuqrah arc (~840 Ma), the Siham arc (750–685 Ma) and the Suwaj arc (695–685 Ma) (Figure 12) and is the type "post-amalgamation basin" in the Arabian Shield. Assembly of the Afif terrane was concurrent with suturing of the Afif terrane with other terranes to the west (Afif suture) during the Nabitah orogeny (680–640 Ma). The Afif terrane is bounded to the east by the Ad Dawadimi terrane, with the two separated by the Halaban suture and the eponymous 695–675 Ma Halaban ophiolite. As evidenced by deepwater sedimentation in the Ad Dawadimi terrane until after ~620 Ma, and metamorphism and deformation of some of the sedimentary rocks at ~620 Ma, the margin was active into the Ediacaran [7]. Soon after its assembly, the Afif terrane was exhumed, uplifted, and eroded, allowing development of the regional unconformity beneath the Murdama basin. The terranes together with the Murdama basin were stitched by granites between about 650 and 565 Ma, and the entire region was subsequently affected by transcurrent strike-slip faults of the Najd fault system (~630–530 Ma), which disrupted the terranes and reworked some of the suture zones (see [11] for further details of tectonic events in the ANS in this time period).

The Murdama basin is named after the Murdama group, a thick succession of sandstone, siltstone, conglomerate, subordinate carbonate, and minor volcanic rocks. The basin rocks also include the volcanic Afif formation, conformably beneath the Murdama group on the west, and the volcanic Hibshi formation, separating the Murdama group from the Ha'il terrane on the north (Figure 11). Superposition of younger volcanic rocks (the Jurdhawiyah group; 612 ± 12 Ma; [36]), intrusions of granite, and disruption by faulting interrupt continuity of exposure and divide the Murdama basin into the Maraghan and Maslum sub-basins (Figure 11). Volcanic and sedimentary rocks lithologically similar to and broadly coeval with the Murdama group crop out west and south of the Murdama basin, where they are known as the Bani Ghayy group [49]. Some authors (e.g., [50]) regard the Murdama and Bani Ghayy groups as the same lithostratigraphic unit, merely deposited in different environments: a large basin in the case of the Murdama group and in narrow fault-controlled basins in the case of the Bani Ghayy.

The thickness of the Murdama group is not known, but individual measured sections are as much as 8000–10,000 m thick [50,51]. The group is moderately to strongly folded [9], and along its southern margin, in the vicinity of the Ar Rika fault, has been affected by brittle-ductile shearing and amphibolite-grade metamorphism with the result that conglomerate clasts have been stretched from their original equant shape into prolate spheroids up to 2 m long and 40 cm wide [52]. The long axes of the stretched clasts align with mineral lineations and mesoscale fold axes along the shear zone. Most rocks in the Murdama basin are otherwise only weakly metamorphosed in the greenschist facies.

Figure 11. Simplified map of post-amalgamation basins in the northeastern Arabian Shield (after [9]). The largest basin, filled by the Murdama group, is located toward the eastern margin of the Afif composite terrane overlying the Khida subterrane, and Nuqrah, Siham, and Suwaj arcs. The Jurdhawiyah group occupies basins unconformable on the Murdama group.

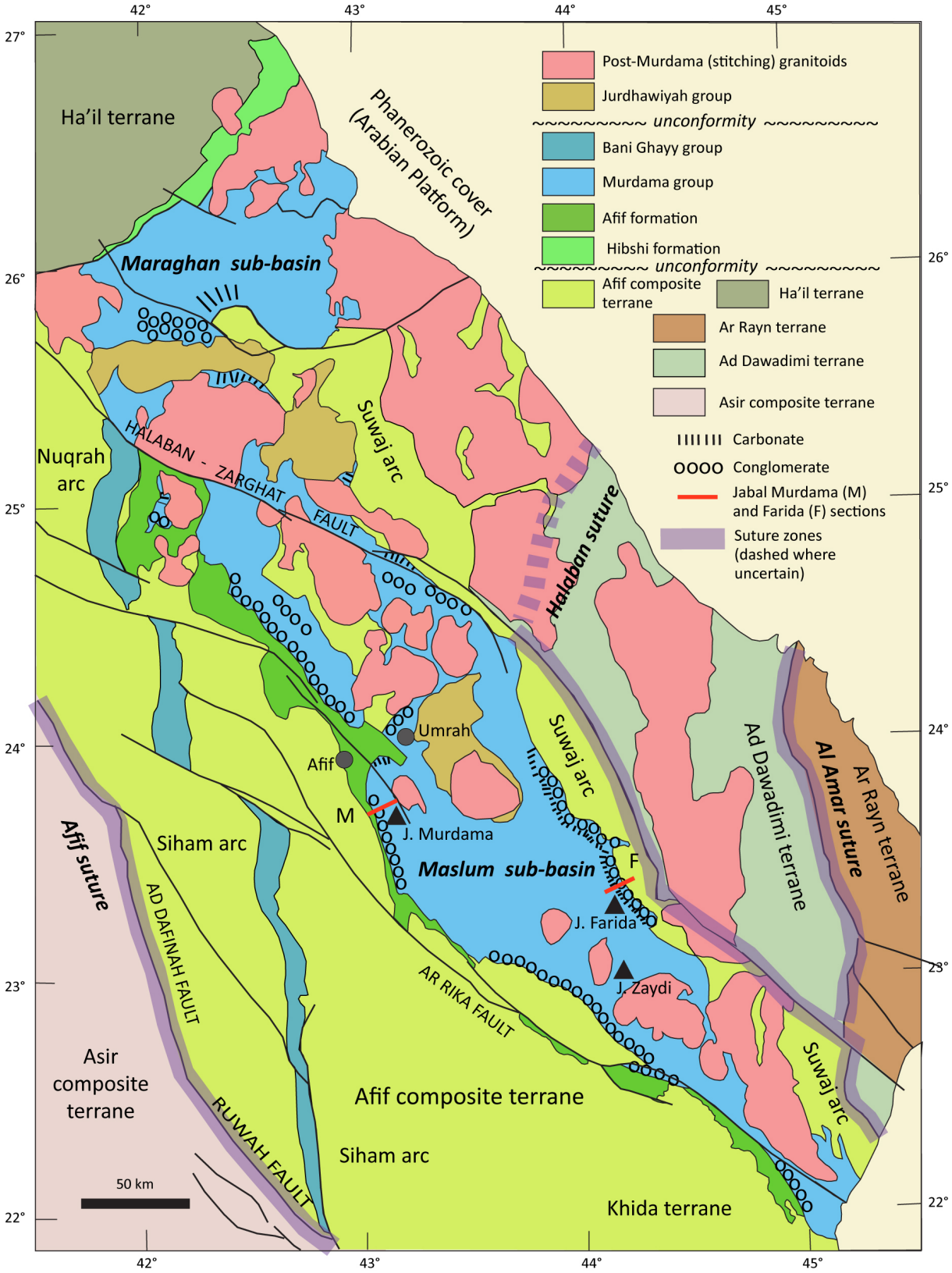

Figure 12. Schematic diagram showing the post-amalgamation setting of the Murdama basin composed of the Murdama group and volcanic units (Afif formation, Hibshi formation) unconformably overlying the Afif composite terrane. Following Murdama deposition, the Murdama basin was unconformably overlain by the Jurdhawiyah group and the entire region was intruded by 650–565 Ma stitching granites and disrupted by Najd faulting.

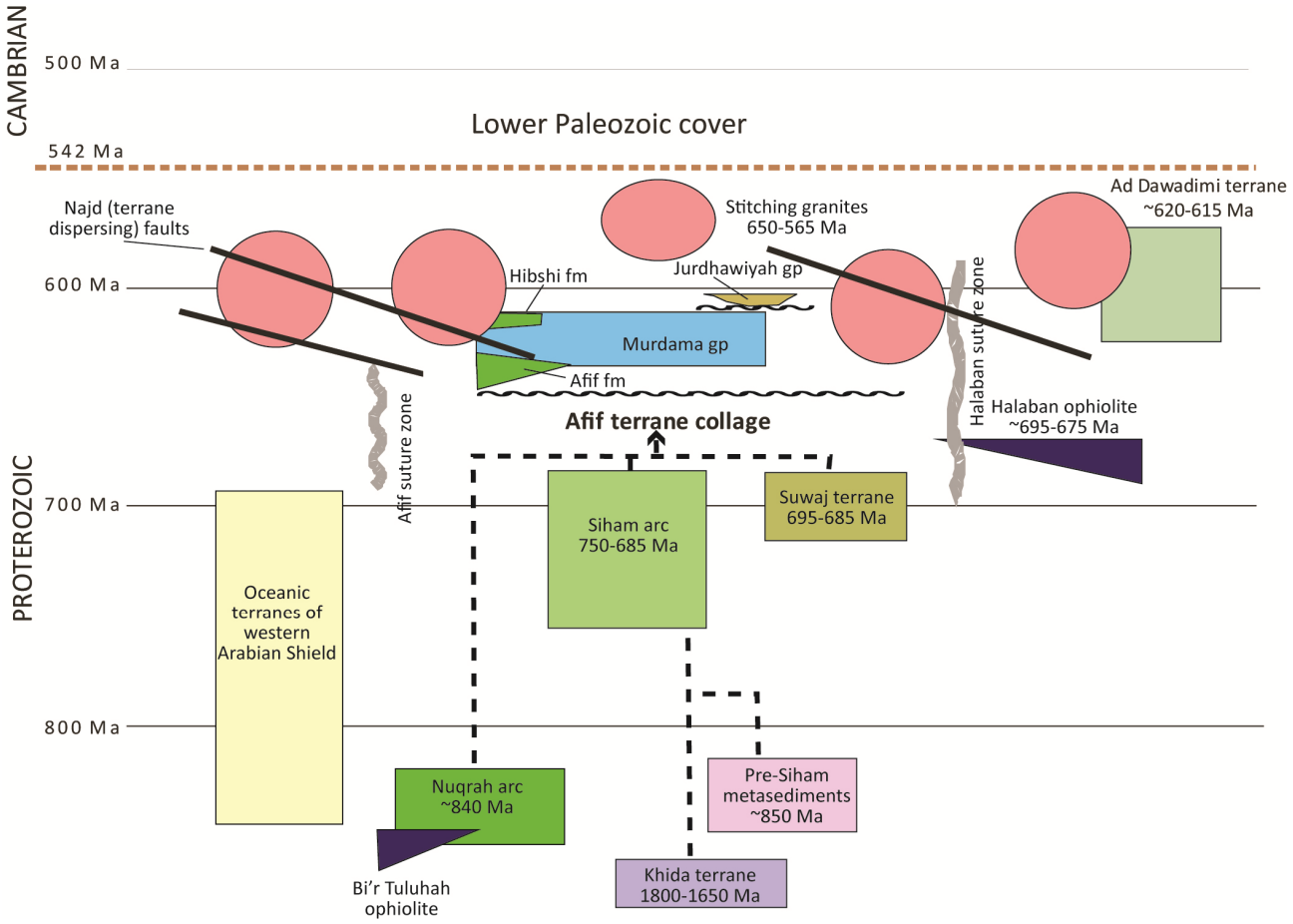

Rhyolitic crystal tuff of the Afif formation yields U-Pb SIMS zircon ages of 649 ± 6 and 639 ± 4 Ma [53], and rhyolitic tuff in the Murdama group yields U-Pb SIMS zircon ages of 630 ± 5 Ma, 629 ± 7 Ma, and 624 ± 6 Ma [53]. The Hibshi formation has a conventional U-Pb zircon concordia age of 632 ± 5 Ma [54]. It is evident from these dates that Murdama basin deposition occurred during and immediately after the Nabitah orogeny (680–640 Ma) and during docking between the Afif and Ad Dawadimi terranes. Murdama basin deposition also spanned the Marinoan glaciation (~645–635 Ma), although neither glacial deposits nor cap carbonates have been reported.

The basement west of the Murdama basin comprises greenschist- and amphibolite-grade metavolcanic, metasedimentary, and plutonic rocks belonging variously to the Khida terrane and Nuqrah and Siham arcs (Figure 12). The rocks include amphibole gneiss, leucocratic gneiss, chlorite-sericite-biotite schist and calc-silicate (diopside, scapolite, and andradite garnet) schist and gneiss [55]. The metamorphic grade of these rocks implies a significant amount of exhumation and erosion prior to Murdama basin deposition. The youngest basement rocks belong to the Siham arc (750–685 Ma) [3]. Along its northeastern margin, the Murdama basin overlies plutonic and volcanic

rocks of the Suwaj arc (~695–685 Ma) [3]. These rocks are metamorphosed in the greenschist and amphibolite facies, and are commonly cataclasized, foliated, and schistose [51,56]. The Suwaj arc is mainly represented by exposures of gabbro, diorite, quartz diorite, trondhjemite, granodiorite, and biotite-amphibolite granite, a predominance of rock types that denotes exposure of the magmatic core of the arc and implies major exhumation and erosion of the basement prior to Murdama deposition. Remnant metamorphic supracrustal layered rocks of the Suwaj arc include meta-andesite, meta-dacite, and metasedimentary schists containing mixtures of chlorite, sericite, muscovite, biotite, hornblende, epidote, diopside, minor scapolite, and locally wollastonite and tourmaline. They also include mica-rich and quartzofeldspathic schist, rare calcareous beds, amphibolite, and fine- to medium-grained, banded, and equigranular mafic granulite. The mafic granulite crops out as roof pendants in post-Murdama granite intrusions. It has a bulk composition of basalt and mafic calcareous rocks and contains assemblages of andesine-diopside-sphene-calcite ± quartz ± scapolite ± garnet or diopside ± vesuvianite ± quartz ± sphene ± scapolite and reportedly has textures typical of granulite-grade metamorphism [56]. If the mafic granulite xenoliths derive from protoliths that were metamorphosed prior to Murdama deposition, their presence may indicate exhumation of basement rocks from considerable depth prior to deposition. However, because the mafic granulite only occurs as roof pendants in post-Murdama granite, correlation with the pre-Murdama basement is not fully established and the high-grade metamorphism and texture could be the result of metamorphism during emplacement of the host batholith [56]. In such a case, the high-grade metamorphism would have no bearing on the amount of exhumation that may be inferred for the pre-Murdama basement, although significant erosion is implied by the limited extent of layered supracrustal rocks belonging to the arc.

The Afif formation consists of rhyolite, andesite, local marble, chert, and conglomerate, overlain by interbedded rhyolite, rhyolite breccia, ignimbrite, dacite, andesite, basalt, and volcaniclastic sedimentary rocks. The rocks have a fairly mature calc-alkalic and high-K calc-alkalic geochemical signature similar to present-day volcanic-arc sequences [57]. Their bimodal character is noteworthy and may be evidence for extension and rifting during the initiation of the Murdama basin. The Afif formation and Murdama group are structurally concordant, with similar inclination of dips and orientation of strikes. In some locations the contact between the two is transitional, with intercalations over a few hundred meters between Afif formation volcanic rocks and Murdama group conglomerate and sandstone [58]. However, the marked change at the contact between the two, from a volcanic environment for the Afif formation to a conglomerate-sandstone sedimentary environment for the Murdama group, the presence of volcanic clasts derived from the Afif formation in basal Murdama conglomerate, and along-strike variability in lithologies of the Afif formation beneath the Murdama group imply a diastrophic contact between the Afif and Murdama. These features suggest erosion of the Afif formation prior to Murdama group deposition, possibly followed by uplift of the wider basin margins leading to an influx of coarse epiclastic sediment.

The volcanic rocks of the Hibshi formation are also bimodal in character. They crop out in a fault-bounded northeast-trending syncline 2–30 km wide and more than 100 km long and constitute a succession more than 5000 m thick [59]. A felsic volcanic center in the central part of the Hibshi formation is marked by basal polymict conglomerate as much as 100 m thick in local channels, fine- to medium-grained, poorly to moderately sorted arkose, lithic (volcanic) wacke, maroon to green siltstone, dacitic and rhyolitic welded and ash-fall tuffs, and dacite and andesite flow rocks and

breccia. The conglomerate is crudely bedded and composed of locally derived clasts of diorite, andesite, dacite, as well as Murdama sandstone. A second center to the northeast consists of rhyolite flows and tuffs and massive basalt flows.

The Murdama group, the main fill of the Murdama basin, is a succession of sandstone, subsidiary conglomerate and limestone, and minor volcanic rocks. Representative stratigraphic columns of the lower 5000 m of the group are shown in Figure 13. Where predominantly composed of sand-sized and coarser fragments, the rocks are referred to as the Zaydi formation. Sections with significant carbonate are referred to as the Farida formation (see below). Conglomerate is abundant, occurring at the base and interbedded with sandstone higher in the section. The conglomerate forms units up to 400 m thick but these thicken and thin along strike. The conglomerate is polymict, poorly sorted, and composed of clast-supported well-rounded pebbles, cobbles, and boulders up to 50 cm in diameter (Figure 14A,B).

Clast lithologies include felsic and mafic lavas, tuff, aplite, siltstone, sandstone, and chert, rhyolitic ignimbrite, rhyolitic lapilli tuff, and andesite derived from the underlying Afif formation or volcanic units elsewhere in the basement. Basement-derived plutonic and metamorphic clasts include quartz microgranite, granodiorite, hornblende and biotite granite, diorite, metavolcanic rocks, and mica schist. The conglomerate is massive, resembling debris mass flow, or moderately well bedded, denoting transportation and deposition by water (Figure 14A). Bedding is accentuated by thin interbeds of cross-bedded sandstone, siltstone, and black marble.

The amount of sandstone in the Zaydi formation increases upsection and above 1500 m is the dominant lithology. The sandstone is remarkably monotonous: a sequence of well-bedded lithic (volcanic) arenite and wacke that does not discernibly change in character over 100 s of kilometers along and across strike. It is typically fine to medium grained, locally coarse grained, and contains subangular fragments of mafic and felsic volcanic rocks, quartz, feldspar, volcanic rocks, and microgranular quartz-feldspar aggregates. The matrix contains chlorite, muscovite, epidote, and carbonate. On a QFL diagram, the sandstone plots in the fields of undissected, transitional, and dissected arcs (Figure 15) consistent with the lithology of the sub-Murdama basement. Individual sandstone beds are decimeters to meters thick and may persist on strike for kilometers. Some are massive, others are laminated, and many are cross-bedded and channelized (Figure 14C,D). In places, the rocks form upward-fining cycles of sandstone, siltstone, and shale less than 1 to several meters thick. Interlayers of siltstone are common (Figure 14E), and in many localities the siltstone is disrupted and redeposited as rip-up conglomerate (Figure 16). Clasts in the rip-up conglomerate are commonly imbricated and together with cross bedding present an opportunity to analyze current directions in the Murdama basin. Other primary sedimentary structures include planar cross bedding, ripple cross lamination, planar lamination, grading, scour-and-fill features, and mud cracks on desiccation surfaces.

Figure 13. Stratigraphic columns of two sections in the lower part of the Murdama group, simplified after [50]. See Figure 11 for locations of sections.

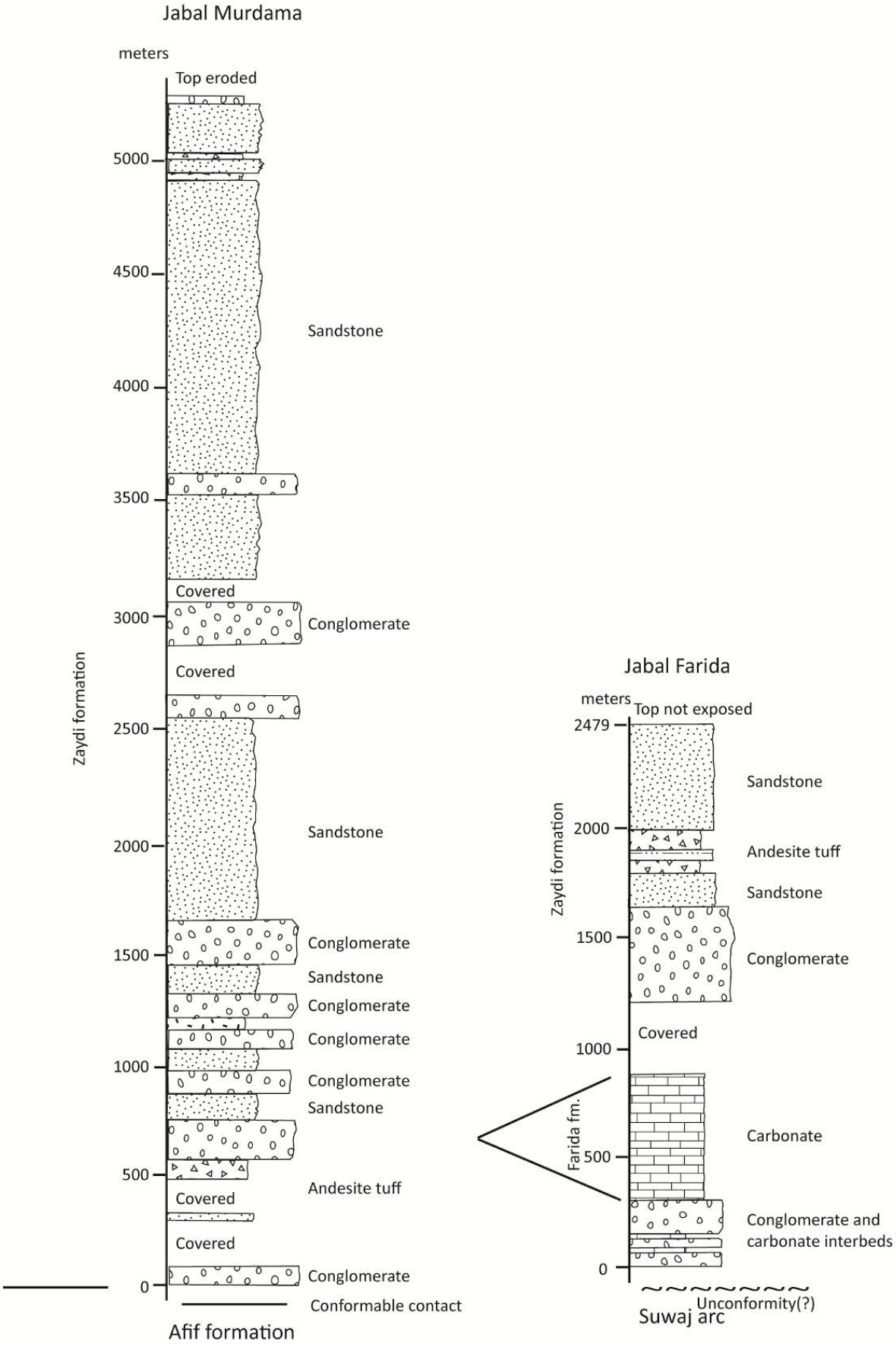

Figure 14. Sedimentary features of the Zaydi formation, Murdama group close to the base of the group at the northern margin of the Maslum basin at Umrah. (**A**) Cobble to boulder, clast-supported polymict conglomerate in beds 1–1.5 m thick; (**B**) Close-up of conglomerate outlined by the box in A, showing the well rounded character of the clasts; (**C**) Planar, tabular set of curved foreset cross beds, ~10 cm thick, interbedded with medium-bedded sandstone below and thin-bedded sandstone above. The cross-bed set is immediately underlain by a bed of fine-grained sandstone to siltstone; (**D**) Slightly channeled sets of cross beds in medium-grained sandstone; (**E**) Thin bed (~5 cm thick) of siltstone interbedded with pebble conglomerate. This type of siltstone is the source for intraformational clasts observed in rip-up conglomerate in the Zaydi formation (see Figure 16).

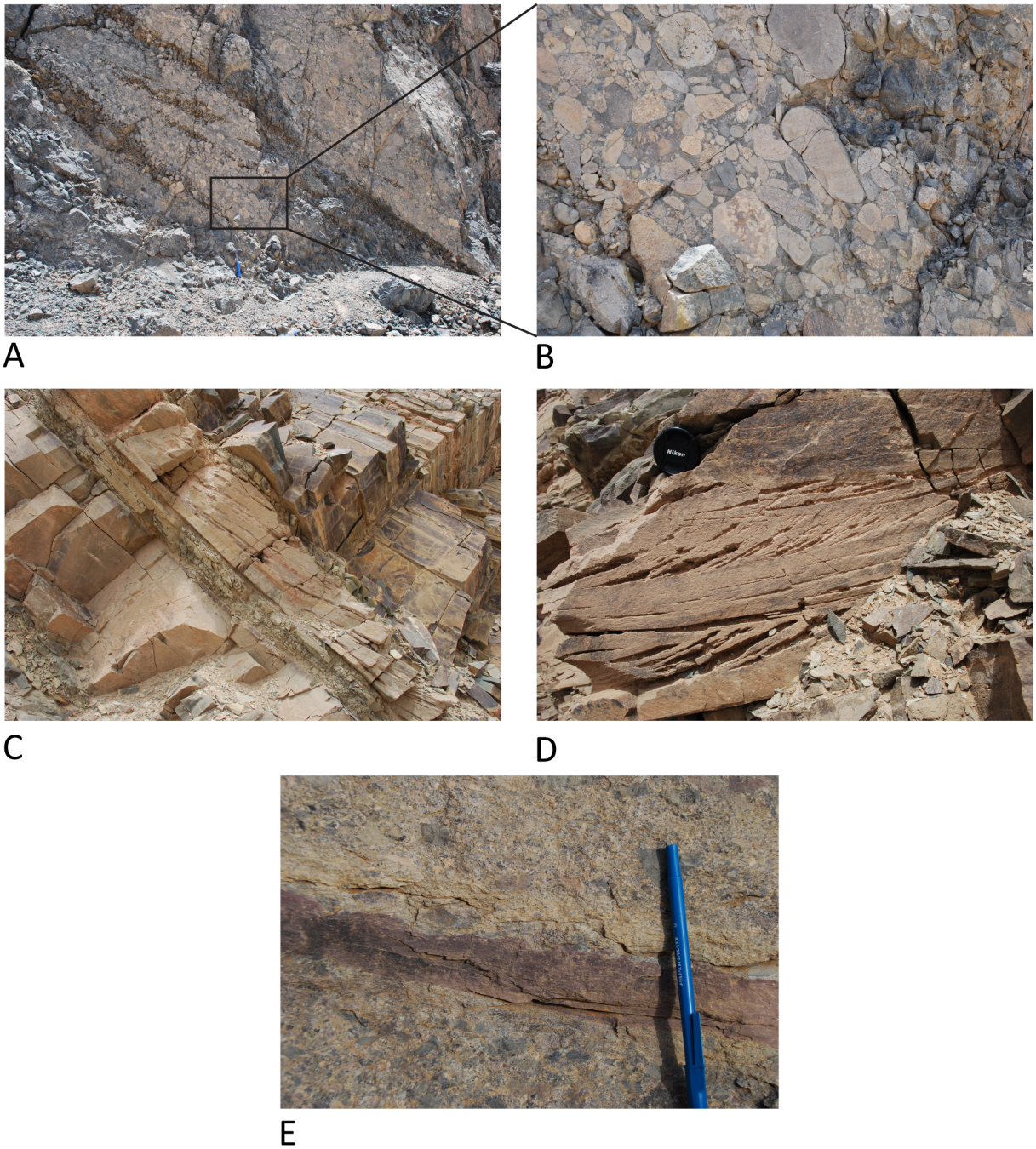

Figure 15. Quartz-feldspar-lithics diagram showing the provenance and plate tectonic setting for sandstone in the Murdama group. Sandstone data (dark gray field) after [50]; provenance fields after [60,61].

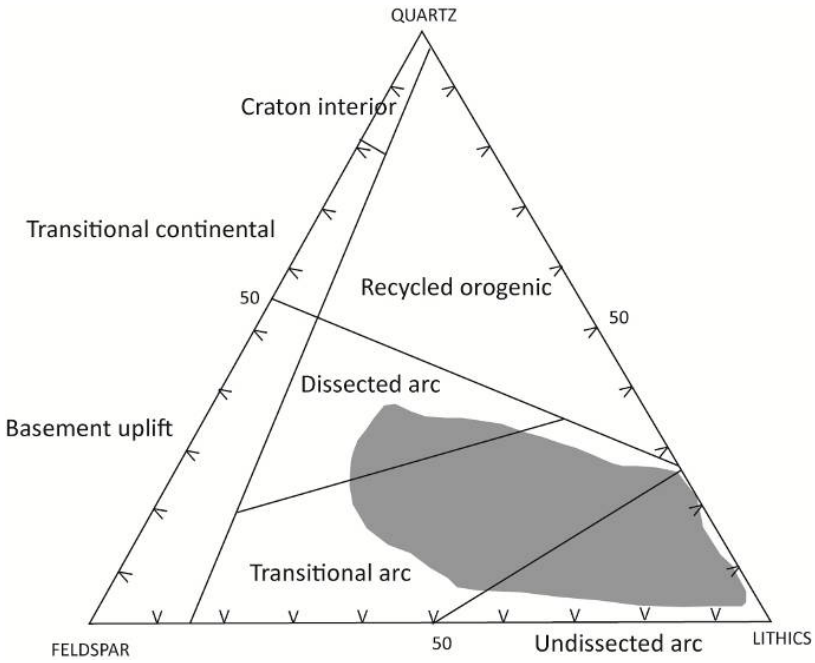

Figure 16. Examples of intraformational conglomerate, Zaydi formation. (**A**) Three beds of upward-fining conglomerate to sandstone; (**B**) Bed of conglomerate interbedded with laminated sandstone. In both examples, the conglomerate comprises rip-up clasts of siltstone. The clasts are conspicuously imbricated, denoting deposition in a high-energy aqueous environment and indicative of current direction (to the left, in these examples; to the east, in the field). Hand lens for scale-2.5 cm diameter.

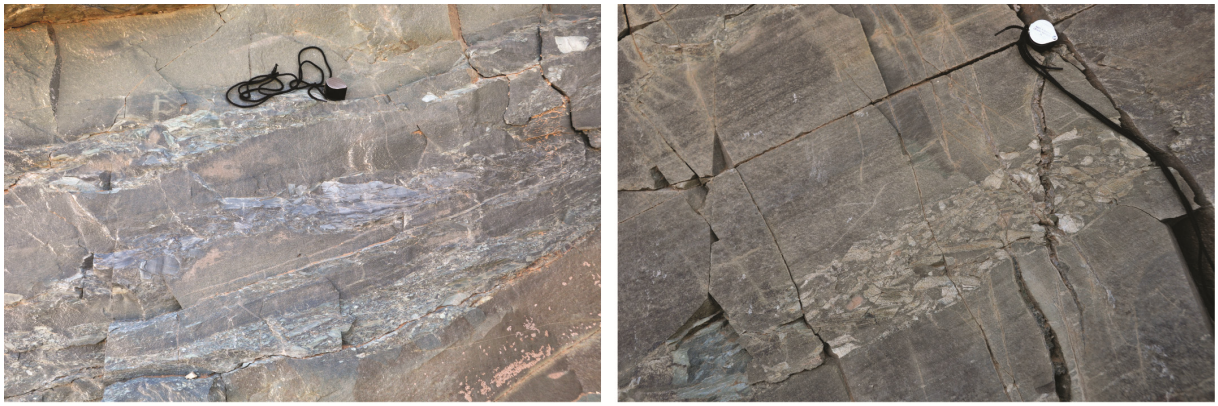

A B

In parts of the Murdama basin, sandstone has a variable amount of carbonate cement and grades into beds and lenses of carbonate several tens of meters to 300 m thick (Figure 17). Where the carbonate rocks are particularly thick and persistent, they are referred to as the Farida formation. The formation characterizes the eastern flank of the Maslum sub-basin. At Jabal Farida, the formation is about 700 m thick (Figure 13), overlying a 200–300 m thick unit of breccia, conglomerate, and sandstone. The Farida formation typically consists of a few meters of black marble, followed upward

by thick beds of well-bedded gray, beige weathering carbonate of probable dolomitic composition with lenticular intercalations of black, carbonaceous marble. In some locations these two carbonate facies are thinly interlayered, resembling varves. Locally, the Farida formation contains columnar stromatolites, and in places the stromatolites contain fresh volcanic fragments, feldspar laths, and shards indicating contemporary volcanism and carbonate sedimentation [56]. The Farida formation also contains pisolites, breccia with angular beige dolomite blocks up to 80 cm across within a black marble matrix, and intercalations of arenitic to conglomeratic marble with well-rounded cobbles of rhyolite, granite, aplite, and marble in a carbonate or locally pelitic cement.

Figure 17. Farida formation, Murdama group, Jabal Farida. View of well-bedded dolomitic limestone in the lower part of the carbonate succession at the eastern margin of the Murdama group in the Maslum basin. Geologists from the Saudi Geological Survey, the Polish Geological Survey, and Adelaide University for scale.

Important depositional features of the Murdama group are (1) its size, making it comparable to orogenic depositional basins elsewhere such as the Mesozoic Pannonian basin in the northern Carpathian foreland and the Himalayan collisional successor basins in northwestern China; (2) deposition above a regional unconformity that developed during or soon after the Nabitah orogeny (680–640 Ma); (3) a remarkable uniformity of sandstone facies, and well developed and persistent bedding suggesting relative structural stability within the basin; (4) the presence of polymict conglomerate of local derivation at the base and to lesser extent higher in the section of the Murdama group; (5) the presence of great thicknesses of locally stromatolitic carbonate; (6) a pervasive distribution of sedimentary structures indicative of shallow water to subaerial environments; and

(7) the presence of bimodal volcanic rocks at the base of the basin in the west (Afif formation) and in the north (Hibshi formation), and andesitic and rhyolitic lavas and tuffs interbeds elsewhere.

Overall, the basin passes from a volcanic-plutonic domain in the west to a marine and shallow-marine basin in the east [62]. Because of the predominance of planar-bedded, poorly sorted sandstone, it is proposed [50] that the Murdama group was deposited in an alluvial to deltaic environment. The thick, locally stromatolitic Farida carbonate suggests a dominantly marine setting in the eastern Maslum sub-basin, whereas lagoonal, lacustrine, or shallow-marine conditions are inferred for the Maraghan sub-basin on the basis of sandstone, siltstone, and shale that are interpreted as deposits in near-shore mud-flat and broad-channel environments with carbonate mud and microbial buildups [63].

No modern basin analysis has been done of the Murdama basin. It has been referred to as a foreland basin [40]. It is located between two active margins—the Afif suture on the west and the Halaban suture on the east—and may be a type of flexural basin developed in response to tectonic loading of new amalgamated crust by obduction of the Halaban ophiolite along the Halaban suture. Alternatively, the basin may reflect subsidence induced by mantle-lithospheric thickening caused by cooling following orogeny or asthenospheric flow reflecting delamination of subducted lithosphere during and soon after the Nabitah orogeny (680–640 Ma) [47]. Bimodal volcanism in the Afif and Hibshi formations additionally suggests an element of crustal extension. The Murdama basin overlies a late Cryogenian unconformity of regional extent that developed on the newly assembled Afif terrane. Exposure of mafic granulite, if the granulite truly reflects Nabitah orogeny metamorphism, and the large extent of plutonic rock in the basement beneath the unconformity implies as much as 15–20 km exhumation and contemporary erosion of parts of the Afif terrane prior to Murdama deposition. The pervasive presence of primary sedimentary structures indicative of a shallow-water environment, along and across strike and up through the stratigraphic column, implies that the rates of subsidence and infill were largely balanced over much of the extent of the basin. Conglomerate in the Murdama group is evidence of sufficient relief of the basin margins to generate cobbles and boulders, perhaps deposited in fan deltas and channels [56]. Yet the sedimentary character of Murdama sandstone and the presence of stromatolitic carbonate in the east is evidence that during the late Cryogenian-Early Ediacaran a vast area in the ANS between the Nabitah mobile belt and the Halaban suture subsided below base level. The thickness of sediment in the Murdama group implies that erosion of the basin margins was intense but the marine carbonates indicate that despite mountain building during Nabitah orogenesis, the basin was at least intermittently connected to an ocean within a relatively short period after orogeny.

8. Ediacaran Basins

Ediacaran post-amalgamation basins are widespread in the ANS (Figure 18) deposited atop regional and local unconformities developed on arc assemblages in the basement. The basins are filled by volcanic and sedimentary rocks of the Dokhan Volcanics, Hammamat Group, Thalbah group, and Elat and Saramuj Conglomerates in the northwest. Somewhat younger rocks of the Jibalah group were deposited close to or immediately along strike-slip faults of the Najd system in the north and northeast, and other Ediacaran sedimentary and volcanic successions fill small basins along north-south shear zones in the southern ANS associated with orogen-normal shortening and suturing. The basins are the result of sedimentation and volcanism in a range of structural and depositional environments that

developed during the final stages of assembly of the ANS, its accretion to the Saharan Metacraton, closure of the Mozambique Ocean, and assembly of eastern and western Gondwana.

Figure 18. Ediacaran sedimentary and volcanic basins in the Arabian-Nubian Shield, showing their common juxtaposition to shear zones, gneiss belts, and core complexes (gneiss domes) (after [11]).

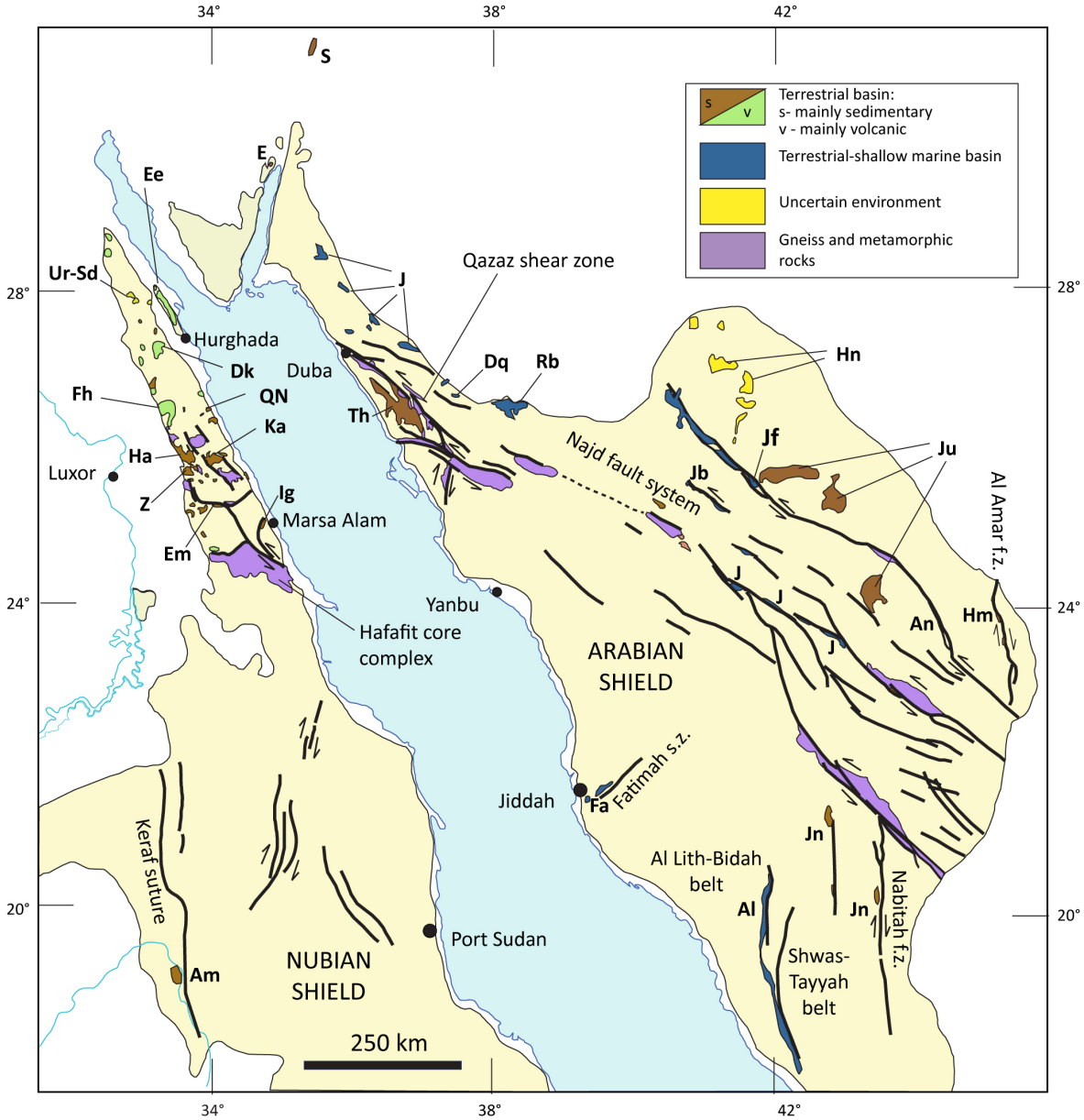

Notes: Identified successions and basins: Al—Ablah; Am—Amaki; An—Antaq; E—Elat Conglomerate; Ee—Esh El Mellaha; Em—El Miyah; Dk—Gebel Dokhan; Dq—Dhaiqa; Fa—Fatima; Fh—Fatirah area; Ha—Wadi Hammamat; Hm—Hamir; Hn—Hadn; Ig—Wadi Igla; J—unnamed Jibalah group basins; Jb—Jibalah; Jf—Jifn; Jn—Junaynah; Ju—Jurdahiway; Ka—Wadi Kareim; QN—Wadi Quieh, Nuqara, and Wassif; Rb—Rubtayn; S—Saramuj Conglomerate; Th—Thalbah; Ur-Sd—Gebel Urf-Wadi Um Sidra; Z—Zeidun. Saramuj Conglomerate is also identified in deep boreholes beneath the Golan Heights, north of the northern margin of this figure.

On the basis of their lithology and depositional character, the basins are divisible into terrestrial and mixed terrestrial to shallow-marine basins (Figure 18). Terrestrial assemblages include the Dokhan

Volcanics and sedimentary rocks of the Hammamat and Thalbah groups (Figure 19). The Ediacaran Elat Conglomerate (~580 Ma) [64] and coeval Saramuj Conglomerate crop out in southern Israel and Jordan and the Saramuj is geophysically inferred to be present over a thickness of ~1000 m at depth beneath the Golan Heights [65]. Other terrestrial Ediacaran basins include volcanic and sedimentary rocks of the Shammar group in the northeast and the small Amaki and Junaynah basins adjacent to the Nile in the southwest and N-trending shears in the southeast. Sedimentary and volcanic rocks of the Jibalah, Fatima, and Ablah groups occupy mixed terrestrial and shallow-marine basins along NW-trending Najd faults in the north-central Arabian Shield, along a NE-trending shear zone immediately east of Jiddah, and along the north-south axis of the zone of weakness at the contact between the Al Lith-Bidah belt and Shwas-Tayyah belt in the south (Figures 3 and 18).

Figure 19. Representative stratigraphic columns for terrestrial Ediacaran successions in the Arabian-Nubian Shield. Zeidun basin after [66]; Gebel Urf succession after [67]; Thalbah group after [68]. See Figures 1 and 18 for locations of these basins. Arrows indicate approximate stratigraphic positions of dated samples discussed in the text.

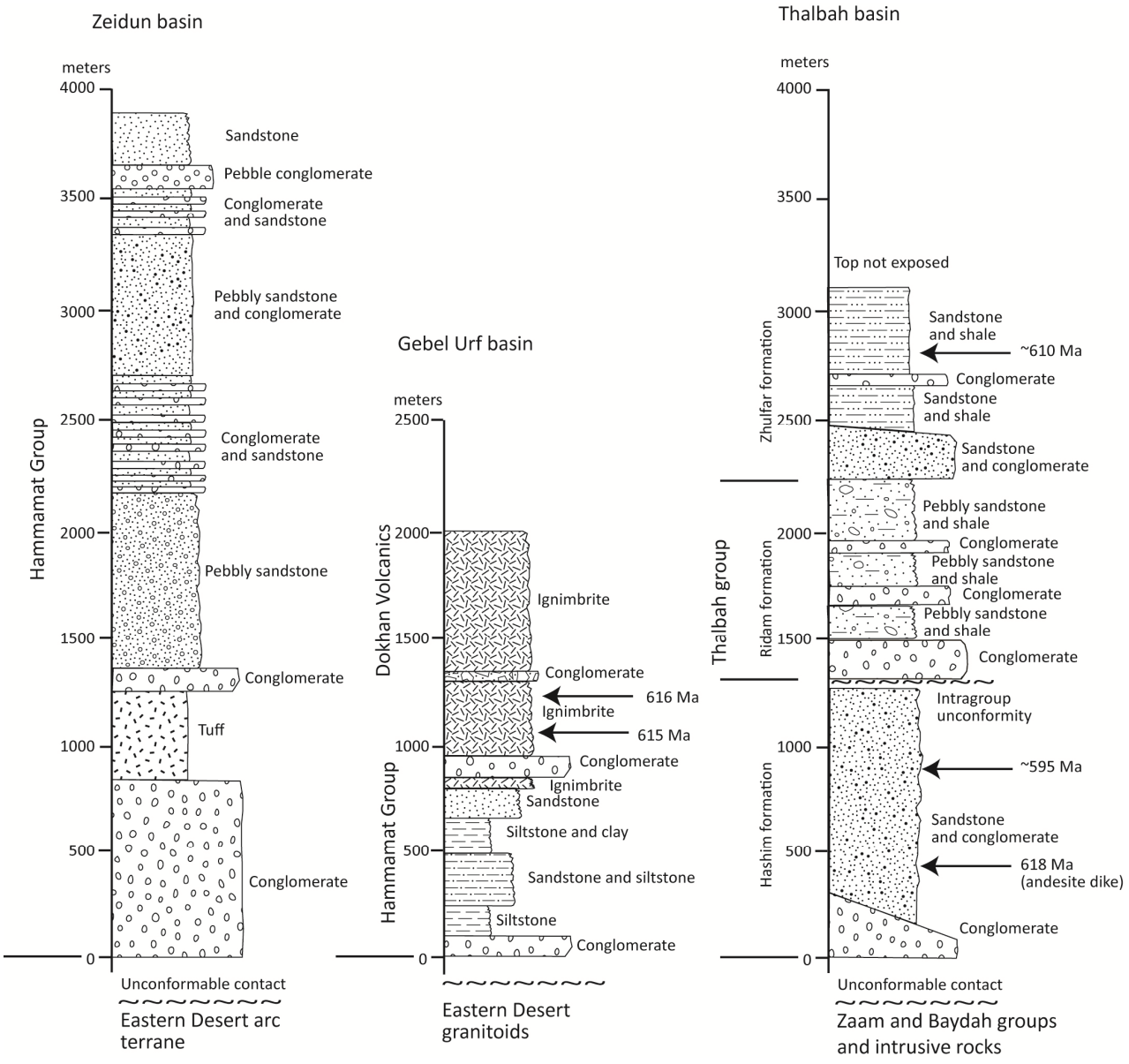

8.1. Terrestrial Basins

The Dokhan Volcanics and Hammamat Group are the names given to Ediacaran volcanic and sedimentary rocks in terrestrial basins in the Nubian Shield. They unconformably overlie eroded, accreted Cryogenian volcanic and plutonic arc rocks of the ANS north of the Yanbu-Sol Hamed-Allaqi suture (Figure 1). Dominantly volcanic sequences are assigned to the Dokhan Volcanics and sedimentary successions are assigned to the Hammamat Group, but there is no consensus about the origins or stratigraphic relationships of the rocks. In some basins, the Hammamat Group underlies the Dokhan Volcanics; in others the Hammamat overlies the Dokhan; and in places the two interfinger.

Whole-rock Rb-Sr ages [69], conventional TIMS zircon U-Pb ages [70], and SIMS zircon U-Pb ages [67,71] indicate that the Dokhan volcanics range in age from 630 to 592 Ma and may have been erupted in two pulses at 630–623 Ma and 618–592 Ma. Detrital zircons yield a U-Pb SHRIMP maximum depositional age of about 585 Ma for the base of the Hammamat succession in the Gebel Um Tawat area, northern Eastern Desert, Egypt, [72], although it is inferred that the group in general was deposited between about 615 to 585 Ma [66,72,73]. Both Hammamat and Dokhan units were affected by rapid hinterland uplift at about 595–588 Ma [74,75]. Equivalent rocks in the Arabian Shield include the Jurdhawiyah (~612–595 Ma) and Thalbah (620–595 Ma) groups. All these groups were deposited in the period between the Marinoan (~635 Ma) and Gaskiers (~582 Ma) glaciations; as such, glaciogenic diamictite and wacke are not expected in these basins.

The Hammamat Group is commonly referred to as molasse [66,72], and was deposited in fluvial systems of continental proportions [72] or in isolated basins [76,77]. The Hammamat basins are variously classified as foreland basins, in the case of the type Hammamat basin [74], intramontane basins in the cases of the Kareim, Quieh, and Igla basins [78], a strike-slip pull-apart basin, in the case of the El Mayah basin [79], and fault-bounded basins [66,77]. The range of inferred structural controls include thrusting, normal faulting, strike-slip faulting, N–S to NW–SE extension, and magmatic doming. In the type Hammamat basin, the Hammamat Group was deformed, metamorphosed, and thrust over younger Dokhan Volcanics, perhaps as a result of deposition in a piggy-back basin in front of a SW-propagating thrust front [80], and was intruded, after folding, by the 596 Ma Um Had granite [80], indicating a minimum deposition age of the Hammamat group in this basin of 596 Ma. Initial subsidence of the Hammamat Group in the Kareim basin was associated with the formation of strike-slip faults around the Sibai gneiss dome as this was beginning to be emplaced and exhumed (~650 Ma) [81] and terminal fanglomerate deposition was associated with the intrusion of young granite at about 580 Ma [82]. The El Mayah basin [79] was initiated as a half-graben and later evolved into a pull-apart basin at a prominent bend in a sinistral shear system of the Najd fault. The Zeidun basin [66] was initiated by subsidence controlled by marginal normal faults during an episode of N-S regional extension in the northwestern ANS. Basin subsidence and sediment delivery rates were linked with exhumation of adjacent core complexes. The basin was subsequently deformed and inverted by folding, E- to ENE-trending steep reverse faulting, and NE- and NW-trending conjugate strike-slip faulting.

The Hammamat succession in the Zeidun basin is as much as ~4000 m thick [66] (Figure 19). The section begins with reddish to purple cobble and boulder clast-supported conglomerate containing volcanic, metavolcanic, and granitic clasts. The conglomerate contains thin, gray, cross-bedded and graded sandstone interbeds, and is overlain by tuffs. The middle part of the section is dominated by

sandy beds with dispersed pebbles that grade up into cm-thick red mudstone. The mudstone is locally disrupted and forms rip-up conglomerate. Interbedded conglomerate and sandstone follows upward, overlain by more pebbly sandstone and conglomerate. The sedimentary rocks in the Zeidun basin are interpreted as molasse deposited in alluvial fan and(or) braided stream environments. Locally cross-bedded sands with pebble horizons possibly represent braided stream reworking of debris flows. Sandstone may result from sheet flood transport of sediment, and red mudstone could be mudflows or lacustrine deposits [66].

The Gebel El Urf basin is an example of a basin containing both Hammamat Group and Dokhan Volcanics. The basin is elongate and folded into an ENE-trending syncline. Hammamat-type sedimentary rocks, about 1000 m thick, occur in its lower part (Figure 19) [83]; Dokhan Volcanic-type rocks, also about 1000 m thick, are above. The Hammamat sequence includes a clast-supported and generally unstratified conglomerate at the base, containing cobbles and boulders 10–30 cm and rarely 1 m in diameter of granitoids, volcanic rocks, and metapelite derived from the underlying arc rocks. The conglomerate is overlain by laminated siltstone with intercalations of fine-grained sandstone and some calcareous concretions. The siltstone shows desiccation cracks and some rip-up clasts. Sandstone is fine to coarse grained and forms laterally continuous beds and lenses. It is generally massive, but locally is laminated and upward fining with cross-bedding and mudstone layers, flame structure and rip-up clasts. The Dokhan Volcanics include dacitic and rhyolitic welded and non-welded ignimbrite containing crystals and crystal fragments of K-feldspar, plagioclase, quartz, biotite, pumice and glass shards, and lithic fragments of metavolcanics, granite, and preexisting ignimbrite.

The origin of Dokhan Volcanics basins is debated. The bimodal character of the unit has been used as evidence for a continental rift environment [84,85]. An alternative proposal is that volcanism was related to the subduction of a hot oceanic ridge before collision and later melting of a hot oceanic slab [86]. In the Gebel Urf basin, the Dokhan Volcanics are modeled as felsic volcanic centers that developed in a structurally controlled intramontane basin with the Hammamat facies representing alluvial fans, fluvial braided rivers, and lakes [83]. Deposition in the Gebel Urf basin began with alluvial-fan and mass-flow conglomerates and sandstone eroded from flanking mountains, followed by development of sandy braided river systems. This was followed by the development of a deep lake, perhaps as a result of continued normal faulting. High-energy arenaceous and rudaceous sedimentation in the middle of the stratigraphic section marked shrinkage of the lake, concurrent with the onset of silica-rich and silica-poor volcanic centers leading to the formation of volcanogenic mass-flow deposits, hyaloclastic deposits, and lavas. The terminal history of the basin included at least two large ignimbrite-forming caldera eruptions.

The Thalbah group [68] resembles the Hammamat group. It crops out in a basin measuring about 100 km NW–SE and 40 km SW–NE unconformably overlying arc rocks of the Midyan terrane in the western Arabian Shield. The group is between 3000 and 4000 m thick, and divided into three overstepping formations (Hashim, Ridam, Zhulfar) separated by internal unconformities (Figure 19). The age of the group is constrained by the arc-related Imdan complex below, dated by U-Pb TIMS at 660 ± 4 Ma [87], and intrusions of diorite and microgranite of the Liban complex, dated at 634 ± 5 by U-Pb SHRIMP [50] and at 621 ± 7 Ma by U-Pb TIMS [87]. An andesite dike intruding the lower Thalbah (Hashim formation) yields a broadly consistent U-Pb zircon SHRIMP age of ~618 Ma [88]. A recent program of detrital zircon dating indicates a sedimentation age consistent with these earlier

results [89], and the data overall suggest that the Thalbah group is ~620 to ~595 Ma, coeval with the Hammamat Group. Given the close lithologic similarity of the two groups, it seems likely that they are counterparts that now crop out on opposite sides of the Red Sea.

The Thalbah group is moderately folded with beds dipping <10° and 70° and well-developed cleavage. The rocks are barely metamorphosed except in the northeast adjacent to the Qazaz shear zone (Figure 18), where conglomerate clasts are stretched and the rocks are metamorphosed to paragneiss. Foliation and mineral/stretching lineations in the Thalbah are coaxial with foliations and lineations in orthogneiss and schist in the shear zone.

The basal Hashim formation begins with massive to weakly bedded clast-supported polymict conglomerate; clasts comprise pebbles and cobbles (5–10 cm) of sandstone, andesite, rhyolite, quartz diorite, and granodiorite. The overlying beds include well-bedded brown and purple litharenite, subordinate siltstone, and intraformational conglomerate. The Ridam formation includes poorly sorted, crudely bedded, pebble-to-boulder polymict conglomerate intercalated with pebbly sandstone and shale. Conglomerate clasts are mostly granite, granodiorite, and diorite; lesser lithologies are rhyolite porphyry, andesite, sandstone, and quartz. The matrix includes feldspar and quartz crystals and grains of volcaniclastic rock. Contemporaneous volcanic rocks are not known in the Thalbah basin and the volcanic material possibly derives from what, prior to Red Sea opening, would have been nearby Dokhan Volcanic centers. The topmost Zhulfar formation consists of well-bedded litharenite, pebble conglomerate, and abundant siltstone.

The geochronological data indicate that the Thalbah group was deposited after amalgamation of the Midyan and Hijaz terranes (~700 Ma) and contemporary with active shearing and gneiss formation on the Qazaz shear zone (635–573 Ma). Its lithology suggests rapid deposition of rudaceous and arenaceous sediments close to an emerging and strongly eroded mountainous hinterland interrupted by quieter intervals of fine-grained sedimentation. The pervasive red coloration and sedimentary structures such as rain prints and mud cracks indicate shallow water to subaerial deposition. Conglomerate units are commonly massive to poorly bedded, indicating mass-flow deposition. Its age and setting are evidence that the group constitutes molasse deposited in a flexural basin along the flank of the Qazaz shear zone [40].

As illustrated in Figure 18, all the ANS Ediacaran volcanosedimentary basins have a close spatial relationship with shear zones, gneiss belts, and core complexes. In most discussions on the origins of these basins, the spatial relationship is also interpreted as implying a genetic relationship, although the precise nature of the genetic relationship is debated. A recent summary of Nubian Shield basins [66], refers to three structural/tectonic types of controls on basin formation: (1) basins associated with active continental margins; (2) basins developing in a transpressional orogen; and (3) basins associated with rifting and extension. In control 1, it is envisaged that sedimentary deposition was associated with continental arc volcanics that provided a significant source of clastic debris. The second control model situates Hammamat basins in areas of subsidence and(or) pull apart contemporary with magmatism, the exhumation and uplift of core complexes, gneiss domes and gneiss belts, and normal and strike-slip fault activity during gravity sliding and transpressional orogeny. Control 3 associates Hammamat Group molasse deposition and Dokhan Volcanic bimodal magmatism with graben formation in an extensional tectonic regime. The basin types have various names such as volcanosedimentary intramontane basins, rim synclines, foreland basins, orthogonal extension and pull-apart basins, piggy-back basins, and rifts and grabens.

8.2. Mixed Terrestrial and Shallow-Marine Basins

Mixed terrestrial and shallow-marine Ediacaran post-amalgamation basins in the ANS are typified by the Jibalah group (Figure 20). Other mixed terrestrial and shallow-marine Ediacaran basins include the Fatimah group [90,91] and Ablah group [22,23]. The Jibalah Group was formally recognized and defined during the 1960s [92,93]. It is widely distributed (Figure 18) [94] although restricted in outcrop extent to isolated areas, almost exclusively along major strands of the northwest-trending Najd fault system. Most basins are small: 5 to 10 km across and 15 to 50 long. However, the Jifn basin and its extension to the northwest, form virtually continuous exposure over a strike length of 175 km. At least one basin (Jifn) may have been initiated during dextral displacement on Najd faulting [95] with inversion and folding caused by subsequent sinistral movement.

Figure 20. Representative stratigraphic columns for terrestrial to shallow-marine Ediacaran successions in the Arabian Shield (not to scale). Rubtayn basin succession after [93]; Jifn basins succession after [95]; Antaq basin succession and age constraint on Antaq basement from [96].

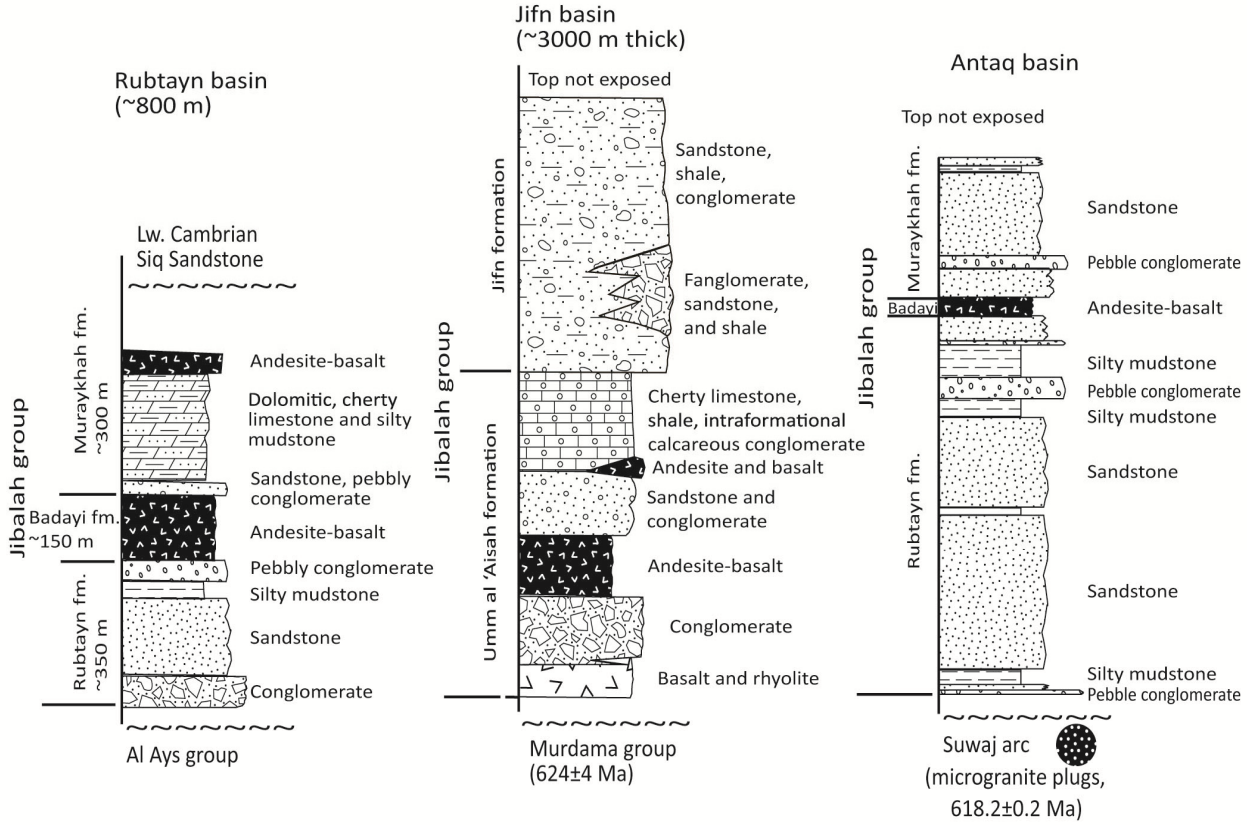

The Jibalah Group mostly rests unconformably on exhumed, uplifted, and eroded volcanic and plutonic arc-associated rocks of the ANS basement and locally overlies ~630 Ma clastic sedimentary and volcanic rocks of the Murdama and Shammar groups. It is very locally intruded by Ediacaran-aged granitoids. The sub-Jibalah unconformity is readily identifiable in the field by the occurrence of a basal conglomerate, which records proximal uplift and the origin of the basins. The age of the Jibalah group is debated, but existing data suggest it is between 600 and 560 Ma. Microgranite plugs in the basement beneath the Antaq basin, yielding a U-Pb chemical abrasion TIMS age of 618 Ma [96], provide the

strongest constraint on the maximum age of sedimentation of the Jibalah Group. Its youngest age of sedimentation is broadly constrained by the age of the Cambrian Siq Sandstone and the ~526 Ma sub-Siq/Angudan unconformity at the base of the lower Paleozoic succession overlying the shield [94]. The minimum deposition age is more tightly constrained by a felsite dike cross-cutting the upper part of the Jibalah group in the Jifn basin, which has a U-Pb concordia age of 577 ± 6 Ma [97]. Carbonate rocks of the Jibalah group in the Dhaiqa basin contain tuff beds that yield a LA-ICP-MS zircon age of 560 ± 4 Ma [98]. Detrital zircon from tuff beds in the Dhaiqa and Rubtayn basins yields U-Pb SIMS ages suggesting deposition between 600 and 570 Ma [99,100]. Three tuffs collected from the upper Rubtayn Formation in the Antaq basin contain abundant equant quartz, feldspar lathes, angular biotite, devitrified glass suggesting a pyroclastic origin, and have broken, stubby, euhedral zircon that yields LA-ICP-MS U-Pb ages of 596 ± 17, 579 ± 17, and 604 ± 18 Ma [96].

Deposition of the lower Jibalah overlapped with the Gaskiers glacial event (~585–~582 Ma) [101]. It is therefore noteworthy that diamictite comprising matrix-supported boulders, cobbles, and possible dropstones are recognized in conglomeratic sandstone in some of the basins (e.g., Figure 21C). It is conceivable that some of these conglomeratic units may represent glaciogenic diamictite, but their glaciogenic origin is not established and most conglomeratic units are probably alluvial fans [95,98,102]. The age of the Jibalah group, additionally, raises the possibility that some of the carbonates in the Jibalah group may have been deposited during the Shuram negative $\delta^{13}C$ anomaly (Figure 22), which is well defined in the Huqf Group of Oman [103], and such carbonates are worthy of further study.

Lithologically, the Jibalah group consists of variable amounts of siltstone, sandstone, conglomerate, bimodal volcanics, and carbonate in sequences more than 3000 m thick (Figure 20). The rocks in several basins in the northwestern Arabian Shield are divided, from bottom to top, into the Rubtayn, Badayi', and Muraykhah formations and similar lithologies are recognized in other basins [94,96] although different names may be used. In the Jifn basin, a lower epiclastic and carbonate interval makes up the Umm al'Aisah formation and an upper arkosic sandstone and conglomeratic unit makes up the Jifn formation (Figure 20).

The Rubtayn formation is typically conglomeratic, varying in thickness from a few meters (e.g., in the Antaq basin) to many hundreds of meters thick (e.g., the Rubtayn basin). The Rubtayn and Umm al'Aisah conglomerate is massive to well bedded (Figure 21D). It is typically poorly sorted, with moderately to well-rounded clasts, of diverse lithologies in a muddy or calcareous wacke matrix [92,93] (Figure 21D,E). Clast lithologies are dominated by the underlying basement lithology. The Rubtayn formation in the Dhaiqa basin contains the prominent diamictite referred to above (Figure 21C). In some basins, such as the Rubtayn [94] and Antaq [96] basins (Figure 20), the basal conglomerate grades upwards into brown to red micaceous and commonly arkosic sandstone and muddy siltstone, in places with interbedded conglomerate, and almost everywhere, only intermittently exposed. Graded beds are common in the sandstone facies and m-scale fluid escape structures have been observed in the Antaq basin [96]. The overlying siltstone is devoid of distinct sedimentary structures. In the Rubtayn basin, siltstone is overlain by 60 m of pebbly conglomerate [93].

The Rubtayn formation is sharply overlain by the Badayi' formation, which consists of subaerially extruded, purple-brown, sodic and iron-rich, porphyritic andesite and basalts [92,93]. Individual flows are discernible based on concentrations of amygdules and occurrence of tuffs between flows. The

Badayi' formation, or its equivalent member within the Umm al'Aisah formation in the Jifn basin, is commonly ~100 m-thick.

Figure 21. Lithologic and bedding features of the Jibalah group. (**A**) Well-bedded limestone, Dhaiqa formation, Dhaiqa basin; (**B**) Detail showing microbial laminites, Dhaiqa formation, Dhaiqa basin; (**C**) Paraconglomerate at the base of the Dhaiqa formation, Dhaiqa basin comprising granite boulders embedded in coarse-grained pebbly sandstone (R.J. Stern for scale); (**D**) View of massive conglomerate (to the left) overlain by well-bedded conglomerate and sandstone (to the right), basal part of the Jifn basin (R. Trindade for scale); (**E**) Rounded-to-subangular pebble-to-boulder clasts of granite and mafic volcanic rock, Jifn basin; (**F**) Cyclic bedding in the eastern Antaq basin composed of arkosic sandstone and siltstone, subordinate conglomerate, and minor carbonate.

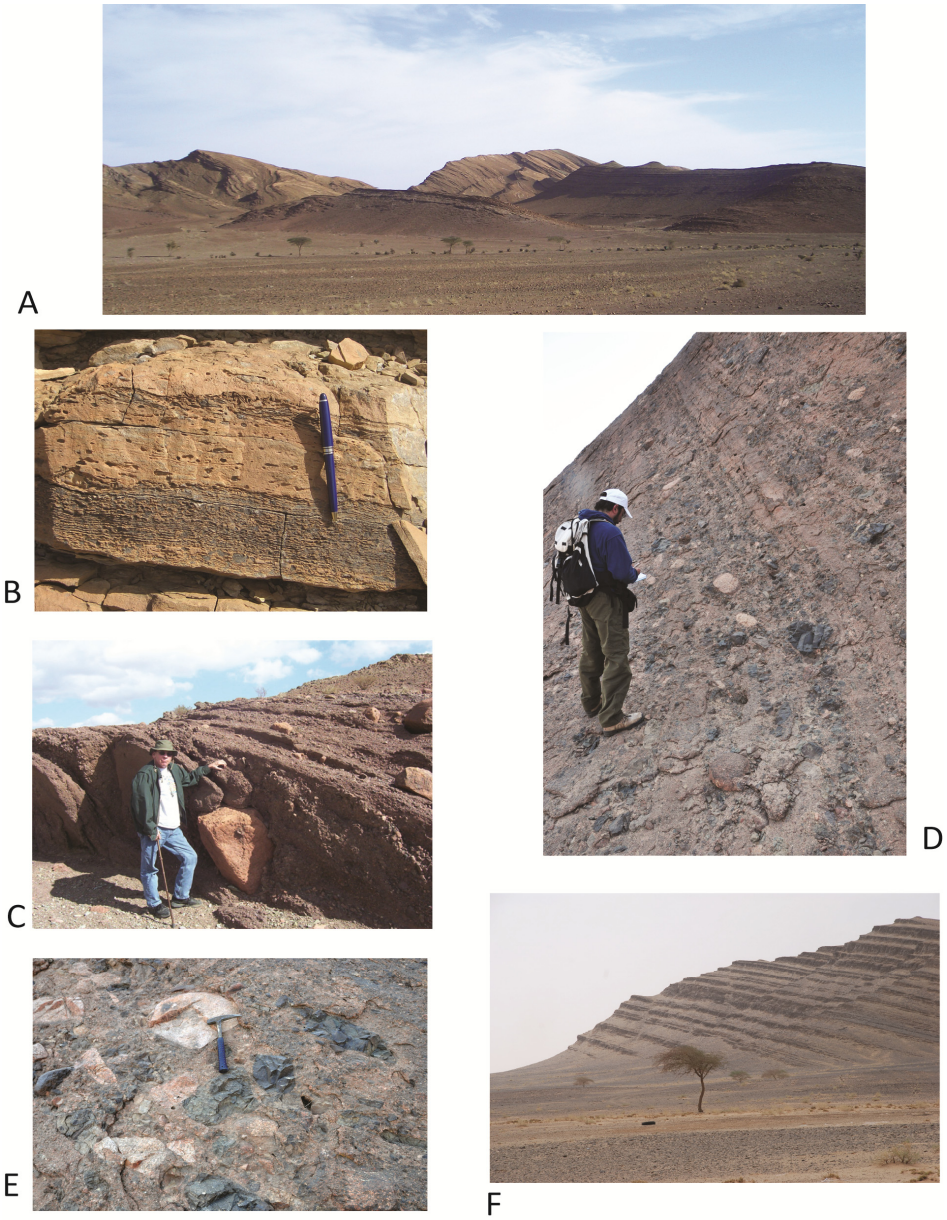

The Badayi' volcanics are typically overlain by an interval of sandstone and pebbly conglomerate marking the base of the overlying Muraykhah formation. The Muraykhah formation otherwise is

characterized by a carbonate-dominated, shallowing upward sequence. In most locations, the Muraykhah formation (and its equivalent interval in the upper Umm al'Aisah formation in the Jifn basin; Figure 20) comprises ~300 m of cherty, gray limestone and dolomite, with interbedded shale, siltstone, minor volcanics (including tuffs), and conglomerate. The carbonates are well bedded (Figure 21A) and show abundant microbial lamination (Figure 21B). Carbonates from the lower Muraykhah formation were likely deposited in relatively deep water, whereas the upper Muraykhah formation carbonates include rippled and crossed-bedded dolarenites, implying a shallow depositional setting [90]. Stromatolites have been described [92,93], but are relatively rare. It has been suggested [94] that the Muraykah formation correlates with the carbonate-dominated Dhaiqa formation in the northwestern Arabian shield [102], which contains a tuff dated at 560 ± 4 Ma [98], as noted above, and the upper Jibalah group in the Antaq basin. However, in the Antaq basin, the upper Jibalah group is dominated by mostly fine sandstone and siltstone arranged in spectacular cycles (Figure 21F). Here, carbonate occurs variably as cement in fine to medium sandstone or in nodules at the tops of the cycles and as massive to poorly laminated beds within the maximum flooding intervals of cycles [96]. It has been argued [94] that the Muraykhah formation records a regional flooding event and marine incursion across the northern and eastern Arabian shield, which is consistent with evidence for shallow marine conditions in the upper Jibalah group in the Antaq basin [96]. However, Sr isotope data from the Dhaiqa formation [102] and from limestone in the Jifn basin (modified from [104]) demonstrate that these basins were at least intermittently restricted. In the Jifn basin, Muraykhah-equivalent carbonates are overlain by a thick wedge of sandstone, shale and conglomerates belonging to the Jifn formation (Figure 20). In the Rubtayn basin, they are overlain by more intermediate to mafic volcanics. Where the upper contact of the Jibalah Group is preserved, it is an angular unconformity, overlain by the lower Cambrian Siq Sandstone [105].

Possible Ediacaran trace and body fossils are reported from the upper part of the Jibalah group. These include *Beltanelloides*-like structures, a putative *Pteridinium* imprint [98,102], and a putative *Harlaniella*-type structure from the Dhaiqa basin [98]. Structures resembling *Aspidella* are reported from the Antaq basin [96], and *Charniodiscus* from the Antaq and Dhaiqa basins [96,98].

Two contrasting depositional models are proposed for the Jibalah group. One envisages that the group was continuously deposited over a large part of the northern Arabian Shield as the result of a shallow-marine incursion, and is now preserved in younger grabens, having been eroded in other places. Based on recent mapping and sampling [100], the same stratigraphy is recognized in several of the Jibalah basins on the Arabian Shield consistent with the interpretation that the unit was originally widespread. The rock assemblages suggest deposition within a single, laterally continuous basin that evolved from proximal fluvial conditions at its base to a marine-shelf setting at the top. The other model envisages that the Jibalah group was never regionally extensive but was deposited syntectonically in fault-controlled basins during Najd faulting under fluvial to shallow-marine or lacustrine conditions [94–96]. In terms of a fault-controlled basin model, the Al Jifn basin (north-central Arabian Shield) is inferred to have developed at a releasing bend along the Halaban-Zarghat fault during a period of dextral shear [95,97]. The Al Kibdi (eastern Arabian Shield) basin is located between two left-stepping strike-slip splays of the Ar Rika fault and is a pull-apart basin that formed during sinistral shear. The Antaq basin (eastern Arabian Shield) is a half-graben that appears to have formed as a result of normal dip-slip movement on the hanging wall, perhaps during

E-W directed extension. The Rubtayn basin (NW Arabian Shield) consists of fault blocks and grabens depressed as a result of subsidence along boundary faults [93].

9. Discussion

The ANS is the product of a ~300 million year cycle of Neoproterozoic accretionary orogeny and crustal growth that evolved from ~870 Ma, the oldest dated rocks in the Makkah batholith and Erkowit pluton in the Jiddah and Haya terranes, to ~560 Ma, the age of some of the youngest granitoids and strata. These rocks formed during a critical episode in Earth history that spanned the transition from Neoproterozoic to Phanerozoic geologic and evolutionary processes and witnessed some of the most important, rapid, and enigmatic changes known in Earth's environment and biota [1,106]. Changes during this period included the breakup of the Rodinia supercontinent, followed by the dispersal and rapid movement of continental nuclei, and the assembly of the new Gondwana supercontinent at the end of the Neoproterozoic. Other changes included important shifts in Earth climate and modifications in the biosphere; some of the most severe glacial episodes known in geologic history covered much of the globe; eukaryotes diversified and gave rise to the first simple animals; the atmosphere and oceans were affected by major fluctuations in their oxygen and iron contents; carbon and strontium isotope compositions of seawater varied dramatically. Orogeny in the ANS began with deformation and metamorphism at about 806 Ma of the juvenile early Neoproterozoic Kurmut terrane and its accretion with the Saharan Metacraton along the Abu Hamed and Dam El Tor fault/thrust belts, precursors of the Keraf suture [107]. The terminal stages of orogeny included the onset of posttectonic A-type granitoid magmatism (~610 Ma onward); orogenic collapse, tectonic escape, and orogen-parallel extension (605–595 Ma); local extension and rifting (620–545 Ma); gneiss core complex formation, exhumation, and cooling (620–580 Ma); NNW-ward thrusting (605–600 Ma); SW-ward and NE-ward thrusting (600–590 Ma); E-W shortening and transpression (620–580 Ma); Najd strike-slip faulting 625–565 Ma); subhorizontal low-angle shearing (605–600 Ma); amalgamation of terranes in the eastern Arabian Shield (<620 Ma); and terminal collision of ANS with the Saharan Metacraton by 580 [11,66]. The large number of volcanosedimentary basins described here evidence the ANS orogenic cycle was punctuated by periods of exhumation, uplift, and erosion, and demonstrate that the tectonic phenomena of mountain building, subsidence, and deposition were closely linked in time and space (Figure 22).

One of the oldest exhumation and erosional events is recorded by deposition of the Hali group (~795–780 Ma). By 795 Ma, volcanic arcs and large TTG-type intrusions had formed in the Al Lith-Bidah and Shwas-Tayyah structural belts. Shortly prior to and during the inferred convergence of these arc systems at 780–765 Ma, part of the Shwas-Tayyah belt was exhumed, uplifted, and eroded. The resulting erosion surface beveled mid-crustal plutonic rocks of the An Nimas complex, suggesting exhumation on the order of 10 km. Epiclastic sediments deposited on this surface were chiefly sand but included pebbles derived from the An Nimas complex. The Hali basin did not last long, and by about 780 Ma, the basin had subsided and was affected by elevated P and T, leading to amphibolite-facies metamorphism of the epiclastics. The rocks were metamorphosed concurrent with shearing within, and on the margin of, the An Nimas complex and emplacement of syntectonic tonalite. Because of overprinting by later orogenesis and lack of focused research, the original size of the Hali basin, its structural controls and likely mechanism of subsidence during and after

sedimentation are unknown. The carbonate member is evidence of subaqueous deposition, but no evidence has been reported to determine whether the environment was lacustrine or marine.

Figure 22. Summary diagram showing temporary relationships between volcanosedimentary basins, glacial intervals, orogenic accretionary events, orogenic collapse events, and secular variation in carbon-isotope composition of shallow-marine carbonates. Timing of glacial events after [41]. See text for discussion of the structural-tectonic features that make up the headings for the two columns labeled "Convergence, amalgamation (sutures, shear zones)" and "Orogenic collapse". The red stars indicate depositional units that contain diamictite–matrix supported pebbles in the case of the Ghamr and Hadiyah groups, and matrix supported boulders in the case of the Jibalah group. These diamictites are consistent with the timing of glacial events, but are not proven to be glacial deposits. Composite seawater carbon-isotope curve on right modified from [104].

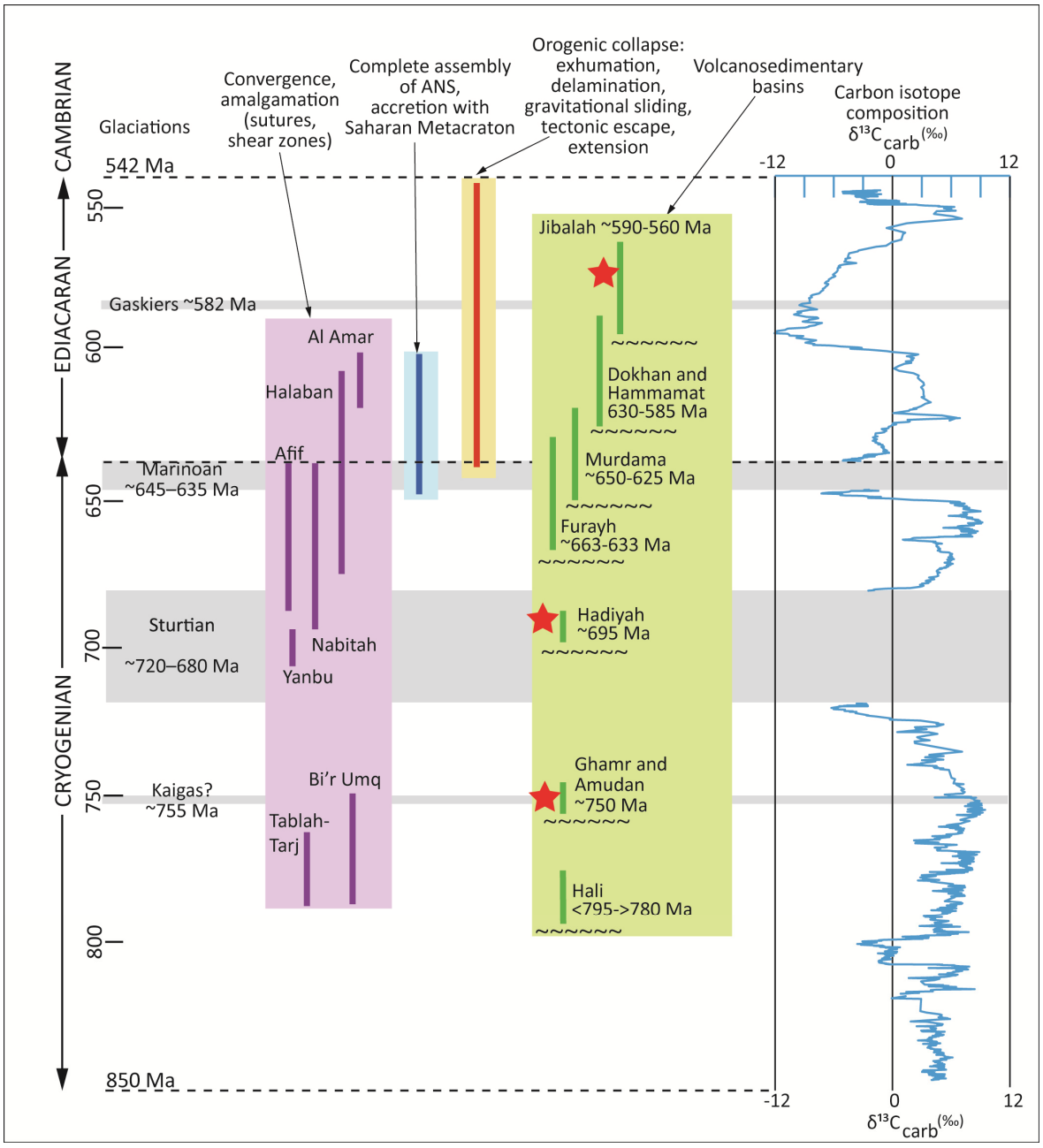

Some 30 million years later, during collision between the Jiddah-Haya and Hijaz-Gebeit terranes along the Bi'r Umq-Nakasib suture, the southern flank of the Jiddah terrane was exhumed. Arc rocks of the Samran, Arj, and Mahd groups and arc-related plutonic rocks were eroded, forming a surface that became covered by sedimentary and volcanic rocks of the Ghamr group and Amudan formation. The Ghamr and Amudan are only weakly metamorphosed implying that, in contrast to the Hali group, they were little buried after deposition. A glaciogeneic diamictite is suspected at the base of the Mahd group beneath the Ghamr group, possibly deposited during an early phase of the Kaigas glacial event, but no glaciogenic deposits are reported for the Ghamr group. It is interesting, however, that broadly coeval metasedimentary rocks in the southern Nubian Shield are reported to contain glaciogenic diamictite and peri-glacial polymict conglomerate and arkose [108]. The location of the Ghamr-Amudan basin on the flank of the Jiddah terrane, alongside the Bi'r Umq suture, on what was probably the upper plate of a convergent margin is consistent with deposition in a retroforeland basin. The rocks were deposited in alluvial fans, drainage channels, and volcanic centers in terrestrial or near-shore submarine environments.

After about 55 million years, orogeny resumed in the ANS with collision between the Jiddah-Gebeit/Gabgaba terranes and the Midyan-Eastern Desert terranes leading to emplacement of ophiolites and development of the Yanbu-Sol Hamed-Allaqi suture. The Hadiyah group was deposited in a trough inboard in the Hijaz terrane from the suture and above the forearc sedimentary wedge of the Al Ays arc. The putative unconformity at the base of the Hadiyah group that cuts down as much as 4 km into the Al Ays arc is evidence of significant exhumation and erosion inboard of the Yanbu suture. We envisage that the Hadiyah basin is a type of retroforeland basin formed in a terrestrial depression on the upper plate adjacent to the Yanbu suture. The basin evolved from a volcanic environment to a locally upward-shallowing sedimentary environment. Coarse clastics derived from the underlying arc rocks of the Al Ays group and its arc-associated intrusion shed into the basin as conglomerate and pebbly sandstone; bimodal volcanic rocks at the base of the group suggest faulting and rifting during initiation of the basin. We note that the Hadiyah group was deposited during the Sturtian glacial event (Figure 22). Further research would be useful to determine whether any of the siliciclastic deposits in the group, such as the matrix-supported pebble and boulder sandstone in the Jammazin member are glaciogenic.

The Furayh basin is a large volcanosedimentary basin at the triple junction between the Jiddah, Hijaz, and Afif terranes. It overlies the Bi'r Umq suture on the south postdating suturing here by about 100 million years, and the Afif suture on the northeast. Volcanism began in the basin ~665 Ma and sedimentation continued until convergence between the Hijaz and Afif terranes and initiation of the Afif suture during the Nabitah orogeny (680–640 Ma). Exhumation along the Bi'r Umq and Afif suture zones allowed Furayh sediments to be deposited on erosion surfaces that locally cut across the sutures. The Furayh basin was dominated by volcanic centers in the west and epiclastic sedimentation in the east. Sedimentary structures are indicative of shallow water to subaerial exposure. Conglomerates in the east and southeast suggest proximity to elevated source regions; volcaniclastic deposits in the west indicate proximity to rapidly unroofing volcanic centers. Carbonates in the Furayh group have not been studied in any detail, but may provide evidence of shallow-marine conditions. If so, they should bear the imprint of the global negative $\delta^{13}C_{carb}$ excursions known to occur globally at this time (Figure 22). Likewise, we might expect some record of the Marinoan glaciation in clastic rocks.

The largest volcanosedimentary basin in the ANS is the Murdama basin. It overlies newly accreted arc systems in the Afif composite terrane and is located between the Nabitah mobile belt on the west and the Halaban suture on the east (Figures 1 and 11). Toward the end of and following these suturing events, a large part of the Afif terrane subsided and became a terrestrial to shallow-marine basin. The underlying arc rocks had been assembled to form the Afif composite terrane by or soon after 685 Ma, but were uplifted and eroded within at least 30 million years, followed by volcanism in the Murdama basin between 650 and 640 Ma, and sedimentation by 630 Ma. The amount of exhumation and erosion was significant, unroofing amphibolite- and granulite-facies metamorphic rocks so that Murdama marine deposits rest on basement probably brought from depths of 15–20 km or more. Subsidence followed major exhumation and erosion of the sub-Murdama basement, affecting a vast region over an area of 700 km by 120 km. The cause of subsidence is unknown. It may have been initiated by faulting and extension, as suggested by bimodal volcanism in the basal volcanic units in the basin. Or it could have been the effect of cooling following Nabitah orogeny and Halaban suturing, the result of delamination, the product of crustal warping as a flexural basin following loading by overthrusting along the Halaban suture, or a combination of these factors; further study is needed to answer this question. What is notable is that, whereas subsidence persisted for perhaps 20 million years while the basin filled and was sufficient to accommodate 10 km or more of sediments, accumulation rates and subsidence were in balance and maintained a shallow sediment-water interface with connections to the sea. The result was that lithologically monotonous sediments containing shallow-water sedimentary structures persisted across the basin and up through the stratigraphic column. As in the case of the Furayh group, the Murdama basin was filled during the Marinoan glacial event. Murdama carbonate is conceivably a favorable rock to sample to detect the Marinoan negative $\delta^{13}C_{carb}$ excursion (Figure 22); arenaceous and rudaceous deposits could be examined for glaciogenic indicators.

Further exhumation and extension marked the development of Ediacaran volcanosedimentary basins. Although consensus on details is lacking, it is generally accepted that Ediacaran exhumation and extension in the ANS resulted from crustal thickening, orogenic collapse, and tectonic escape during terminal orogenesis and assembly of the shield [109]. The process of orogenic collapse and exhumation entailed crustal thinning and widespread extension manifest by normal faulting and low-angle detachments associated with exhumation of gneiss domes and strike-slip sinistral and dextral shearing of the Najd fault system. It is modeled as the result of removal and replacement of thickened lithospheric mantle by delamination [110], was contemporary with a transition from calc-alkaline to alkaline magmatism [111], the emplacement of a significant number of dike swarms [40,112], and enhanced heat along fault systems leading to the formation of syn-extensional plutonism and a triggering of exhumation of hot middle crust [109]. On the basis of Rb-Sr and $^{40}Ar/^{39}Ar$ cooling ages it appears that exhumation was relatively long lived across the region, beginning by ~650 Ma, continuing between 620 and 606 Ma, and ceasing before ~580 Ma [80,113]. Basement rocks in northern Sinai were rapidly exhumed and eroded at about 600 Ma [108] following peak regional metamorphism at about 620 Ma at 7 ± 1 kbar (20–25 km depth) and 650–700 °C. Erosional models for the northern ANS envisage that the region underwent more than 3 km uplift following mantle delamination, which triggered rapid unroofing of about 10–12 km of crust in about 20 million years. This lowered the average relief by about 2 km and formed the surface and basins covered by the Elat and Saramuj Conglomerates [109,114]. The Elat Conglomerate overlies

630–605 Ma granitoids [64]; the Saramuj Conglomerate overlies 625–600 Ma granitoids [115]. Erosional denudation may have been followed by isostatic uplift but erosion, as well as thermal subsidence, ultimately lowered the surface to sea level [110]. Metamorphism and cooling during exhumation is dated in the eastern ANS by hornblende $^{40}Ar/^{39}Ar$ ages between about ~616 and 601 Ma [116,117]. In the southern ANS, hornblende and biotite $^{40}Ar/^{39}Ar$ cooling ages of 577 ± 2 Ma and 577 ± 5 Ma [118] are interpreted as evidence of rapid Ediacaran cooling and exhumation following terminal collision and the cessation of ductile deformation in the vicinity of the Keraf suture.

Ediacaran subsidence and depositional centers developed in many parts of the ANS during this period of orogenic collapse, extension, and exhumation. Basins associated with strike-slip faulting may be variably classified as transform, transpressional or transtensional. Others, having no causal link with strike-slip faulting, originated during normal faulting in regional extension regimes. Some basins had complex origins that began as fault-bounded rifts and half-grabens and evolved into pull-apart basins at bends in Najd shear zones. Others are referred to variously by terms that include foreland, intramontane, and piggy-back basins. The lithologic character of the Ediacaran basins suggest that the western ANS was at a higher elevation than the eastern ANS during the closing stages of ANS orogeny. Molasse in the western basins was deposited in terrestrial basins, under subaerial to shallow-water conditions. The eastern basins, characterized by the Jibalah group, had mixed terrestrial and shallow-marine environments. They were affected by a late Ediacaran marine transgression [40] and regional flooding event or had at least some connection to the ocean. Clastic material in the basins was shed from elevated basin margins in the case of individual fault-bounded basins, or possibly introduced by major fluvial systems of continental proportions. Conglomerates contain clasts derived from underlying arc rocks. Carbonates indicate shallow-marine or more restricted environments. Isotopic data consistent with the prominent Shuram negative $\delta^{13}C_{carb}$ excursion are not reported, although boulder-clast diamictite and paraconglomerate in some Jibalah basins are conceivably glaciogenic.

The most prominent unconformity in the ANS is the extensive erosion surface that removed between 2 and 10 km of basement rock [114,119] prior to deposition of lower Paleozoic siliciclastic rocks that blanket the shield. This surface, the sub-Siq or Angudan unconformity [94], had originated by about 535 Ma. The unconformities beneath the Ediacaran basins predated but were probably precursors of the sub-Siq surface. All these surfaces may be multigenerational, the result of more than one period of erosion during the Ediacaran. In the northeastern ANS, for example, erosion between 640 and 615 Ma formed the surface on which the Hibshi (632 Ma) and Jurdhawiyah (612–594 Ma) groups were deposited [54]; the Jibalah group was deposited on a surface that truncates 625 Ma rhyolite and 618 Ma microgranite; and granites are differentially preserved whereby late Ediacaran granites (580–570 Ma) retain their apical parts and their extrusive equivalents, whereas early Ediacaran plutons (Idah suite: 620–615 Ma) are deeply eroded. This granite pattern suggests that Abanat suite plutons were intruded into crust that had already been exhumed and denuded, but were themselves little eroded prior to deposition of the lower Paleozoic sandstone. Similar multiple periods of erosion are suggested for the northern parts of the Arabian Shield and Sinai Peninsula in a region where the emplacement of A-type rocks was preceded by a phase of extensive erosion associated with lithospheric extension and crustal rupture [120].

As stated many times, the unconformities at the bases of the volcanosedimentary successions considered in this review are unambiguous evidence of periodic exhumation and erosion of basement

crust; they imply strong uplift of rocks that were once deep-seated in the crust and removal of material. The causes of basement exhumation in the process of ANS orogeny are far from clear however. Exhumation can occur in virtually any geologic setting. It is conventionally considered to be driven by three main processes: normal faulting or extension, ductile lithospheric thinning, and erosion [121], to which can be added, with specific reference to the Eastern Desert in the Nubian Shield, gravitational sliding of supracrustal rocks from core complexes. In this context it is important to recognize that convergent margins can exhibit coeval compressional and extensional strain, so that orogens may undergo horizontal contraction and horizontal extension at different levels at the same time. This is an important constraint for models that may be developed to account for exhumations considered in this review. The specific causes of the periodic phases of ANS exhumation described here, evidenced by the volcancosedimentary basins, need to be established by further structural and tectonic analysis. Other major gaps in relevant information about the volcanosedimentary basins concern the cause(s) and rates of basin subsidence and whether or not basins coeval with global glacial periods contain glaciogenic deposits or evidence of glacial-related isotopic excursions. Although potential glacial diamictite is reported for the Ghamr, Hadiyah, and some Jibalah basins, the character and origin of the diamictite needs to be unambiguously determined. The Ghamr, Hadiyah, Furayh, and Murdama basins, broadly contemporary with the Kaigas and Marinoan events, should be searched for solid evidence of glaciation and if such evidence is absent, reasons should be considered for its absence such as whether glaciation had restricted extents in the ANS because of topography and(or) variable paleoclimatic conditions or that conditions were not conducive to preservation of appropriate rocks.

10. Conclusions

The main conclusion we draw from this survey of volcanosedimentary basins is that orogeny in the ANS was closely linked with subsidence and deposition. Mountain building created uplands, but erosion denuded exhumed basement and created vast amounts of clastic debris that shed into terrestrial and shallow-marine basins. Sectors of the ANS orogenic belt, particularly in the east, were penetrated by seaways or flooded by marine incursions. Western parts, at least during the late Cryogenian and Ediacaran, were above sea level and were subaerial to shallow-water depocenters of volcanic rocks and terrigenous sediments.

Importantly, the preservation of the volcanosedimentary successions in the ANS, despite ongoing orogeny, motivates research aimed at elucidating Neoproterozoic geologic processes. The mineralogy and textures of sandstones and siltstones, examination of sedimentary facies and isotopic compositions of seawater precipitates, and reconstructions of depositional environments will provide information about weathering and, by implication, of Neoproterozoic climate. The Ediacaran basins have potential to yield more information on late Neoproterozoic biospheric evolution, possibly including the earliest animals. Detrital zircon analysis in these basins will give information about the sources of sediment and the distribution of Neoproterozoic, Paleoproterozoic, and Archean crustal blocks in the Mozambique Ocean. Overall, because of their excellent exposure and preservation despite being part of an accretionary orogen, these volcanosedimentary basins are a world-class natural laboratory for testing concepts about crustal growth at the end of the Precambrian and a prime target for calibrating Neoproterozoic Earth history.

References

1. Stern, R.J. Arc assembly and continental collision in the neoproterozoic East African Orogen: Implications for the consolidation of Gondwanaland. *Annu. Rev. Earth Planet Sci*. **1994**, *22*, 319–351.
2. Collins, A.S.; Pisarevsky, S.A. Amalgamating eastern Gondwana: The evolution of the circum-Indian Orogens. *Earth-Sci. Rev.* **2005**, *71*, 229–270.
3. Johnson, P.R.; Kattan, F.H. *The Geology of the Saudi Arabian Shield*; Saudi Geological Survey: Jiddah, Saudi Arabia, 2012; pp. 1–479.
4. Stern, R.J. Crustal evolution in the East African Orogen: A neodymium isotopic perspective. *J. Afr. Earth Sci*. **2002**, *34*, 109–117.
5. Whitehouse, M.J.; Windley, B.F.; Stoeser, D.B.; Al-Khirbash, S.; Ba-Bttat, M.A.O.; Haider, A. Precambrian basement character of Yemen and correlations with Saudi Arabia and Somalia. *Precambrian Res*. **2001**, *105*, 357–369.
6. Whitehouse, M.J.; Stoeser, D.B.; Stacey, J.S. The Khida terrane-geochronological and isotopic evidence for Paleoproterozoic and Archean crust in the Eastern Arabian Shield of Saudi Arabia. *Gondwana Res*. **2001**, *4*, 200–202.
7. Cox, G.M.; Lewis, C.J.; Collins, A.S.; Halverson, G.P.; Jourdan, F.; Foden, J.; Nettle, D.; Kattan, F. Ediacaran Terrane accretion within the Arabian-Nubian Shield. *Gondwana Res.* **2011**, *21*, 341–352.
8. Abdelsalam, M.G.; Abdel-Rahman, E.M.; El-Faki, E.M.; Al-Hur, B.; El-Bashier, F.R.M.; Stern, R.J.; Thurmond, A.L. Neoproterozoic deformation in the northeastern part of the Saharan Metacraton, northern Sudan. *Precambrian Res*. **2003**, *123*, 203–221.
9. Johnson, P.R. Post-amalgamation basins of the NE Arabian Shield and implications for Neoproterozoic III tectonism in the Northern East African Orogen. *Precambrian Res*. **2003**, *123*, 321–337.
10. Igersoll, R.V. Tectonics of sedimentary basins, with revised nomenclature. In *Tectonics of Sedimentary Basins, Recent Advances*; Busby, C., Azor, A., Eds.; Wiley-Blackwell: Chichester, UK, 2012; pp. 3–43.
11. Johnson, P.R.; Andresen, A.; Collins, A.S.; Fowler, A.R.; Fritz, H.; Ghebreab, W.; Kusky, T.; Stern, R.J. Late Cryogenian-Ediacaran history of the Arabian-Nubian Shield: A review of depositional, plutonic, structural, and tectonic events in the closing stages of the northern East African Orogen. *J. Afr. Earth Sci.* **2011**, *61*, 167–232.
12. Hadley, D.G.; Schmidt, D.L. Sedimentary rocks and basins of the Arabian Shield and Their evolution. In *Evolution and Mineralization of the Arabian-Nubian Shield*; Cooray, P.G., Tahoun, S.A., Eds.; Institute of Applied Geology, King Abdulaziz University: Jiddah, Saudi Arabia, 1980; Bulletin 3, Volume 4, pp. 26–50.
13. Ahmed Suliman, E.T.B. Keraf shear zone, NE Sudan: Geodynamic characteristics of the Nile Craton-Nubian Shield boundary. Ph.D. Thesis, Technical University Berlin, Berlin, Germany, 2000.
14. Kemp, J. The Kuara formation (northern Arabian Shield); definition and interpretation: A probable fault-trough sedimentary succession. *J. Afr. Earth Sci.* **1996**, *27*, 507–523.

15. Kemp, J. Caldera-related Volcanic Rocks in the Shammar Group, northern Arabian Shield. *J. Afr. Earth Sci.* **1996**, *27*, 551–572.
16. Schmidt, D.L.; Hadley, D.G.; Greenwood, W.R.; Gonzalez, L.; Coleman, R.G.; Brown, G.F. *Stratigraphy and Tectonism of the Southern Part of the Precambrian SHIELD of Saudi Arabia*; Saudi Arabian Directorate General of Mineral Resources: Jiddah, Saudi Arabia, 1973; Bulletin 8, pp. 1–13.
17. Greenwood, W.R. *Geologic Map of the Abha Quadrangle, Sheet 18F, Kingdom of Saudi Arabia*; Saudi Arabian Deputy Ministry for Mineral Resources: Jiddah, Saudi Arabia, 1985; GM 75, pp. 1–27.
18. Genna, A.; Guerrot, C.; Deschamps, Y.; Nehlig, P.; Shanti, M. Les formations Ablah d'Arabie Saoudite (datation et implication géologique). *C.R. Acad. Sci. IIA* **1999**, *329*, 661–667.
19. Johnson, P.R.; Kattan, F.H.; Wooden, J.L. Implications of SHRIMP and microstructural data on the age and kinematics of shearing in the Asir Terrane, southern Arabian Shield, Saudi Arabia. *Gondwana Res.* **2001**, *4*, 172–173.
20. Cooper, J.A.; Stacey, J.S.; Stoeser, D.B.; Fleck, R.J. An evaluation of the zircon method of isotopic dating in the southern Arabian Craton. *Contrib. Mineral. Petr.* **1979**, *68*, 429–439.
21. Blasband, B.B. Neoproterozoic Tectonics of the Arabian-Nubian Shield. Ph.D. Thesis, Mededelingen van die Faculteit Geowetenschappen, Universiteit Utrecht, Utrecht, The Netherlands, 2006.
22. Hamimi, Z.; El-Shafei, M.; Kattu, G.; Matsah, M. Transpressional regime in southern Arabian Shield: Insights from Wadi Yiba area, Saudi Arabia. *Miner. Petrol*. **2012**, doi:10.1007/s00710-012-0198-6.
23. Kattu, G.; Hamimi, Z.; El-Shafei, M. *Transpressional Regime in Asir Tectonic Terrane, Saudi Arabia*; Lap Lambert Academic Press: Saarbrücken, Germany, 2013; pp. 1–120.
24. Kemp, J.; Gros, Y.; Prian, J.P. *Geologic Map of the Mahd adh Dhahab Quadrangle, Sheet 23E, Kingdom of Saudi Arabia*; Saudi Arabian Deputy Ministry for Mineral Resources: Jiddah, Saudi Arabia, 1982; GM 64, pp. 1–39.
25. Ramsay, C.R. *Geologic Map of the Rabigh Quadrangle, Sheet 22D, Kingdom of Saudi Arabia*; Saudi Arabian Deputy Ministry for Mineral Resources: Jiddah, Saudi Arabia, 1986; GM 84, pp. 1–49.
26. Johnson, P.R.; Abdelsalam, M.G.; Stern, R.J. The Bi'r Umq-Nakasib suture zone in the Arabian-Nubian Shield: A key to understanding crustal growth in the east African Orogen. *Gondwana Res.* **2003**, *6*, 523–530.
27. Hargrove, U.S. Crustal evolution of the Neoproterozoic Bi'r Umq suture zone, Kingdom of Saudi Arabia: Geochronological, Isotopic, and Geochemical Constraints. Ph.D. Thesis, University of Texas, Dallas, TX, USA, 2006.
28. Calvez, J.Y.; Kemp, J. *Geochronological Investigations in the Mahd Adh Dhahab Quadrangle, Central Arabian Shield*; Deputy Ministry for Mineral Resources: Jiddah, Saudi Arabia, 1982; BRGM-TR-02-5, pp. 1–41.
29. Sahl, M.; Smith, J.W. *Geologic Map of the Al Muwayh Quadrangle Sheet 22E, Kingdom of Saudi Arabia*; Saudi Arabian Directorate General of Mineral Resources: Jiddah, Saudi Arabia, 1986; GM 88, pp. 1–29.

30. Stern, R.J.; Avigad, D.; Miller, N.R.; Beyth, M. Evidence for the snowball Earth hypothesis in the Arabian-Nubian Shield and the east African Orogen. *J. Afr. Earth Sci.* **2006**, *44*, 1–20.
31. Stern, R.J.; Johnson, P.R.; Ali, K.A.; Mukherjee, S. Evidence for early and mid-cryogenian glaciation in the northern Arabian-Nubian Shield (Egypt, Sudan, and western Arabia). In *The Geological Record of Neoproterozoic Glaciation*; Arnaud, E., Halverson, G.P., Shield-Zhou, G., Eds.; Geological Society: London, UK, 2011; Memoirs 36, pp. 277–284.
32. Pallister, J.S.; Stacey, J.S.; Fischer, L.B.; Premo, W.R. Precambrian ophiolites of Arabia: Geologic settings, U-Pb geochronology, Pb-isotope characteristics, and implications for continental accretion. *Precambrian Res.* **1988**, *38*, 1–54.
33. Pellaton, C. *Geologic Map of the Yanbu'al Bahr Quadrangle, Sheet 24C, Kingdom of Saudi Arabia*; Saudi Arabian Directorate General of Mineral Resources: Jiddah, Saudi Arabia, 1979; GM 48, pp.1–16.
34. Kemp, J. *Geologic map of the Wadi Al Ays Quadrangle, Sheet 25C, Kingdom of Saudi Arabia*; Saudi Arabian Deputy Ministry for Mineral Resources: Jiddah, Saudi Arabia, 1981; GM 53, pp. 1–39.
35. Hassan, M.M.; Abu-Alam, T.S.; Stuewe, K.; Meyer, S.; Passchier, C.W. On the Evolution of the Arabian-Nubian Shield and the Largest Shear Zone on Earth. In Proceedings of American Geophysical Union Fall Meeting, San Francisco, CA, USA, 3–7 December 2012.
36. Kennedy, A.; Johnson, P.R.; Kattan, F.H. *SHRIMP Geochronology in the Northern Arabian Shield Part I: Data Acquisition*; Saudi Geological Survey: Jiddah, Saudi Arabia, 2004; SGS-OF-2004-11, pp. 1–28.
37. Kennedy, A.; Johnson, P.R.; Kattan, F.H. *SHRIMP Geochronology in the Northern Arabian Shield Part II: Data Acquisition 2004*; Saudi Geological Survey: Jiddah, Saudi Arabia, 2005; SGS-OF-2005–10, pp. 1–44.
38. Hadley, D.G. *Geologic Map of the Sahl al Matran Quadrangle, Sheet 26C, Kingdom of Saudi Arabia*; Saudi Arabian Deputy Ministry for Mineral Resources: Jiddah, Saudi Arabia, 1987; GM 86, pp. 1–24.
39. Johnson, P.R. *Proterozoic Geology of Western Saudi Arabia—North-Central Sheet: Explanatory Notes on Precambrian Stratigraphic Relations*; Saudi Arabian Deputy Ministry for Mineral Resources: Jiddah, Saudi Arabia, 1995; USGS-OF-95-5, pp. 1–44.
40. Genna, A.; Nehlig, P.; le Goff, E.; Guerrot, C.; Shanti, M. Proterozoic tectonism of the Arabian Shield. *Precambrian Res.* **2002**, *117*, 21–40.
41. MacGabhann, B.A. Age Constraints on Precambrian Glaciations and the Subdivision of Neoproterozoic Time. Available online: http://www.academia.edu/1773698/Age_constraints_on_Precambrian_glaciations_and_the_subdivision_of_Neoproterozoic_time (accessed on 25 April 2013).
42. Macdonald, F.A.; Schmidt, M.D.; Crowley, J.L.; Roots, C.F.; Jones, D.S.; Maloof, A.C.; Strauss, J.V.; Cohen, P.A.; Johnston, D.T.; Schrag, D.P. Calibrating the Cryogenian. *Science* **2010**, *327*, 1241–1243.
43. Delfour, J. *Geologic Map of the Al Hissu Quadrangle, Sheet 24E, Kingdom of Saudi Arabia*; Saudi Arabian Deputy Ministry for Mineral Resources: Jiddah, Saudi Arabia, 1981; GM 58, pp. 1–47.

44. Johnson, P.R. *Proterozoic Geology of Western Saudi Arabia, North-Central Sheet (Revised, Digital Edition): Notes on Proterozoic Stratigraphy*; Saudi Geological Survey: Jiddah, Saudi Arabia, 2004; SGS-OF-2004-5, pp. 1–31.
45. Camp, V.E. *Geologic map of the Umm al Birk Quadrangle, Sheet 23D, Kingdom of Saudi Arabia*; Saudi Arabian Directorate General of Mineral Resources: Jiddah, Saudi Arabia, 1986; GM 87, pp. 1–30.
46. Pellaton, C. *Geologic Map of the Al Madinah Quadrangle, Sheet 24D, Kingdom of Saudi Arabia*; Saudi Arabian Deputy Ministry for Mineral Resources: Jiddah, Saudi Arabia, 1981; GM 52, pp. 1–19.
47. Stoeser, D.B.; Stacey, J.S. Evolution, U-BP geochronology, and isotope geology of the Pan-African Nabitah orogenic belt of the Saudi Arabian Shield. In *The Pan-African belt of NE Africa and Adjacent Areas*; Friedrich Viewig and Sohn: Braunschweig/Wiesbaden, Germany, 1988; pp. 227–288.
48. Zahran, A.M.; Stewart, I.C.F.; Johnson, P.R.; Basahel, M.H. *Aeromagnetic-Anomaly Maps of Central and Western Saudi Arabia*; Saudi Geological Survey: Jiddah, Saudi Arabia, 2003; SGS-OF-2002-8, pp.1–6.
49. Agar, R.A. The Bani Ghayy group: Sedimentation and volcanism in pull-apart grabens of the Najd strike-slip orogen, Saudi Arabian Shield. *Precambrian Res*. **1986**, *31*, 259–274.
50. Greene, R.C. *Stratigraphy of the Late Proterozoic Murdama Group, Saudi Arabia*; U.S. Government Printing Office: Washington, DC, USA, 1993.
51. Delfour, J. *Geologic Map of the Halaban Quadrangle, Sheet 23G, Kingdom of Saudi Arabia*; Saudi Arabian Directorate General of Mineral Resources: Jiddah, Saudi Arabia, 1979; GM 46, pp. 1–32.
52. Delfour, J. *Geologic Map of the Wadi ar Rika Quadrangle, Sheet 22G, Kingdom of Saudi Arabia*; Saudi Arabian Directorate General of Mineral Resources: Jiddah, Saudi Arabia, 1980; GM 51, pp. 1–34.
53. Kennedy, A.; Kozdroj, W.; Kattan, F.H.; Ziolkowska-Kozdroj, M.; Johnson, P.R. *SHRIMP Geochronology in the Arabian Shield (Midyan Terrane, Afif Terrane, Ad Dawadi Terrane) and Nubian Shield (Central Eastern Desert Terrane) Part IV: Data Acquisition 2008*; Saudi Geological Survey: Jiddah, Saudi Arabia, 2010; SGS-OF-2010-10, pp. 1–101.
54. Cole, J.C.; Hedge, C.E. *Geochronologic Investigation of Late Proterozoic Rocks in the Northeastern Shield of Saudi Arabia*; Saudi Arabian Deputy Ministry of Mineral Resources; Jiddah, Saudi Arabia, 1986; USGS-TR-05-5, pp. 1–42.
55. Letalenet, J. *Geologic Map of the Afif Quadrangle, Sheet 23F, Kingdom of Saudi Arabia*; Saudi Arabian Directorate General of Mineral Resources: Jiddah, Saudi Arabia, 1979; GM 47, pp. 1–20.
56. Cole, J.C. *Geologic Map of the Aban al Ahmar Quadrangle, Sheet 25F, Kingdom of Saudi Arabia*; Saudi Arabian Deputy Ministry for Mineral Resources: Jiddah, Saudi Arabia, 1988; GM 105, pp. 1–45.
57. Roobol, M.J.; Ramsay, C.R.; Jackson, N.J.; Darbyshire, D.P.F. Late Proterozoic lavas of the central Arabian Shield—Evolution of an ancient volcanic arc system. *J. Geol. Soc. Lond.* **1983**, *140*, 185–202.

58. Johnson, P.R. *Proterozoic Geology of Western Saudi Arabia, East-Central Sheet: Description of Proterozoic Map Units*; Saudi Arabian Deputy Ministry for Mineral Resources: Jiddah, Saudi Arabia, 1996; USGS-OF-96-4, pp. 1–71.
59. Williams, P.L.; Vaslet, D.; Johnson, P.R.; Berthiaux, A.; Le Strat, P.; Fourniguet, J. *Geologic Map of the Jabal Habashi Quadrangle, Sheet 26F, Kingdom of Saudi Arabia*; Saudi Arabian Deputy Ministry for Mineral Resources: Jiddah, Saudi Arabia, 1986; GM 98, pp. 1–52.
60. Dickinson, W.R.; Suczek, C.A. Plate tectonics and sandstone compositions. *Am. Assoc. Petroleum Geol. Bull.* **1979**, *63*, 2164–2182.
61. Dickinson, W.R.; Beard, L.S.; Brakenridge, G.R.; Erjavec, J.L.; Ferguson, R.C.; Inman, K.F.; Knepp, R.A.; Lindberg, F.A.; Ryberg, P.T. Provenance of North American Phanerozoic sandstones in relation to tectonic setting. *Geol. Soc. Am. Bull.* **1983**, *93*, 222–235.
62. Jackson, N.J.; Basahel, A.N.; Cooray, P.G., Darbyshire, D.P.F. *Late Precambrian (Sequence A) Rocks of the East Central Shield of Saudi Arabia*; Faculty of Earth Sciences, King Abdulaziz University: Jiddah, Saudi Arabia, 1983; Bulletin 5, pp. 119–134.
63. Wallace, C.A. *Lithofacies and Depositional Environments of the Maraghan Formation and Speculation on the Origin of Gold in Ancient Mines, an Najadi Area, Kingdom of Saudi Arabia*; Saudi Arabian Deputy Ministry for Mineral Resources: Jiddah, Saudi Arabia, 1986; USGS-OF-06-6, pp. 1–19.
64. Morag, N.; Avigad, D.; Gerdes, A.; Harlavan, Y. 1000–580 Ma crustal evolution in the northern Arabian-Nubian Shield revealed by U-Pb-Hf of detrital zircons from late Neoproterozoic sediments (Elat area, Israel). *Precambrian Res.* **2012**, *206–211*, 197–212.
65. Meiler, M.; Reshef, M.; Shulman, H. Late Proterozoic-Paleozoic geology of the Golan Heights and its relation to the surrounding Arabian Platform. In *Earth and Environmental Sciences*; Dar, I.A., Dar, M.A., Eds.; InTech: Rijeka, Croatia, 2011.
66. Fowler, A.; Osman, A.F. Sedimentation and inversion history of three molasse basins of the western Central Eastern Desert of Egypt: Implications for the tectonic significance of Hammamat basins. *Gondwana Res.* **2013**, *23*, 1511–1534.
67. Breitkreuz, C.; Eliwa, H.; Khalaf, I.; El Gameel, K.; Bühler, B.; Sergeev, S.; Larinov, A.; Murata, M. Neoproterozoic SHRIMP U-BP zircon agers of silica-rich Dokhan Volcanics in the Northeastern Desert, Egypt. *Precambrian Res.* **2010**, *182*, 163–174.
68. Davies, F.B. *Geologic Map of the Al Wajh Quadrangle, Sheet 26B, Kingdom of Saudi Arabia*; Saudi Arabian Deputy Ministry for Mineral Resources: Jiddah, Saudi Arabia, 1985; GM 83, pp. 1–27.
69. Abdel-Rahman, A.M.; Doig, R. The Rb-Sr geochronologic evolution of the Ras Gharib segment of the northern Nubian Shield. *J. Geol. Soc. Lond.* **1987**, *144*, 577–586.
70. Stern, R.J.; Hedge, C.E. Geochronologic and isotopic constraints on late Precambrian crustal evolution in the Eastern desert of Egypt. *Am. J. Sci.* **1985**, *285*, 97–127.
71. Wilde, S.A.; Youssef, K. Significance of SHRIMP U-BP dating of the Imperial Porphyry and associated Dokhan Volcanics, Gebel Dokhan, north Eastern Desert, Egypt. *J. Afr. Earth Sci.* **2000**, *31*, 403–413.

72. Wilde, S.A.; Youssef, K. A re-evaluation of the origin and setting of the late Precambrian Hammamat Group based on SHRIMP U-Pb dating of detrital zircons from Gebel Umm Tawat, North Eastern Desert, Egypt. *J. Geol. Soc. Lond.* **2002**, *159*, 595–604.
73. Willis, K.M.; Stern, R.J.; Clauer, N. Age and geochemistry of late Precambrian sediments of the Hammamat Series from the Northeastern Desert of Egypt. *Precambrian Res.* **1988**, *42*, 173–187.
74. Fritz, H.; Wallbrecher, E.; Khudeir, A.A.; Abu El Ela, F.; Dallmeyer, D.R. Formation of Neoproterozoic metamorphic core complexes during oblique convergence (Eastern Desert, Egypt). *J. Afr. Earth Sci.* **1996**, *32*, 311–329.
75. Loizenbauer, J.; Wallbrecher, E.; Fritz, H.; Neumayer, P.; Khudeir, A.A.; Kloetzli, U. Structural geology, single zircon ages and fluid inclusion studies of the Meatiq metamorphic core complex: Implications for Neoproterozoic tectonics in the Eastern Desert of Egypt. *Precambrian Res.* **2001**, *110*, 357–383.
76. Grothaus, B.; Eppler, D.; Ehrlich, R. Depositional environments and structural implications of the Hammamat Formation, Egypt. *Annu. Geol. Surv. Egypt* **1979**, *9*, 564–590.
77. Abdeen, M.M.; Greiling, R.O. A quantitative structural study of late Pan-African compressional deformation in the Central Eastern Desert (Egypt) during Gondwana assembly. *Gondwana Res*. **2005**, *8*, 457–471.
78. El-Wahed, M.A.A. The role of the Najd Fault System in the tectonic evolution of the Hammamat molasse sediments, Eastern Desert, Egypt. *Arab. J. Geosci*. **2009**, *3*, 1–26.
79. Shalaby, A.; Stüwe, K.; Fritz, H.; Makroum, F. The El Mayah molasse basin in the Eastern Desert of Egypt. *J. Afr. Earth Sci.* **2006**, *45*, 1–15.
80. Andresen, A.; El-Rus, M.A.A.; Myhre, P.I.; Boghdady, G.Y. U-Pb TIMS age constraints on the evolution of the Neoproterozoic Meatiq gneiss dome, Eastern Desert. Egypt. *Int. J. Earth Sci*. **2009**, *98*, 481–497.
81. Bregar, M.; Bauernhofer, A.; Pelz, K.; Kloetzli, U.; Fritz, H.; Neumayr, P. A late Neoproterozoic magmatic core complex in the Eastern Desert of Egypt: Emplacement of granitoids in a wrench-tectonic setting. *Precambrian Res.* **2002**, *118*, 59–82.
82. Fritz, H.; Messner, M. Intramontane basin formation during oblique convergence in the Eastern Desert of Egypt: Magmatically versus tectonically induced subsidence. *Tectonophysics* **1999**, *315*, 145–162.
83. Eliwa, H.; Breitkreuz, C.; Khalaf, I.; El Gameel, K. Depositional styles of early Ediacaran terrestrial volcanosedimentary succession in Gebel El Urf area, North Eastern Desert, Egypt. *J. Afr. Earth Sci.* **2010**, *57*, 328–344.
84. Stern, R.J.; Gottfried, D. Petrogenesis of late Precambrian (575–600 Ma) bimodal suite in northeast Africa. *Contrib. Mineral. Petr.* **1986**, *92*, 492–501.
85. Mohammed, F.H.; Moghazi, A.M.; Hassanen, M.A. Geochemistry, petrogenesis and tectonic setting of late Neoproterozoic Dokhan-type volcanic rocks in the Fatira area, eastern Egypt. *Inter. J. Earth Sci.* **2000**, *88*, 764–777.
86. Eliwa, H.A.; Kimura, J.-I.; Itaya, T. Late Neoproterozoic Dokhan Volcanics, north Eastern Desert, Egypt: Geochemistry and petrogenesis. *Precambrian Res*. **2006**, *151*, 31–52.
87. Hedge, C.E. *Precambrian Geochronology of Part of Northwestern Saudi Arabia*; Saudi Arabian Deputy Ministry for Mineral Resources: Jiddah, Saudi Arabia, 1984; USGS-OF-04-31, pp. 1–12.

88. Kennedy, A.; Kozdroj, W.; Kadi, K.; Ziolkowska-Kozdroj, M.; Johnson, P.R. *SHRIMP Geochronology of the Arabian Shield (Midyan Terrane, Afif Terrane) and Nubian Shield (Central Eastern Desert Terrane) Part V: Data Acquisition 2009*; Saudi Geological Survey: Jiddah, Saudi Arabia, 2010; SGS-OF-2010-11, pp. 1–80.
89. Pease, V.; Kadi, K.; Whitehouse, M.; Kozdroj, W. The provenance of Proterozoic sediments of the Midyan terrane, Saudi Arabia from U-Pb zircon SIMS ages. *Precambrian Res.* **2013**, Submitted for Publication.
90. Hamimi, Z.; Matsah, M.; El-Shafei, M.; El-Fakharani, A.; Shujoon, A.; Al-Gabali, M. Wadi Fatima thin-skinned foreland FAT belt: A post-amalgamation marine basin in the Arabian Shield. *Open J. Geol*. **2012**, *2*, 271–293.
91. Grainger, D.J. GeoArabia field trips: The late Proterozoic Fatima group near Jiddah. *Geoarabia* **2001**, *6*, 103–114.
92. Delfour, J. Le Groupe de J'Balah, une nouvelle unité du bouclier arabe (The Jubaylah group, a new unit of the Arabian Shield). *Fr. Bur. Rech. Géol. Min. Bull.* **1970**, *4*, 19–32.
93. Hadley, D.G. *The Taphrogeosynclinal Jubaylah Group in the Mashhad Area, Northwestern Hijaz, Kingdom of Saudi Arabia*; Saudi Arabian Directorate General of Mineral Resources: Jiddah, Saudi Arabia, 1975; Bulletin 10, pp. 1–10.
94. Al-Husseini, M. Late Ediacaran to early Cambrian (Infracambrian) Jibalah group of Saudi Arabia. *Geoarabia* **2011**, *16*, 69–90.
95. Kusky, T.M.; Matsah, M.I. Neoproterozoic dextral faulting on the Najd fault system, Saudi Arabia, preceded sinistral faulting and escape tectonics related to closure of the Mozambique Ocean. *Geol. Soc. Spec. Publ.* **2003**, *206*, 327–361.
96. Nettle, D. A sequence stratigraphic, geochronological and chemostratigraphic investigation of the Ediacaran Antaq basin, eastern Arabian Shield, Saudi Arabia. M.Sc. Thesis, University of Adelaide, Adelaide, Australia, 2009; pp. 1–84.
97. Matsah, M.I.; Kusky, T.M. Sedimentary facies of the Neoproterozoic Al-Jifn basin, NE Arabian Shield: relationships to the Halaban-Zarghat (Najd) fault system and the closure of the Mozambique Ocean. In *Aspects of Pan-African Tectonics*; De Wall, H., Greiling, R.O., Eds.; Forschungszentrum Jülich: Jülich, Germany, 1999; Bilateral Series of the International Bureau 32; pp. 17–21.
98. Vickers-Rich, P.; Ivantsov, A.; Kattan, F.H.; Johnson, P.R.; Al Qubsani, A.; Kashghari, W.; Leonov, M.; Rich, T.; Linnemann, U.; Hofmann, M. *In Search of the Kingdom's Ediacarans: The First Genuine Metazoans (Macroscopic Body and Trace Fossils) from the Neoproterozoic Jibalah Group (Vendian/Ediacaran) on the Arabian Shield*; Saudi Geological Survey: Jiddah, Saudi Arabia, 2013; in press.
99. Kennedy, A.; Kozdroj, W.; Johnson, P.R.; Kattan, F.H. *SHRIMP Geochronology of the Northern Arabian Shield Part III: Data acquisition 2006*; Saudi Geological Survey: Jiddah, Saudi Arabia, 2011; SGS-OF-2007-9, pp. 1–85.
100. Nicholson, P.G.; Janjou, D.; Fanning, C.M.; Heaman, L.M.; Grotzinger, J.P. Deposition, age and Pan-African correlation of late Neoproterozoic outcrops in Saudi Arabia. In Proceedings of 8th Middle East Geoscience Conference and Exhibition, Manama, Bahrain, 2–5 March 2008.

101. Condon, D.J.; Bowring, S.A. A user's guide to Neoproterozoic geochronology. In *The Geological Record of Neoproterozoic Glaciations*; Arnaud, E., Halverson, G., Eds.; Geological Society: London, UK, 2011; pp. 135–149.
102. Miller, N.; Johnson, P.R.; Stern, R.J. Marine versus non-marine environments for the Jibalah group, NW Arabian Shield: A sedimentologic and geochemical survey and report of possible Metazoa in the Dhaiqa formation. *Arab. J. Sci. Eng.* **2008**, *33*, 55–77.
103. Fike, D.A.; Grotzinger, J.P.; Pratt, L.M.; Summons, R.E. Oxidation of the Ediacaran ocean. *Nature* **2006**, *444*, 744–747.
104. Halverson, G.; Shield-Zhou, G. Chemostratigraphy and the Neoproterozoic glaciations. In *The Geological Record of Neoproterozoic Glaciations*; Arnaud, E., Halverson, G., Eds.; Geological Society: London, UK, 2011; pp. 51–66.
105. Brown, G.F.; Schmidt, D.L.; Huffman, A.C., Jr. *Geology of the Arabian Peninsula: Shield Area of Western Saudi Arabia*; Professional Paper 560-A; U.S. Geological Survey: Denver, CO, USA, 1989; pp. 1–180.
106. Kusky, T.M.; Abdelsalam, M.; Stern, R.J. Tucker, Preface to Special Issue Precambrian Research on the East African and related Orogen and the assembly of Gondwana. *Precambrian Res*. **2003**, *123*, 81–85.
107. Küster, D.; Liégeois, J.P.; Sergeev, S.; Lucassen, F. Zircon geochronology and Sr, Nd, Pb isotope geochemistry of granitoids from Bayuda Desert and Sabaloka (Sudan): Evidence for a Bayudian event (920–900 Ma) preceding the Pan-African orogenic cycle (860–590 Ma) at the eastern boundary of the Saharan Metacraton. *Precambrian Res.* **2008**, *164*, 16–39.
108. Avigad, D.; Stern, R.J.; Beyth, M.; Miller, N.; McWilliams, M.O. Detrital zircon U-BP geochronology of Cryogenian diamictites and lower Paleozoic sandstone in Ethiopia (Tigrai): age constraints on Neoproterozoic glaciation and crustal evolution of the southern Arabian-Nubian Shield. *Precambrian Res.* **2007**, *154*, 88–106.
109. Cosca, M.A.; Shimron, A.; Caby, R. Late Precambrian metamorphism and cooling in the Arabian-Nubian Shield. Petrology and $^{40}Ar/^{39}Ar$ geochronology of metamorphic rocks of the Elat area (southern Israel). *Precambrian Res.* **1999**, *98*, 107–127.
110. Avigad, D.; Cvirtzman, Z. Late Neoproerozoic rise and fall of the northern Arabian-Nubian Shield: the role of lithospheric mantle delamination and subsequent thermal subsidence. *Tectonophysics* **2009**, *477*, 217–228.
111. Be'eri-Shlevin, Y.; Katzir, Y.; Blichert-Toft, J.; Kleinhanns, I.C.; Whitehouse, M.J. Nd-Sr-Hf-O isotope provinciality in the northernmost Arabian-Nubian Shield: Implications for crustal evolution. *Contrib. Mineral. Petr.* **2010**, *160*, 181–201.
112. Be'eri-Shlevin, Y.; Katzir, Y.; Whitehouse, M. Post-collisional tectonomagmatic evolution in the northern Arabian-Nubian Shield: Constraints from ion-probe U-BP dating of zircon. *J. Geol. Soc. Lond.* **2009**, *166*, 71–85.
113. Fritz, H.; Dallmeyer, D.R.; Wallbrecher, E.; Loizenbauer, J.; Hoinkes, G.; Neymayr, P.; Khudeir, A.A. Neoproterozoic tectonothermal evolution of the Central Eastern Desert, Egypt: A slow velocity tectonic process of core complex exhumation. *J. Afr. Earth Sci.* **2002**, *34*, 137–155.

114. Garfunkel, Z. History and paleogeography during the Pan-African orogen to stable platform transition: Reappraisal of the evidence from the Elat area and the northern Arabian-Nubian Shield. *Israeli J. Earth Sci*. **1999**, *48*, 135–157.
115. Jarrar, G.; Stern, R.J.; Saffarini, G.; Al-Zubi, H. Late- and post-orogenic Neoproterozoic intrusions of Jordan: Implications for crustal growth in the northernmost segment of the East African Orogen. *Precambrian Res.* **2003**, *123*, 295–319.
116. Al-Saleh, A.M.; Boyle, A.P. Structural rejuvenation of the eastern Arabian Shield during continental collision: $^{40}Ar/^{39}Ar$ evidence from the Ar Ridaniyah ophiolite mélange. *J. Afr. Earth Sci*. **2001**, *33*, 135–141.
117. Al-Saleh, A.M.; Boyle, A.P.; Mussett, A.E. Metamorphism and $^{40}Ar/^{39}Ar$ dating of the Halaban ophiolite and associated units: Evidence for two-stage orogenesis in the eastern Arabian Shield. *J. Geol. Soc. Lond.* **1998**, *155*, 165–175.
118. Abdelsalam, M.G.; Stern, R.J.; Copeland, P.; Elfaki, E.M.; Elhur, B.; Ibrahim, F.M. The Neoproterozoic Keraf suture in NE Sudan: Sinistral transpression along the eastern margin of West Gondwana. *J. Geol.* **1998**, *106*, 133–147.
119. Dabbagh, M.E.; Rogers, J.J.W. Depositional environments and tectonic significance of the Wajid Sandstone of southern Saudi Arabia. *J. Afr. Earth Sci.* **1983**, *1*, 47–57.
120. Samuel, M.D.; Moussa, H.E.; Azer, M.K. A-type volcanics in central eastern Sinai, Egypt. *J. Afr. Earth Sci.* **2007**, *47*, 203–226.
121. Ring, U.; Brandon, M.T.; Willett, S.D.; Lister, G. Exhumation processes. In *Exhumation Processes: Normal Faulting, Ductile Flow, and Erosion*; Ring, U., Brandon, M.T., Lister, G.S., Willett, S.D., Eds.; Geological Society: London, UK, 1999; pp. 1–27.

© 2013 by the authors; licensee MDPI, Basel, Switzerland. This article is an open access article distributed under the terms and conditions of the Creative Commons Attribution license (http://creativecommons.org/licenses/by/3.0/).